Università degli Studi di Salerno
and
Universitat Politècnica de Catalunya

DEPARTMENT OF CIVIL ENGINEERING, DICIV - DECA
Master of Degree in Building and Architectural Engineering
Master of Degree in Civil Engineering

MASTER OF DEGREE THESIS

Experimental and numerical wave overflow modelling typical of Catalan coast

Thesis Advisors
Dott. Corrado Altomare
Prof. Francesc Xavier Gironella I Cobos
Prof. Giacomo Viccione

Candidate
Maria Luigia Robustelli
Serial Number: 0660100510
Serial Number: 590100 044093560 8

Thesis submitted in 2018-2019

"Se qualcosa è destinato a te, troverà sempre il modo di raggiungerti"

(Hester Brown)

Thanksgiving

É vero sono stati cinque anni e mezzo intensi, vissuti senza nessuna pausa e con tantissimi ostacoli, ma accompagnati da altrettante soddisfazioni. Ricordo che durante l'ultimo anno di scuole medie tutti sognavano di essere attrici, calciatori, modelle, piloti mentre io no. Ero "diversa". Io volevo diventare ingegnere, accompagnata da quella voglia matta di progettare ancora più grande quelle casette che, fino a quel momento, creavo solo per le mie lumachine in campagna. Ripercorrere questi anni è di una difficoltà immane, mi vengono in mente tanti aneddoti ma, il più importante resta il giorno in cui scoprii di aver superato il test di ingresso nazionale; non ci credevo era iniziato il mio sogno. Da quel momento tutto è stato una scoperta continua: un nuovo mondo, nuove conoscenze, nuovi ostacoli, nuovi obiettivi da raggiungere eppure ora mi ritrovo qui, a scrivere la parte più "significativa" di un'intera tesi. Il mio lavoro si apre con una frase la quale racchiude tutta la mia vita, o meglio, l'inizio di questa avventura nata dal destino.

In primo luogo, vorrei ringraziare chi mi ha dato la possibilità di lavorare a questa tesi: il Prof. Giacomo Viccione, il Prof. Xavi Gironella ed il Dott. Corrado Altomare. Un ringraziamento dal cuore, poiché hanno creduto in me, nelle mie capacità e sono stati un appoggio continuo, grazie a loro sono cresciuta tanto, sia dal punto di vista professionale ma, soprattutto da quello umano; i vostri insegnamenti mi accompagneranno per sempre.

Un ringraziamento particolare lo dedico a Corrado che, per me, non è stato solo un tutor ma un amico, un fratello, il mio vero punto di riferimento qui a Barcellona. Ti ringrazio per aver avuto sempre un secondo per me, penso che senza il tuo aiuto non sarei riuscita a completare questo percorso, spero di

esser stata all'altezza delle tue aspettative e di non averti deluso.
Un grazie immenso va ai miei compagni di avventura: Tuozzo, Carmine, Debora, Martina e Sante, senza di voi quelle otto ore rinchiuse in un'aula non avrebbero avuto senso. Ci siamo divertiti un mondo, abbiamo "studiato", siamo cresciuti insieme: tra progetti infiniti, viaggi idimenticabili, risate, scherzi e litigate, grazie per tutto. Tuozzo grazie per la tua simpatia contagiosa e per avermi sempre strappato un sorriso; con Martina invece, si è "combattuto" insieme, grazie per la tua schiettezza e per avermi tranquillizzato in molti momenti, Sante grazie per il tuo modo di fare all'antica e per aver dispensato consigli preziosi sulla vita e sull'università, mi sono stati davvero utili e a Carmine dico grazie per le tue battute che non fanno mai ridere e per i tuoi silenzi che a volte, valgono più di mille parole. Debora merita un ringraziamento speciale perchè lei, più di ogni altro, c'è stata per me. L'Università mi ha donato non un'amica ma una sorella, ricordati che per te ci sarò sempre. Sono sicura che i nostri percorsi continueranno ad intrecciarsi, vi voglio davvero bene, è stato un onore percorrere questi anni insieme a voi.
Per Giuseppe invece, dovrei far costruire una statua d'oro raffigurante il suo viso, grazie per essere stato il mio psicolgo, per aver sopportato tutti i miei sfoghi pre esame ma, soprattutto grazie per essere stato il mio portafortuna, sei un amico vero.
Ringrazio Teresa, la mia compagna di avventura a Barcellona, solo lei sa quanto ho sudato per scrivere questa tesi, ti ringrazio per le risate, le chiacchiere in camera tua, le camminate e soprattutto grazie per aver sopportato le mie continue lamentele.
A Isabella (il mio plinto di fondazione), Elena (la mia amica di risate e scherzi), Dainali (la mia "mamma"), Alessia (l'amica della porta accanto), Rosangela (la mia dispensatrice di consigli), a Michela, Valentina, Severino (i primi che hanno creduto i me) e a tutte le persone che ho incontrato durante questo percorso dico grazie, perchè con una parola, con un gesto siete stati sempre presenti.
Ringrazio i miei due angeli custodi, mia nonna e mio cugino Antonio, coloro che, in ogni momento, in ogni esame, mi "poggiavano" la mano sulla spalla

dandomi quel coraggio che non sapevo neanche di possedere, siete stati la mia spinta in più. Nonna ho realizzato il tuo sogno!!
Ringrazio i miei genitori perchè so che per me ci sarete sempre e, nonostante, abbia iniziato questo percorso da sola, sono convinta che lo finiremo insieme. Spero che oggi siate orgogliosi di avere una figlia come me. Ringrazio i miei due fratelloni, i miei altri due papà, che hanno sempre appoggiato le mie scelte e mi hanno sempre invogliato a combattere per realizzare i miei sogni, grazie davvero per tutto quello che avete fatto e continuate a fare per me.
Il ringraziamento più grande va a Gerardo, la persona più importante della mia vita, se sono qui oggi è solo grazie a lui. Mi ha supportato e sopportato fin dai test d'ingresso, è stato l'unico a credere fermamente che, nella vita, avrei raggiunto tutti i miei obiettivi. É stato tutto per me: consigliere, amico, professore, tifoso, motivatore, mi ha spinto a dare sempre il massimo, proprio per questo tutti i miei successi li dividiamo insieme. La frase scritta nella prima pagina è soprattutto dedicata a te perchè, in fin dei conti, la mia più grande vittoria nella vita è stata incontrarti.
Infine voglio dedicare due righe a me, alla mia forza di volontà, alla mia tenacia, al mio non arrendermi mai di fronte alle difficoltà. A volte sembrava che tutto fosse più grande di me ma, lottando con caparbietà, ero sicura che tutta la fatica mi sarebbe stata ricompensata. Oggi, alla fine di questo percorso, posso finalmente urlare con fierezza ed orgoglio di AVERCELA FATTA!!

Contents

List of Figures

CHAPTER 1

Introduction

This thesis work is the result of collaboration between the "Università degli Studi di Salerno" (Italy) and the "Universitat Politècnica de Catalunya-BarcelonaTech" (BCN, Spain), in particular with the Maritime Engineering Laboratory (LIM). The thesis is focussing on the analysis of the wave overtopping and post-overtopping processes on coastal defense structures in highly urbanized areas. In fact, one of the most common and major risks for people happens when the waves crash against the coastal deferences and a flow is generated at the top of the structures, which can have enough energy to knock over and injure a person, or even carry them into the sea. To prevent or reduce these consequences, coastal defenses are built, the most common are:

- sloping sea dikes;
- vertical walls;
- armoured rubble slopes.

In particular, the present work analyzes the overtopping volumes, discharges and velocities that can lead to risk scenarios for people and vehicles along the coastline. The analyzed case study, "Premiá de Mar", schematically represents the coastline north of Barcelona, Spain, where every year the railway line is

exposed to overflowing phenomena so that, in the worst conditions, rail traffic is interrupted to prevent the train from overturning.
The main purpose of this thesis work is to verify that coastal safety limits and design criteria recommended by the current literature, such as EurOtop manual (2018) [13], require to be amended. To reach this objective, a methodology consisting of three distinct phases will be illustrated:

1. physical model tests were carried out, modelling a layout that resembles the case study for different wave conditions corresponding to events with different return periods. The small scale flume "CIEMito" at LIM/UPC was for the purpose;

2. the acquired experimental data were collected, analyzed and compared with the state-of-the-art semi-empirical formulas;

3. the results, finally, have been compared with the safety criteria from EurOtop (2018) and with the stability curves for people and vehicle proposed by literature (e.g., Sandoval and Arrighi).

The application description is preceded, in the following chapters, by a section of theoretical references; the different formulations for the determination of mean overtopping discharge, the wave evolution period, the individual overtopping volume and, in particular, the methodologies for the definition of the stability curves are illustrated. This research is a preliminary study that will be investigated and discussed in further works.

CHAPTER 2

Literature

The scientific literature available on wave overtopping prediction is very extensive, but it is not the same on the stability of people under the effect of wave overtopping flows, that is limited to a modest number of studies. In this area several studies have tested human subjects in controlled flows which have generated a quantification of the critical flows parameters and mechanisms that can lead to make a person lose stability and fall into the flow. The chapter summarizes the literature about wave overtopping for steep low-crested structures and presents an extended review of studies related with human stability under different types of flows, and a novel analysis of real overtopping accidents.

2.1 Wave overtopping

Wave overtopping happens when waves run up the seaward face of the coastal defenses, reach the crest and pass over it. This phenomenon causes flooding of the areas above the structures and by reaching high speeds, endanger people and infrastructures. Hereafter the main structural and hydraulic parameters that might affect the overtopping are described. The structural parameters are the crest freeboards R_c, defined as the height of the crest of a structure relative

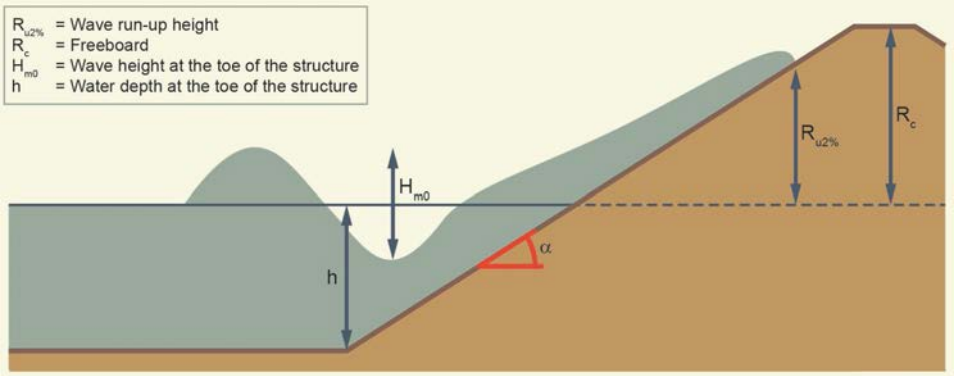

Figure 2.1: Sketch of overtopping phenomena. Image by [13]

to the water level, the slope angle of the structure α, the water depth at toe of the structures h_{toe} and the roughness of seaward face γ_{f}. The wave parameters are the incident significant wave height H_{m0} and spectral wave period $T_{\mathrm{m\text{-}1,0}}$ defined as:

$$H_{\mathrm{m0}} = 4\sqrt{m_0} \tag{2.1}$$

$$T_{\mathrm{m\text{-}1,0}} = \frac{m_{\text{-}1}}{m_0} \tag{2.2}$$

Other parameters of use when studying the overtopping process are the linear wavelength $L_{m-1,0}$, the wave steepness $s_{m-1,0}$ and the breaker parameter $\xi_{\mathrm{m\text{-}1,0}}$, defined as:

$$L_{m-1,0} = \frac{gT_{m-1,0}^2}{2\pi} \tanh\left(\frac{2\pi h}{T_{m-1,0}}\right) \tag{2.3}$$

$$s_{m-1,0} = \frac{H_{m0}}{L_{m-1,0}} \tag{2.4}$$

$$\xi_{\mathrm{m\text{-}1,0}} = \frac{\tan(\alpha)}{\sqrt{\frac{2\pi H_{\mathrm{m0}}}{gT^2{}_{\mathrm{m\text{-}1,0}}}}} \tag{2.5}$$

It is here important distinguish between deep, shallow and very shallow foreshores, even if today does not exist a clear criterion for the differentiation them. **Van Gent et al.** (1999) [1] proposed a criterion to determine if the foreshore is characterized by deepwater, intermediate, shallow or very shallow water: if the ratio between the wave height in deepwater, $H_{m0-DEEP}$, and the water depth the toe of the dike, h_{toe}, is greater than 0.75 and less than 1.50, then the foreshore can be considered as shallow; if the same ratio is greater than 3.0, then the foreshore can be assumed very shallow. In all the other cases, the

foreshore must be considered as intermediate or deep. The criteria from Van Gent [1] is summarized in the table:

Depth condition	$H_{\mathrm{m0,deep}}/h$ [-]
Very shallow	$H_{\mathrm{m0,deep}}/h > 1.5$
Shallow	$1.5 > H_{\mathrm{m0,deep}}/h > 0.75$
Intermediate	$0.75 > H_{\mathrm{m0,deep}}/h > 0.4$
Deep	$H_{\mathrm{m0,deep}}/h < 0.4$

In a shallow foreshore breaking waves and wave height are lower, but there is still a spectrum similar to the original spectrum. At a very shallow foreshore is difficult to recognize a spectrum with a peak. Generally speaking, the transition between shallow and very shallow foreshores can be defined as the situation where the original incident wave height has been decreased by 50% or more, due to wave breaking. The effect of a (very) shallow foreshore translates into a high value of the breaker parameter ($\xi_{m-1,0} > 5/7$) with relatively gentle dike slopes (1:2.5). In this thesis work has been used the foreshore's classification by **Hofland** [5]:

Depth condition	$h_t/H_{\mathrm{m0,o}}$ [-]
Deep	$h_t/H_{\mathrm{m0,o}} > 4$
Shallow	$1 < h_t/H_{\mathrm{m0,o}} < 4$
Very shallow	$0.3 < h_t/H_{\mathrm{m0,o}} < 1$
Extremely shallow	$h_t/H_{\mathrm{m0,o}} < 0.3$

2.1.1 Wave period evolution

The spectral wave period is preferred to either as the peak period T_{p} or the average period T_{m} in wave overtopping calculations, because it gives more weight to the longer periods in the spectrum. Furthermore, the same $T_{\mathrm{m\text{-}1,0}}$ along with same wave heights lead to similar overtopping discharges, independently of the spectrum type, even in case of double-peaked or flatted spectra. A detailed analysis on the use of the spectral period for overtopping prediction is contained

in Van Gent et al. (1999) [1] where the author demonstrated that the spectral period shows a better performance than the other wave periods both for wave overtopping and wave run-up predictions (Fig 2.2, 2.3).

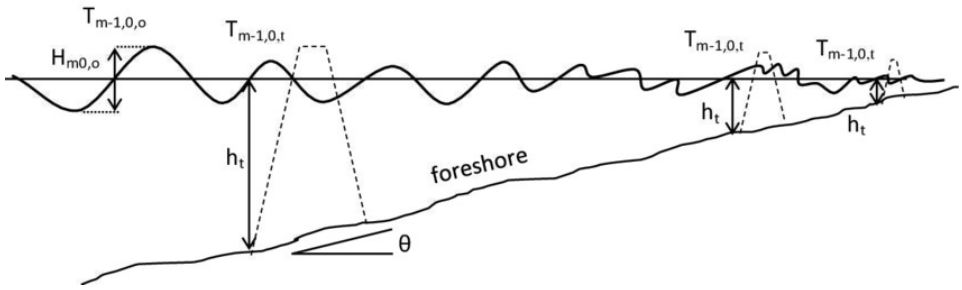

Figure 2.2: Foreshore configuration with 3 different setting of structures [1]

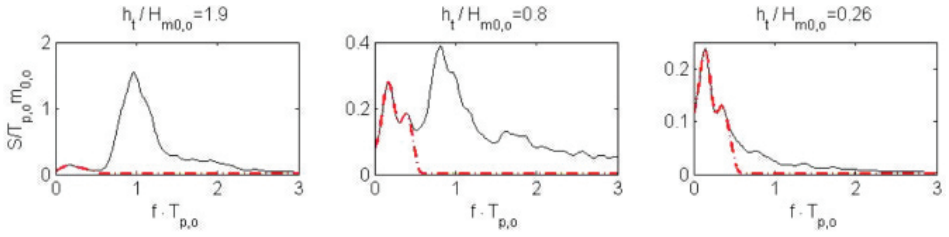

Figure 2.3: Measured wave spectra for the different structures [1]

Van Gent et al. (1999) [1] carried out small scale mode model tests on a 1:100 and 1:250 foreshores with smooth structure slopes of 1:4 and 1:2.5. Due to the heavy breaking the spectral wave period, $T_{\text{m-1,0}}$, can changed drastically. One example shows that the spectral wave period was changed from 2 to 3 s at deep water to 8 s at the toe of the structure. This implies a significant change of spectral shape as well. Wave heights are also reduced from roughly 0.14 m to 0.04 m in this case. With such small wave heights and very long periods at the toe of the structure, the breaker parameter becomes very large, around $\xi_{\text{m-1,0}}$=14 for a 1:4 slope and $\xi_{\text{m-1,0}}$=20 for a 1:2.5 slope.

The studied used now in the EurOTop (2018) is that of **Hofland et al.** (2017) [6]. He introduced the new parameter, $\tilde{h}$, in which is incorporated the foreshore slope θ besides the relative depth.

$$\tilde{h} = \frac{h_t}{H_{m0,o}} \left(\frac{\cot \theta}{100} \right)^{0.2} \tag{2.6}$$

Hofland et al. (2017) was carried the test with the straight foreshore, it can be seen from the Fig 2.4 for shallow foreshore, the wave period increases slightly with the decreasing depth, for the very shallow foreshores $T_{m-1,0,s}$ increases quicker with depth, finally for the extremally shallow foreshore the increase is even bigger.

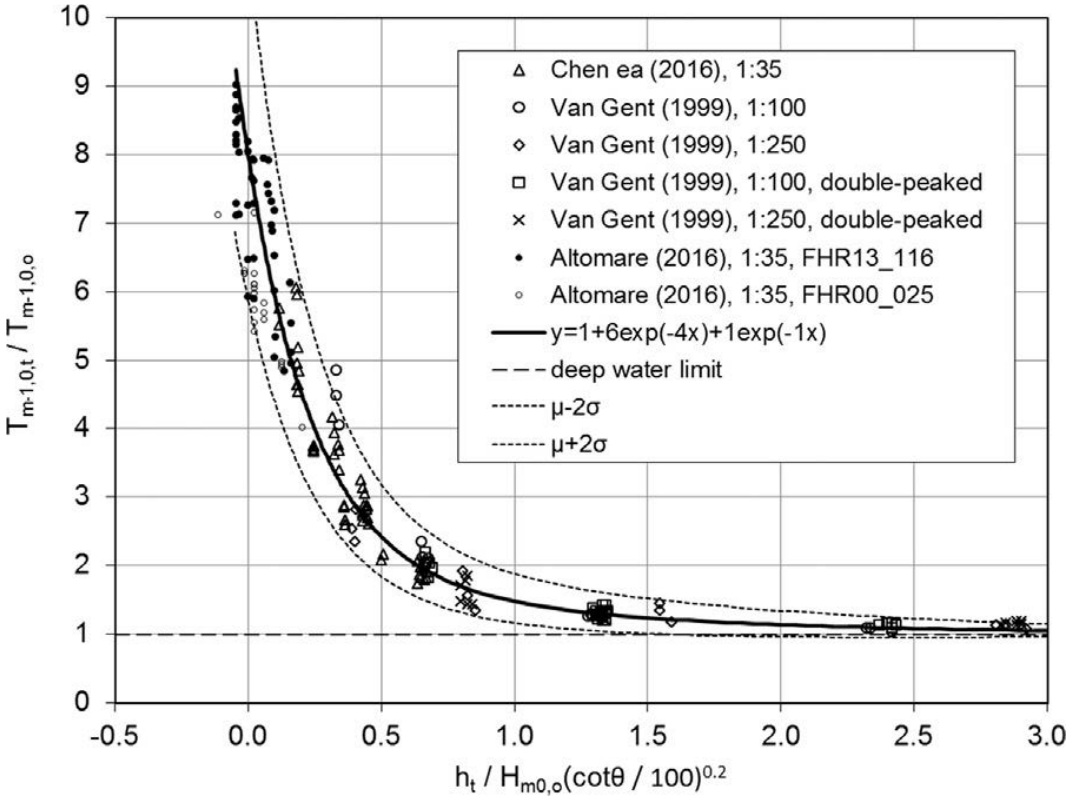

Figure 2.4: Data of the (increase in) measured wave period $T_{m-1,0}$ of long-crested waves on a straight mildly sloping foreshore, as a function of relative depth with slope correction. The solid line is the fit through the data given in Eq. (2.7). The dashed lines indicate the $\pm 2\sigma$ (root-mean-square variation) error bands. [6]

For the wave period calculation he used the new formula, defined as:

$$\frac{T_{m-1,0,t}}{T_{m-1,0,o}} - 1 = 6\exp(-4\tilde{h}) + \exp(-\tilde{h}) \tag{2.7}$$

Two exponential terms are very important for the calculation of the period in conditions of shallow and extremally shallow foreshores: for the extremally shallow conditions is dominant the second exponential term while for shallow

conditions $\tilde{h} > 1$ the first exponential term. With the Hofland prediction it's possible to defined the spectral wave period for long - crested waves.

2.1.2 Mean overtopping discharge

The first study used for the calculation of discharge for seadike with shallow foreshore is proposed by **Van Gent et al.** (1999) and also reported in TAW (2002) [3] and EurOtop (2007) [2], the formula is expressed by the following two equations:

$$\frac{q}{\sqrt{gH^3{}_{\mathrm{m0}}}} = 10^c \exp\left(- \frac{R_{\mathrm{c}}}{H_{\mathrm{m0}}\gamma_f\gamma_\beta(0.33 + 0.22\xi_{\mathrm{m\text{-}1,0}})}\right) \tag{2.8}$$

$$\frac{q}{\sqrt{gH^3{}_{\mathrm{m0}}}} = 0.21 \exp\left(- \frac{R_{\mathrm{c}}}{H_{\mathrm{m0}}\gamma_f\gamma_\beta(0.33 + 0.22\xi_{\mathrm{m\text{-}1,0}})}\right) \tag{2.9}$$

where:

- q is the overtopping discharge per meter width of the structure [m^3/s/m]
- R_{c} is the crest freeboard [m]
- γ_f is the reduction coefficient that considers the effects of the slope roughness [-]
- γ_β is the reduction coefficient that considers the effects of the obliqueness [-]
- c parameter assumed as normally distributed with mean value to 0-0.92 and a standard deviation σ equal to 0.24

The equations are valid for $\xi_{\mathrm{m\text{-}1,0}} \geq 7$ [2][3][4]. In the case of $\xi_{\mathrm{m\text{-}1,0}} \leq 5$, it is recommended to use the following pair of formulas:

$$\frac{q}{\sqrt{gH^3{}_{\mathrm{m0}}}} = \frac{0.067}{\sqrt{\tan(\alpha)}}\gamma_\beta\xi_{\mathrm{m\text{-}1,0}} \exp\left(- 4.75\frac{R_{\mathrm{c}}}{H_{\mathrm{m0}}\gamma_f\gamma_\beta\gamma_v\gamma_b\xi_{\mathrm{m\text{-}1,0}}}\right) \tag{2.10}$$

with maximum of:

$$\frac{q}{\sqrt{gH^3{}_{\mathrm{m0}}}} = 0.2 \exp\left(- 2.6\frac{R_{\mathrm{c}}}{H_{\mathrm{m0}}\gamma_f\gamma_\beta}\right) \tag{2.11}$$

In the case of $5 < \xi_{\text{m-1,0}} < 7$, a linear interpolation is recommended between the two sets of formulas.

Goda (2009) [14] proposed a simple exponential functional from for the overtopping formula, defined as follows:

$$\frac{q}{\sqrt{gH^3{}_{\text{m0}}}} = \exp\left[-\left(A + B\frac{R_{\text{c}}}{H_{\text{m0}}}\right)\right] \tag{2.12}$$

where:

$$A = A_0\left[(0.956 + 4.44\tan\theta)\left(\frac{h_{\text{toe}}}{H_{\text{m0}}} + 1.242 - 2.032(\tan\theta)^{0.25}\right)\right] \tag{2.13}$$

$$B = B_0\left[(0.822 + 2.22\tan\theta)\left(\frac{h_{\text{toe}}}{H_{\text{m0}}} + 0.578 - 2.22\tan\theta\right)\right] \tag{2.14}$$

where θ is the angle of the foreshore and h_{toe} is the water depth at te toe of the structure. The coefficient A_0 and B_0 are expressed as functions of the dike slope α:

$$A_0 = 3.4 - 0.734\cot\alpha + 0.239\cot^2\alpha - 0.0162\cot^3\alpha \tag{2.15}$$

$$B_0 = 3.4 - 0.5\cot\alpha + 0.15\cot^2\alpha - 0.011\cot^3\alpha \tag{2.16}$$

the equations were derived by Goda using 715 data points for vertical walls and 1254 data points for sloping dikes respectively, both extracted form CLASH database. To cover a lack of data in shallow foreshore Goda also used data from Tamada et al. (2002) [17]. However very few data refer to zero or to very low water depth at the toe of the dike and no data with emergent toes are included, therefore, in many case the new set of equations proposed by Goda have to be used for a preliminary assessment.

Altomare et al. (2016) [11] modified the Van Gent formulation. From the previous studies it has already been possible to verify a correlation between the $Q_{measured}$ and the R_c/H_{m0}, but through the use of the scatter - plot - matrix he identifies a new bond (Fig 2.5). The select data by Altomare are: the measured discharge, the incident wave height and period. the water depth at the toe of the dike, the dike slope and the foreshore slope.

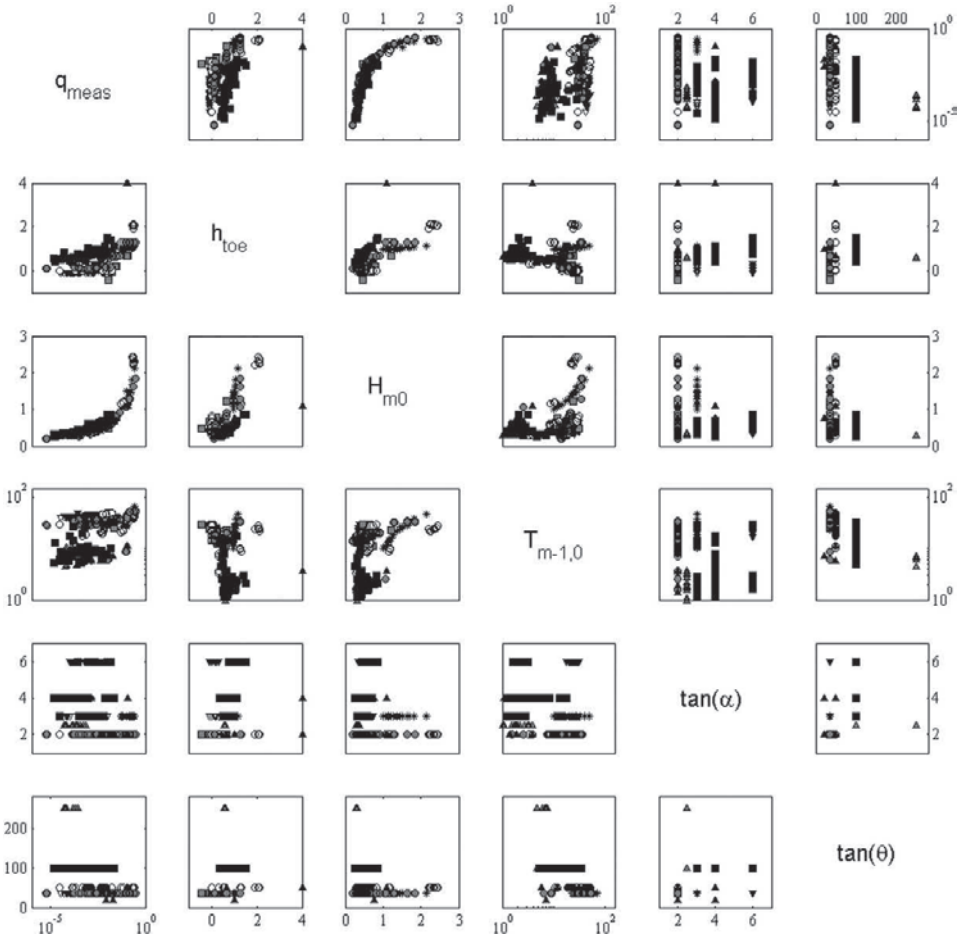

Figure 2.5: Scatter-plot matrix of uniformly scaled variables by [11]

From the Fig 2.6 it can be see:

- the overtopping discharge increases with the wave height;
- a non linear correlation between the wave height and water depth;
- the correlation between the wave overtopping and water depth, for very shallow water the wave breaking is heavier resulting in smaller wave height and then smaller overtopping rates.

Altomare et al. (2016) proposed the new formulation for very shallow condition:

$$\frac{q}{\sqrt{gH_{m0}^3}} = 10^{c_{new}} \exp\left(-\frac{R_c}{H_{m0}(0.33 + 0.022\xi_{m-1,0})}\right) \tag{2.17}$$

He assumed to use an equivalent slope by combining the foreshore slope and the dike. The new parameter c is based by the datasets of CLASH, is assumed

to be normally distributed and is equal to -0.791 and the standard deviation σ is 0.294. Altomare et al. formula is used in EurOtop (2018) for the design of coastal structures.

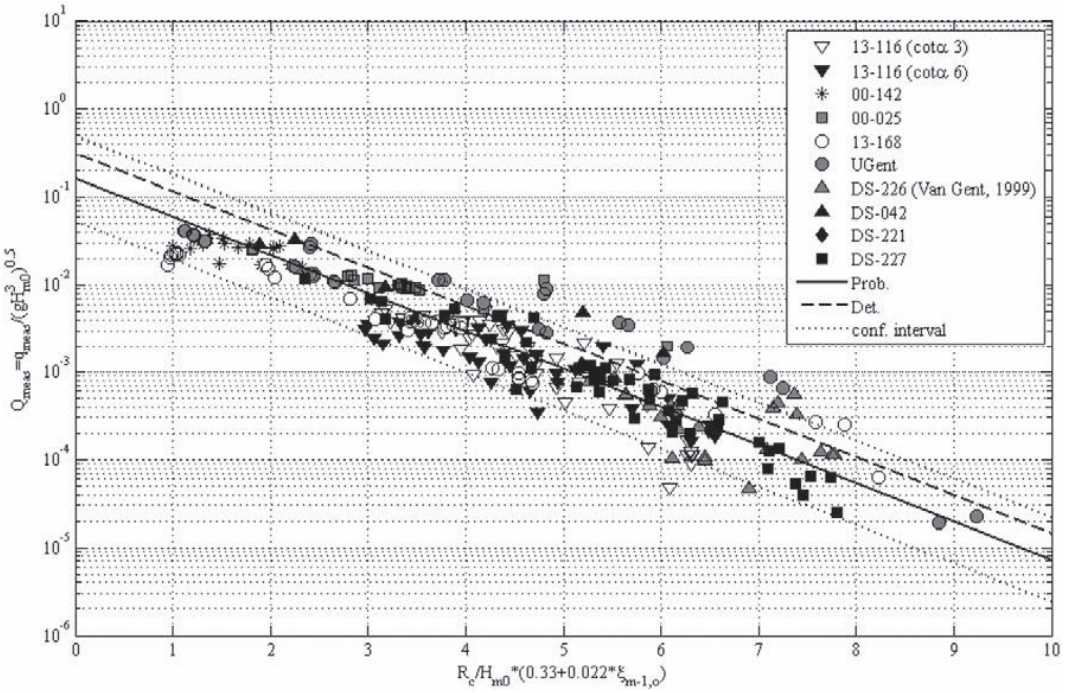

Figure 2.6: Wave overtopping data and prediction using Eq. 2.17 with 5% under and upper exceed limits [11]

Gallach (2018) [6] proposed the formula based of three coefficients:

$$\frac{q}{\sqrt{gH^3{}_{\mathrm{m0}}}} = a_{update} \cdot \exp\left[-\left(b_{update} \frac{R_c}{H_{m0}\gamma_\beta\gamma_f} \right)^{c_{update}} \right] \tag{2.18}$$

where:

- $a_{update} = 0.0109 - 0.035(1.05 - \cot\alpha)$ and $a_{update} = 0.109$ for $\cot\alpha > 1.5$;
- $b_{update} = 2 + 0.56(1.5 - \cot\alpha)^{1.3}$ and $b_{update} = 2$ for $\cot\alpha > 1.5$;
- $c_{update} = 1.1$

The range of application of the formula is for slope angles $0 < \cot\alpha < 4$ and the relative crest R_c/H_{m0}. Also in this formulation the coefficients of roughness and the obliqueness are equal to one, like Altomare et al. study.

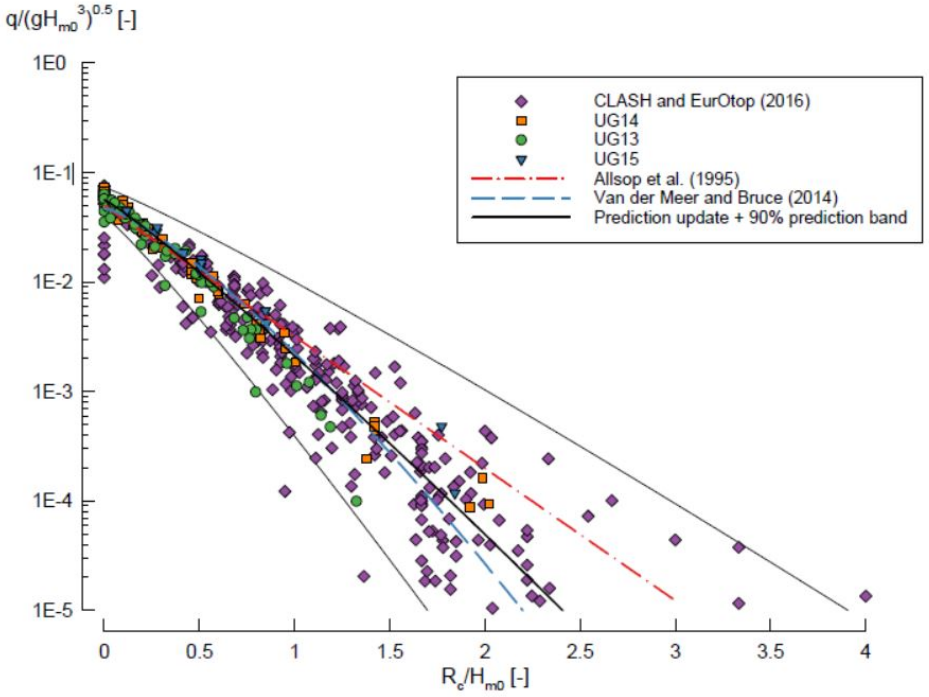

Figure 2.7: Vertical structures overtopping data compared to the updated prediction (Eq. 2.18) with its 90% prediction band, Van der Meer and Bruce (2014) and Allsop et al. (1995). [6]

2.1.3 Individual overtopping volumes

If the structure is not submerged, the overtopping process can be interpreted as a succession of different individual overtopping events, characterized by a certain volume and a certain velocity. Therefore, it is a statistical process, where discharge is expressed in probability overtopping terms (P_{ov}), multiplied for the ratio between maximum overtopping volume expected (V_t) and wave period expected (T_m):

$$q = \frac{\sum_{onde} Volumes}{\sum_{onde} Periods} = \frac{N_{\text{ov}} E(V_t)}{N_w E(T)} = P_{\text{ov}} \frac{(V_t)}{T_m} \tag{2.19}$$

where P_{ov} is the ratio between the number of overflowing waves N_{ov} and the number of recognizable waves N_w. Since every wave that overflows exceeds the crest of the structure, P_{ov} sea edge coincides with the probability that the wave causes an ascent higher than the ridge itself R_c, ie that it results:$R_u > R_c$.
For regular waves P_{ov} is 0.0 if $R_u \leq R_c$ or is 1.0 is $R_u > R_c$.

For irregular waves, **Van der Meer et al** (1995) [15] suggested we adopt a Weibull probability distribution, with parameters α and β depending on the characteristics of the incident waves and on the slope of the parameter, to calculate the wave ascent in the presence of permissible structures in rocks. The cumulative density function of the Weibull distribution is defined as:

$$P_{\text{ov}} = \exp\left[-\left(\frac{R_c}{\alpha}\right)^{\beta}\right] \tag{2.20}$$

The value of the shape parameter β has an important influence on prediction of the maximum overtopping volume. Large value of β means more individual overtopping volumes with roughly the same value. For a small value of the shape factor, the tail of the distribution become steep meaning that the majority of the volumes are small and there are few very large overtopping volumes. **Van der Meer and Janssen** [15] analyzed wave run-up and wave overtopping for sloped coastal structures like revetments and seawall. In particular, the authors has analyzed 14 sets of measurements with a range of relative crest freeboard $0.99 \leq R_c/H_{m0} \leq 3.16$ for mild seaward slopes (1:3 and 1:4). They found that the shape factor β has a constant value of 0.75; the scale factor α depends of mean average overtopping discharge q [m^3/m], the average wave period T_m [s] and the probability of overtopping waves P_{ov}.

$$\alpha = 0.84\left(\frac{qT_m}{P_{\text{ov}}}\right) \tag{2.21}$$

The definition of this equation results from the average overtopping discharge, defined as the total volume overtopped V_t and the duration of the event T_t. The latter can be defined as the product of the number of waves N_w and the mean wave period T_m. Thus, the following mathematical expression can be written:

$$\alpha = \frac{V_t}{N_w T_m} \tag{2.22}$$

From this, can be obtained:

$$\frac{qN_w T_m}{N_{\text{ow}}} = \frac{V_t}{N_{\text{ow}}} \tag{2.23}$$

The right term can be defined as the measured average overtopping volume $\bar{V}_{\text{measured}}[m^3/m]$. We can still defined the theoretical average overtopping

discharge as:

$$V_{\text{theoretical}} = \alpha\Gamma\left(1 + \frac{1}{\beta}\right) \tag{2.24}$$

We can defined the parameter α as:

$$\alpha = \frac{1}{\Gamma\left(1 + \frac{1}{\beta}\right)} \frac{qT_m}{P_{\text{ov}}} \tag{2.25}$$

The terms $\Gamma\left(1 + \frac{1}{\beta}\right)$ is defined α' and the relation with β is shown in Fig 2.8.

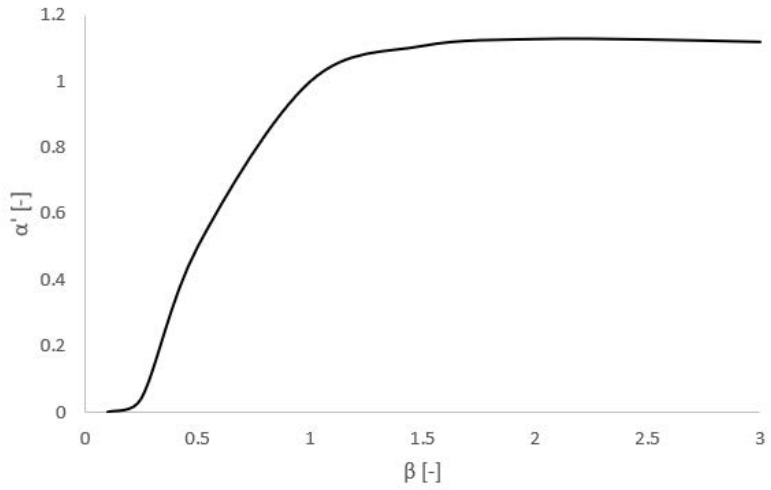

Figure 2.8: Relation between α' and β

Victor et al. (2012) [16] analyzed data of steep-low crested structures, using the 50% of the highest from dataset UG10 (364 tests). In particular, the ranges of application are:

- relative crest freeboard: $0.10 \leq R_c/H_{\text{m0}} \leq 1.69$
- slope angol:$\cot\alpha \in$ [0.36,0.58,0.85,1.00,1.43,1.73,2.14,2.75]
- wave steepness: $0.02 \leq s_{\text{m-1,0}} \leq 0.05$

The author studied the effect of slope angle α, relative crest freeboard R_c/H_{m0} and the waves steepness $s_{\text{m-1,0}}$ on the shape factor β. The found that the latter is influenced by the slope angle and the relative crest freeboards whereas the wave steepness has no influences on shape factor. The new α' and β are:

$$\beta = \exp\left(-2.0\frac{R_c}{H_{\text{m0}}}\right) + 0.526 + 0.15\cot\alpha \tag{2.26}$$

$$\alpha' = 1.13 \tanh(1.132\beta) \tag{2.27}$$

Hughes et al (2012) [18] collected three different dataset (27 tests from Hughes and Nadal (2009) [19]), 364 values from Victor et al (2012) [18] and 14 wave-only overtopping from Van der Meer and Janssen (1995) [15] and plotted them versus relative crest freeboard. For each test, the 10% of the highest has been selected to represent the extreme events (Fig 2.9). The authors suggested a new formula valid in the range of relative crest freeboard $-2.0 \leq R_c/H_{\mathrm{m0}} \leq 4.0$:

$$\beta = \left[\exp\left(-0.6\frac{R_c}{H_{\mathrm{m0}}}\right)\right]^{1.8} + 0.64 \tag{2.28}$$

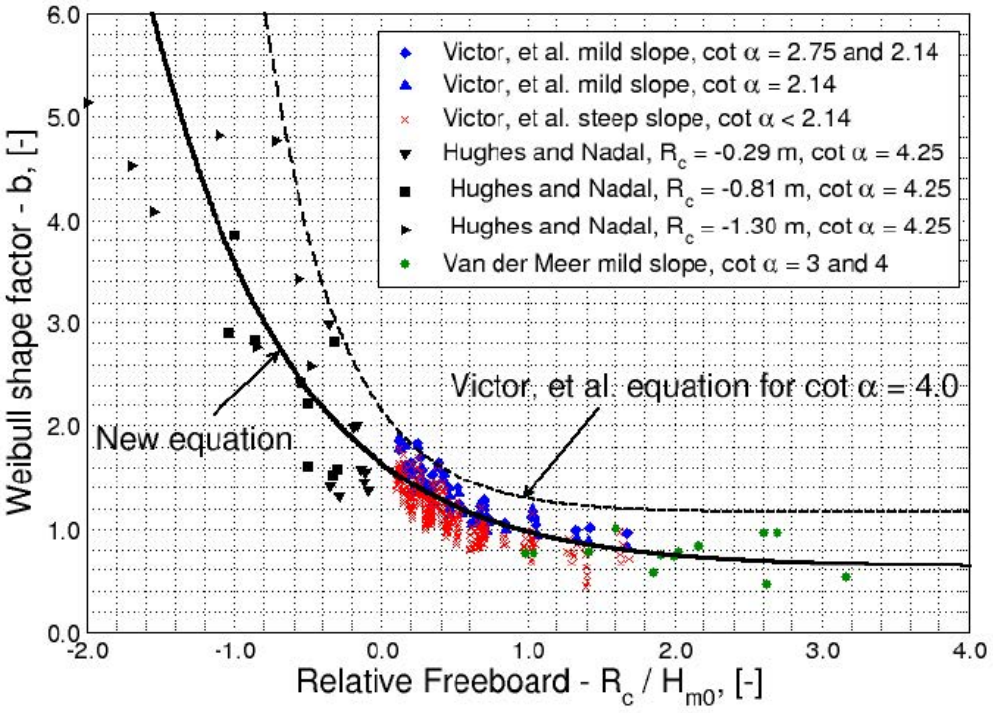

Figure 2.9: Weibull shape factor proposed by Hughens et al (2012) [18]

Zanuttigh et al. (2013) [7] analyzed the β values for rubble mound breakwaters and for low crested structures (crest at or just above the water level). In particular, the authors used two sources of wave-by-wave overtopping data:

- DELOS project: 2D an 3D data for low-crested structures

- CLASH: rouble mound breakwaters and smooth impermeable sloping structures

The β factor for smooth structures found by the authors depends on the mean average overtopping discharge q, the spectral wave period $T_{\text{m-1;0}}$ and the spectral wave height at the toe of the dike H_{m0} and that has also been used bu EurOTop (2016):

$$\beta = 0.73 + 55\left(\frac{q}{gH_{\text{m0}}T_{\text{m-1;0}}}\right)^{1.8} \tag{2.29}$$

Gallach Sanchez (2018) [6] gathered different tests carried out at the wave flume of the Department of Civil Engineering at Ghent University (UG10, UG13, UG14, UG15 and UG16) covering a wide range of hydraulic condition. In table, a summary of the conditions for all tests:

Parameters	Range
Crest freeboard R_c [m]	0-0.2
Incident spectral wave height H_{m0} [m]	0.018 - 0.225
Relative crest freeboard R_c/H_{m0} [-]	0 - 3.25
Relative wave height H_{m0}/h	0.03 - 0.5

The author found that the probability distribution of the individual overtopping volumes follows a Weibull distribution. He suggests a new prediction formula (Eq. 2.30) to evaluate shape factor β that improves the accuracy for those cases with zero freeboard.

$$\beta = (0.59 + 0.23\cot\alpha)\exp\left(-0.6\frac{R_c}{H_{\text{m0}}}\right) + 0.83 \tag{2.30}$$

The maximum individual overtopping volume per meter width can be calculated starting from the non-exceedance probability of the statistical distribution. If the volumes follow a Weibull distribution, as indicated by several authors, the non-exceedance probability is given by Eq. 2.31:

$$P(V \geq V_i) = 1 - \exp\left[-\left(\frac{V_i}{\alpha}\right)^{\beta}\right] \tag{2.31}$$

Using the Weibull plotting position formula $P(Vi) = i/(N_{\mathrm{ow}} + 1)$ and setting the rank $i = 1$, the maximum volume can be calculated as:

$$V_{\mathrm{max}} = \alpha[\ln(N_{\mathrm{ow}} + 1)]^{1/\beta} \tag{2.32}$$

which depends of the shape factor β, the scale factor α and the number of overtopping waves. The latter, which is proportionally to overtopping probability P_{ov} and the number of incident waves N_w, it can be calculated as $N_{ow} = P_{ov} \cdot N_w$. Using Eq. 2.20 and Eq. 2.25, Eq. 2.32 can be rewritten as:

$$V_{max} = \alpha' \, \frac{qT_{tot}}{N_{ow}} \cdot [\ln(N_{\mathrm{ow}} + 1)]^{1/\beta} \tag{2.33}$$

2.2 Human stability in overtopping flows

The first that examined the critical characteristics of human stability flow was **Abt et al.** (1989) [8], aiming to find a general criterion for defining an area at high risk of flooding for humans. At that time, safety agencies used a variety of methods to study floods that were unsafe for the people impacted, furthermore, none of them were based on the fundamental consideration of human ability to remain stable during water flood. The parameters studied in the aforementioned work were flow velocity and depth that make a person lose stability. A series of tests were carried out in a 61 m long, 2.44 m wide and 1.22 m deep recirculation channel at the Engineering Research Center of Colorado State University. On the floor of channel were installed a series of different materials to study a range of floor/roughness conditions: grass, smooth concrete, steel and shavings were all tested. In addition, there was the possibility to change the slope of the channel that gave the opportunity to study the effects of the tilted floor, with slopes of 0.5% and 1.5% used. The first phase of Abt et al. (1989) [8] was made using a rigid monolithic to simulate human body (Fig. 2.10).

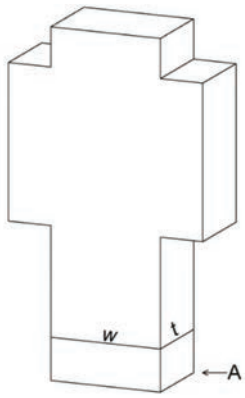

Figure 2.10: Rigid monolith used by Abt et al. (1989) research no information of w and t is given

Results were then used to verify the theoretical envelope for rotational instability. The rotational instability results from the balance of moment around the point A in figure, being the main force acting over the body are: the monolith weight

(W), the buoyancy (B), and the hydrodynamic force (P).

$$\sum M_A = [(W - B)(0.5t)] - [P(0.5d)] = 0 \tag{2.34}$$

where:

- $B = twd\gamma_w$
- γ_w=unit weight of water
- $P = C_d\rho\frac{u^2}{2}A_n$
- C_d=coefficient of drag
- ρ=water density [kg/m^3]
- u=flow speed [m/s]
- A_n=projected area against the flow [m^2]

Assuming a uniform velocity in the cross section of the flow, equation was solved by the author to give a toppling envelope for the rigid monolith. The curves outlined by the author define the safe condition for the monolithic block (below the curve) and the one in which it can be overturned by the water (above the curve) (Fig 2.11).

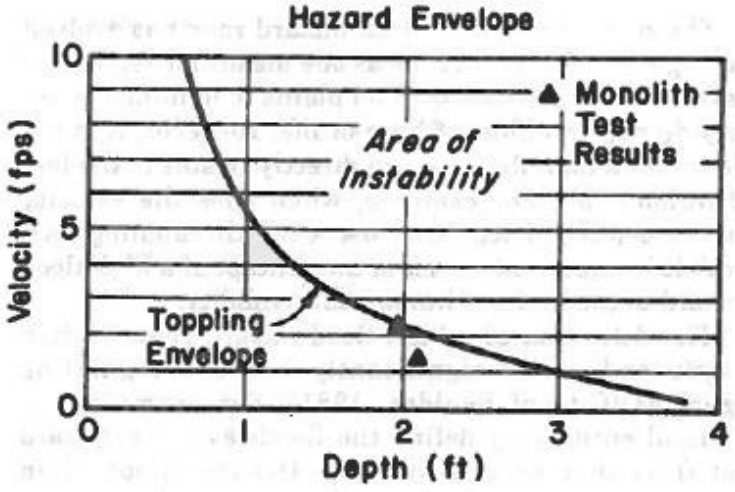

Figure 2.11: Toppling envelope for rigid body monolith [8]

The experimental results for critical flow depths and velocities at the point of

toppling were in good agreement with the predicted range. Subsequently, 20 human subjects were tested under a controlled flow: 2 females and 18 males; weight between 40.9 kg, and 91.4 kg; height from 1.52m to 1.90m. All subjects wore similar clothing. In addition for safety reasons all subjects wore a helmet and a harness, connected to a beam over the flume (Fig. 2.12).

Figure 2.12: Experimental setup carried out by Abt et al. (1989) [8]

At the beginning of each test, the subject took position in the test section of the flume and was exposed to a pre-test, low velocity and depth condition. All the subjects were allowed to accustom the test, giving her/him the chance to feel safe in the flow. Then the flow was slowly increased in order to avoid the generation of waves. During the test, the subject was asked to move in three directions: against the flow; with the flow, and across the flow. The test continued until it was impossible for the subject remain stable standing or walking. Parameters at this points, critical average velocity (u_{cr}) and the critical depth of the flow (d_{cr}) was recorded. Moreover it was calculated a product number ("P.N.") $u_{cr} \cdot d_{cr}$ as an indicator of resistance for each test. 71 tests were conducted, the results of which are shown in Fig. 2.13. It was concluded by the authors that the monolith results are very conservative, since its PN was significantly smaller than the found for the human subjects. A wide range of results for the human subjects were found, explained due to each person having to inform the team when they could no longer stay stable. In conclusion, the absence of an actual fall, this is a subjective evaluation likely to be influenced by each person's characteristics: their height and weight, and

also their particular skills, confidence and perception of risk.

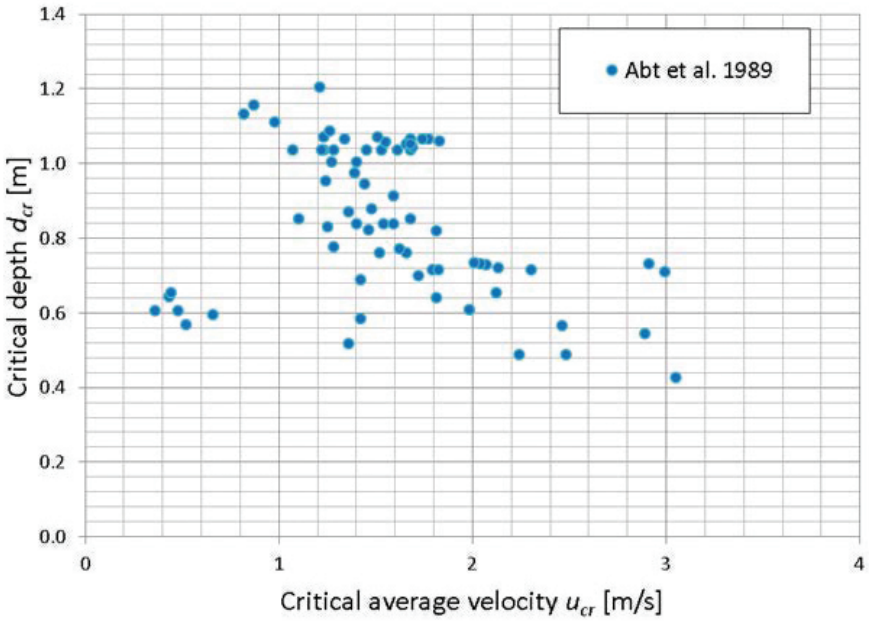

Figure 2.13: Critical speed and depth from Abt et al. (1989) experiment [8]

The ability of each person to react and adapt to the flow, through e.g. changing the position of the feet; leaning into the flow, or using arms for balance, was a very important factor in determining each subject's ability to withstand the flow for longer. For the conditions tested, the results shown that stability was not affected by the type of surface used, and no clear effect of the floor's slope was found. With the results, a methodology to predict the P.N. which could cause instability of a person was proposed based upon a semi-logarithmic curve, and as a function of the person's weight and height.

$$P.N. = \exp\left(m \cdot hp\frac{0.222}{1000} + 1.088\right) \tag{2.35}$$

with:

- $P.N$=Product number [fp_2/s]
- m=person's mass [pounds]
- hp=person's height [inches]

The first study with the purpose to study the human stability in wave overtopping flows, reporting on an initiative carried out the 1995 by the Japanese Port and Harbour Research Institute (PARI), with results reported in **Endoh and Takahashi** (1994) [9]. This study was focused on wave overtopping on breakwaters, which have dual objectives to protect the harbour from storm waves and also provide public areas for recreation. Three human subjects, with heights 1.64 m to 1.83 m and weights 64 kg to 73 kg, were tested in a large current basin, 50 m long and 20 m width, but only the results of two subjects were reported in Endoh and Takahashi (1994). As in Abt et al. (1989) study, a flow in a flume was generated and increased until the person lost his balance, at which point the critical depth (d_{cr}) and velocity (u_{cr}) of the flow was recorded. In addition to the previous study, in this new study, the forces due to the flow against the subject were measured with load cells. The influence of different alignments of the persons against the flow and different leg separations was included in this study. Moreover,the study of the frictional coefficient between two types of shoe soles and the different floors was also included. From the results Endoh and Takahashi (1994) studied two models of human instability:"slipping" and "tumbling" (Fig 2.14).

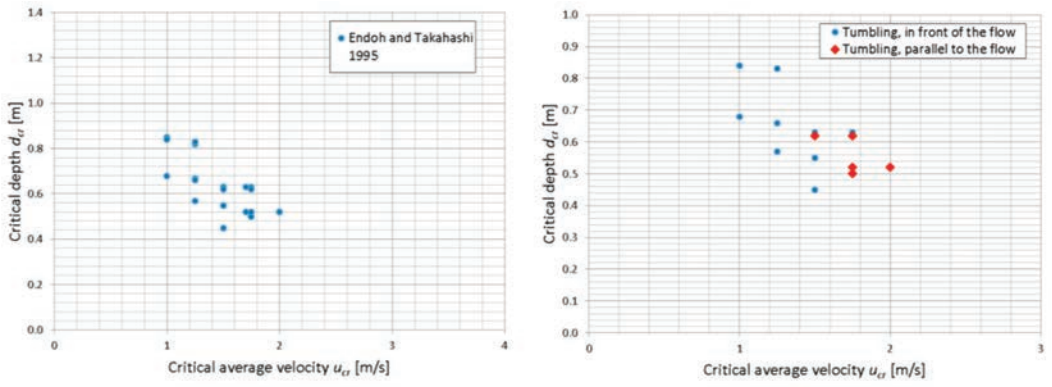

Figure 2.14: Critical speed and depth from Endoh and Takahashi (1994) [9].(a) General results (b) Results of the subject B.

The first one occurs when the flow force against the body (F_f) is bigger than the maximum available friction resistance of the subject (F_r) (this considering various type of shoe soles) . It is anticipated that for fall due to this mecha-

nism, the person will tend to fall with legs pointing downstream. The second mechanism models the falling process rising when the moment produced by the flow around the feet of the subject is bigger than the restoring moment produced by the weight of the person.

From figure, a wide scatter in the results is evident, but a trend between the critical depth at loss of stability (u_{cr}) and the critical velocity of the flow (d_{cr}) is however evident, even though the subjects used had different characteristics and different flow tolerance to be unstable (Fig. 2.15).

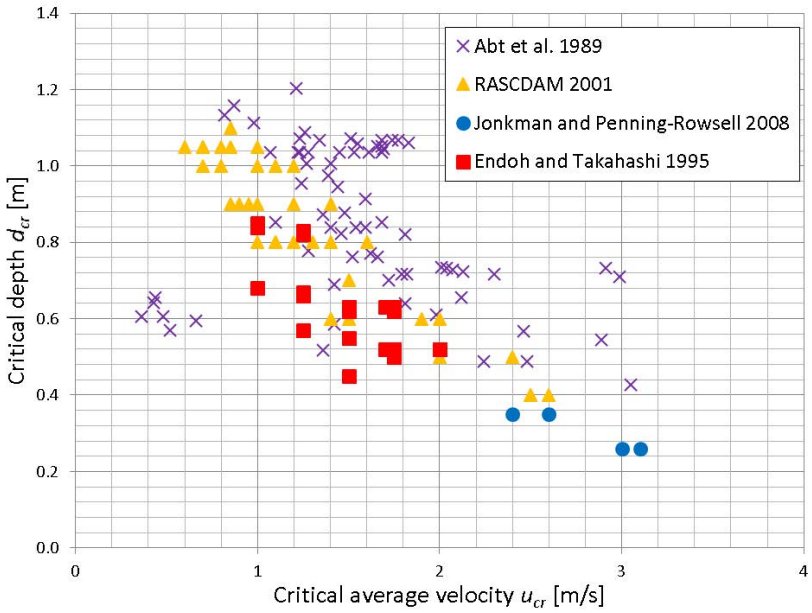

Figure 2.15: Critical speed and depth from previous studies [9].

In the literature there is a complete absence of quantified data on human accidents caused by wave overtopping flows. **Sandoval** (2015) [10], for the first time, studies real events by analyzing videos, made available by "YouTube" or using the camera of mobile phones. Moreover, an extensive INTERNET search was conducted, finding video evidence from real situations which show pedestrians being exposed to real wave overtopping flows. From these, it was possible to analyse the different ways in which the water interacted with the persons and how they reacted to it. These new results are an important value because they are estimation from real events, with no scale effects, furthermore, it was possible to watch the real reaction of people, without safety equipment,

avoiding the opportunity to get used to pre-test condition and being free to react instinctively.

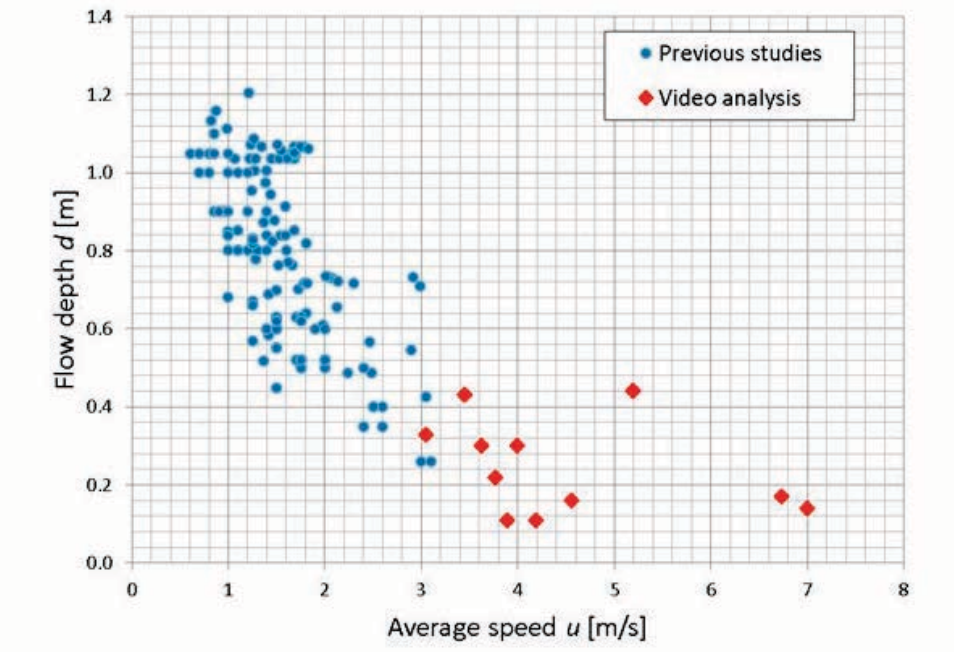

Figure 2.16: Flow speed and depth data from the video analysis of actual events, plotted together with the results of studies from literature by Sandoval (2015) [10].

In the Fig. 2.16 it is possible to compare the results obtained by Sandoval, with the analysis of real situation and those obtained from the previous studies. According to the theories of Endoh and Takahashi (1994), Sandoval understands that the stability not depends only on the person's weight and height, but is also influenced by the position of the person, their way of standing and also by the coefficient of friction between shoe sole and ground. The analysis for each mechanism of instability can be derived as follows:

- **Friction stability**

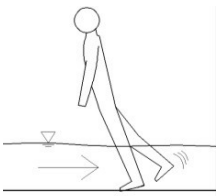

$$F_f - F_r \tag{2.36}$$

where:

F_f is the drag force of the flow and it's the function of the velocity, depth, the shape of the submerge body and the drag coefficient.

F_r is the friction resistance function of the body weight and friction coefficient.

$$C_d \cdot \frac{\rho}{2} \cdot u^2 \cdot B \cdot d - \mu \cdot m \cdot g \tag{2.37}$$

From this equation the critical combination $u-d$ for the friction instability can be found.

$$u^2 \cdot d = \frac{2 \cdot \mu \cdot m \cdot g}{C_d \cdot \rho \cdot B} \tag{2.38}$$

- **Momentum stability**

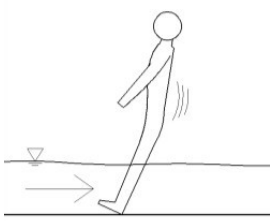

$$M_r - M_f \tag{2.39}$$

The moments generated by the flows (M_f) can be calculated as the drag force applied at the half of the depth. One the other hand the restoring moment (M_r) is function of the person weight and the distance to the pivot point (d_1).

$$m \cdot g \cdot d_1 - f_f \cdot \frac{d}{2} = 0 \tag{2.40}$$

Replacing the value of the drag force the critical combination $u - d$ for the moment stability can be found:

$$m \cdot g \cdot d_1 - C_d \cdot \frac{\rho}{2} \cdot u^2 \cdot B \cdot d \cdot \frac{d}{2} = 0 \tag{2.41}$$

$$u \cdot d = 2 \cdot \sqrt{\frac{m \cdot g \cdot d_p}{C_d \cdot \rho \cdot B}} \tag{2.42}$$

whit:

$$F_f = C_d \cdot \frac{\rho}{2} \cdot u^2 \cdot B \tag{2.43}$$

C_d=drag coefficient [-], calculated according to Endoh and Takahashi (1994):

$$C_d = 1.1\left(1 - \frac{L_f}{h_p}\right) \; with \; \theta = 0° \tag{2.44}$$

$$C_d = 1.1\left(1 + \frac{L_f}{h_p}\right) \; with \; \theta = 45°, 90° \tag{2.45}$$

where:

u=average flow velocity [m/s]

d=average flow depth [m]

ρ=density of water [kg/m^3]

μ=coefficient of friction between shoe sole and ground [-]

L_f=width between the feet [m]

θ=angle of the person against the current [°]

h_p=person height [m]

B=average diameter of the subject legs [m]

$A = Bd$=the projected area of the submerged part of the body normal to the flow [m^2]

d_1= distance form pivot point to the centre gravity [m]

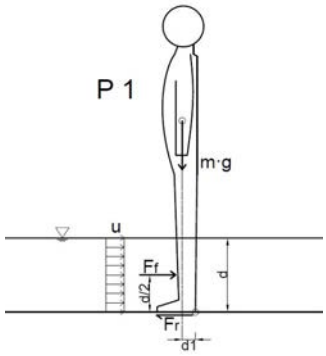

Figure 2.17: Human model standing in front of the flow.

To extrapolate the risk curves using this methodology, Sandoval, on first, identified an initial position (see Fig. 2.17), this represents a very conservative assumption because it represents a person surprised by the flow and has not adjusted position to resist to flow. It is also important define height and weight of the person. Firstly, it can be seen that the two mechanisms occupies different

zones where they are the dominant cause of instability. The friction instability verified in shallow and fast waters and, instead, the moment instability is dominant in deeper and slower waters. This is explained because the moment instability mechanism is the one responsible for knocking down a person, indeed, a considerable depth is needed to generate a large enough moment to defeat the restoring moment due to the person's weight.

By the equations found above is possible to find the condition of u and d where the transition occurs.

$$d_{\text{tr}} = \frac{2 \cdot d_p}{\mu} \tag{2.46}$$

$$u_{\text{tr}} = \mu \sqrt{\frac{m \cdot g}{c_d \cdot \rho \; B \cdot d_p}} \tag{2.47}$$

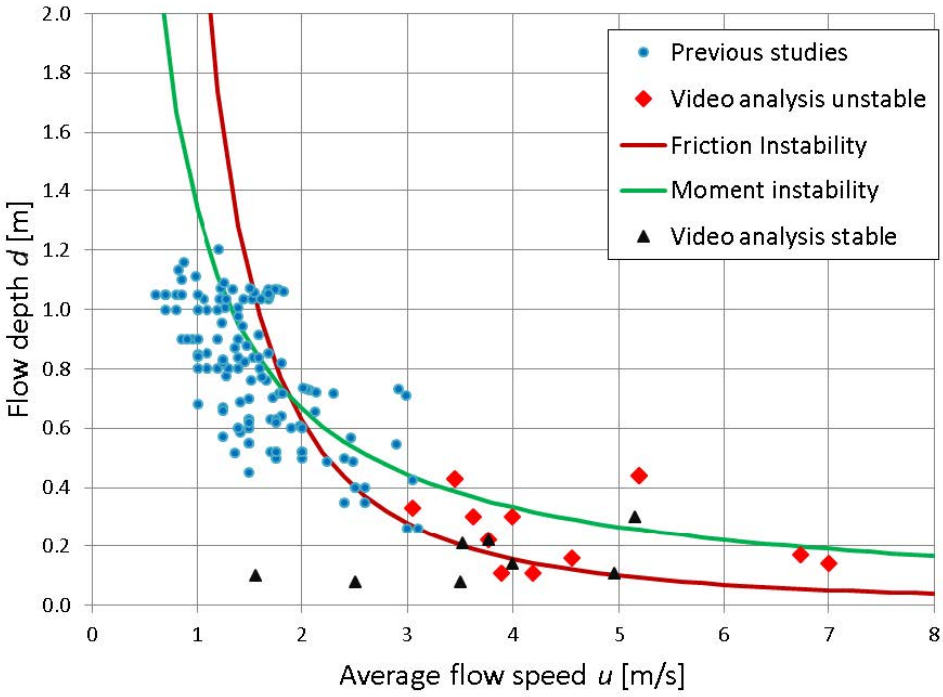

Figure 2.18: Comparison of instability prediction and data from video analysis of actual event and the results of studies from literature by Sandoval (2015) [10].

Good agreement is observed considering the shape of the instability curve and the distribution of the critical points, but only the 34% of the points are located

in the hazard zone. Moreover, it can be seen that in the lower part of the graph (friction instability) the prediction work better, instead, in deeper water the models don't work very well. In general the points calculated in the video analysis are located more or less in the zone of the graph where they supposed to be. In the upper part of the graph the prediction lines lie significantly above the trend of the data. The buoyancy not being considered as could explain this one of the forces acting on the person in the derivations of the models. This produces an unrealistic prediction in situations where the depth is similar to or greater than the subject's height. In such a case, it would be expected that the resistance to being swept away by the flow will reduce to zero, since the available ground-to-footwear friction will disappear. This omission could produce and overestimation of the stability under considerable deep flows.
The buoyancy force is simply weight of the water displaced by the submerged body. This add another variable in this study, because it depends upon the shape of the human body, changing from person to person, and the clothing could also affect considerable. Assumptions must therefore be made in order to solve the problem. Using a body model (Fig. 2.19), Sandoval calculated the buoyancy as a function of the depth of the flow.

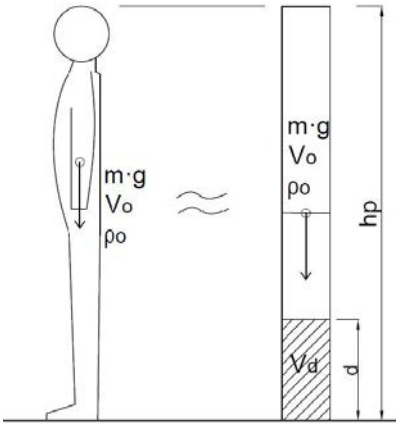

Figure 2.19: Model of the distribution of a person's volume with height

$$V_d(d) = \frac{V_0}{h_p} d \tag{2.48}$$

$$V_d(d) = \frac{m}{\rho_0 \cdot h_p} d \tag{2.49}$$

We can calculated $F_b(d)$ as follow:

$$F_b(d) = \begin{cases} \frac{m}{\rho_0 \cdot h_p} \cdot d \cdot \rho \cdot g & for\ 0 \leq d \leq h_p \\ V_0 \cdot \rho \cdot g = \frac{m}{\rho_0} \cdot \rho \cdot g & for\ h_p \leq d \end{cases} \tag{2.50}$$

with:

- $F_b(d)$=buoyancy force [N]
- $V_d(d)$=submerged volume of the body [m^3]
- d=water depth [m]
- ρ=water density [1000 kg/m^3]
- g=gravitational acceleration [m/s^2]
- m=subject's mass [kg]
- ρ_0=density of the human body [≈1,062 kg/m^3]
- h_p=subject's height [m]
- V_0=total volume of the subject [m]

Using these new expressions, it is possible to modify the relations of Endoh and Takahashi (1994), as follows:

- **Friction stability for $0 \leq d \leq h_p$**

$$F_f - F_r = 0 \tag{2.51}$$

Now the friction resistance is reduced by the buoyancy force:

$$C_d \frac{\rho}{2} u^2 b d - \mu \cdot \Big(mg - V_d \rho g \Big) = 0 \tag{2.52}$$

We can be estimated V_d and so the relationship becomes:

$$C_d \frac{\rho}{2} u^2 b d - \mu \cdot \left(mg - \frac{md}{\rho_0 h_p} \rho g \right) = 0 \tag{2.53}$$

and so the relationship between velocity and depth is:

$$u = \sqrt{C_F m} \cdot \sqrt{\frac{1}{d}} \cdot \sqrt{\left(1 - \frac{d\rho}{\rho_0 h_p} \right)} \ with\ C_F = \frac{2g\mu}{\rho C_d B} \tag{2.54}$$

- **Momentum stability for $0 \leq d \leq h_p$**

$$F_r \cdot d_1 - F_f \cdot \frac{d}{2} = 0 \tag{2.55}$$

as the friction resistance, here the restoring momento is reduced by the buoyancy force

$$(m \cdot g - V_d \cdot \rho \cdot g) \cdot d_1 - C_d \cdot \frac{\rho}{2} u^2 \cdot B \cdot d \cdot \frac{d}{2} = 0 \tag{2.56}$$

and so the relationship between velocity and depth is:

$$u = \frac{2}{d} \cdot \sqrt{\frac{m \cdot g \cdot d_1}{C_d \cdot \rho \cdot B} \cdot \left(1 - \frac{d \cdot \rho}{\rho_0 h_p}\right)} \tag{2.57}$$

$$u = \frac{C_M}{d} \cdot \sqrt{m} \cdot \sqrt{\left(1 - \frac{d \cdot \rho}{\rho_0 h_p}\right)} \qquad where\ C_M = 2 \cdot \sqrt{\frac{g \cdot g_1}{C_d \cdot \rho \cdot B}} \tag{2.58}$$

The new equations modified the graphics (Fig. 2.20):

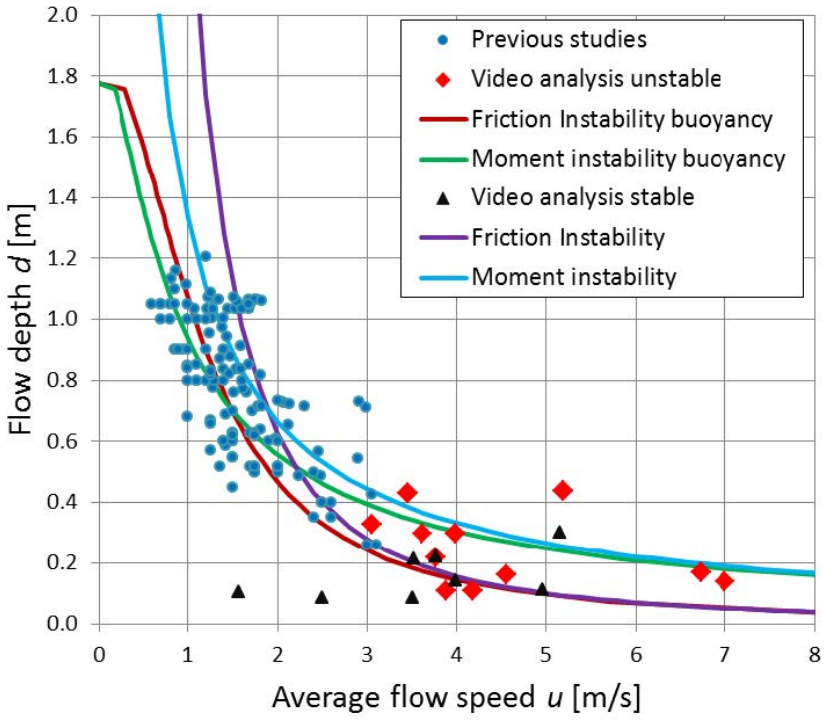

Figure 2.20: Comparison of instability prediction regardless buoyancy and considering buoyancy and data from video analysis of actual event and the results of studies from literature by Sandoval [10].

It can be seen that the new prediction work better in the higher part of the graph, now the 70% of the points are well located in the hazardous zone of the graph, this give us the indication that the buoyancy force has a significant effect in the stability of the subjects under deeper waters. Also it is important that the good agreement in lower part of the graph is not lost due to the modification of the equations because in shallow waters, the buoyancy force does not play a significant role in comparison with the person's weight. It can also be noted that when the buoyancy force is taken in consideration, the difference between the moment model and the friction model is smaller when $u < u_{\text{tr}}$ compared with the past figure.

Sandoval, through the reports found, was able to examine people of different sex to better identify the risk zones and also examined a new position (Fig. 2.21). It is supposed that the person reacts to the flow by moving one leg back-thought to be an instinctive reaction of a person in this kind of situation. This response generates a larger distance between the pivot point and the centre of gravity, d_1, increasing the restoring moment available. In addition, the projected area exposed to the flow decreases, as only one leg is receiving the drag force directly.

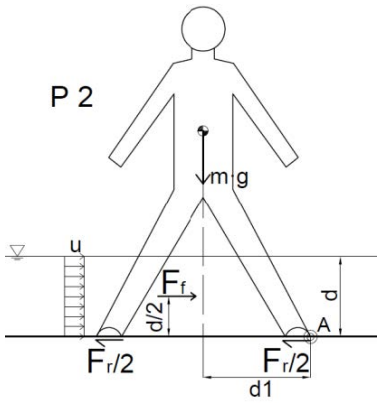

Figure 2.21: Second stability position

From Fig 2.22 it can be seen that the change of position from P1 to P2 increase considerably the moment resistance, due to the increase of d_1, but it does not have a significant effect on the friction stability model since even though the area against the flow get reduced, the factor C_d increases its value.

From this, it follows that the change of position will be more effective in case of deeper-slow flows than in shallow-faster waters.

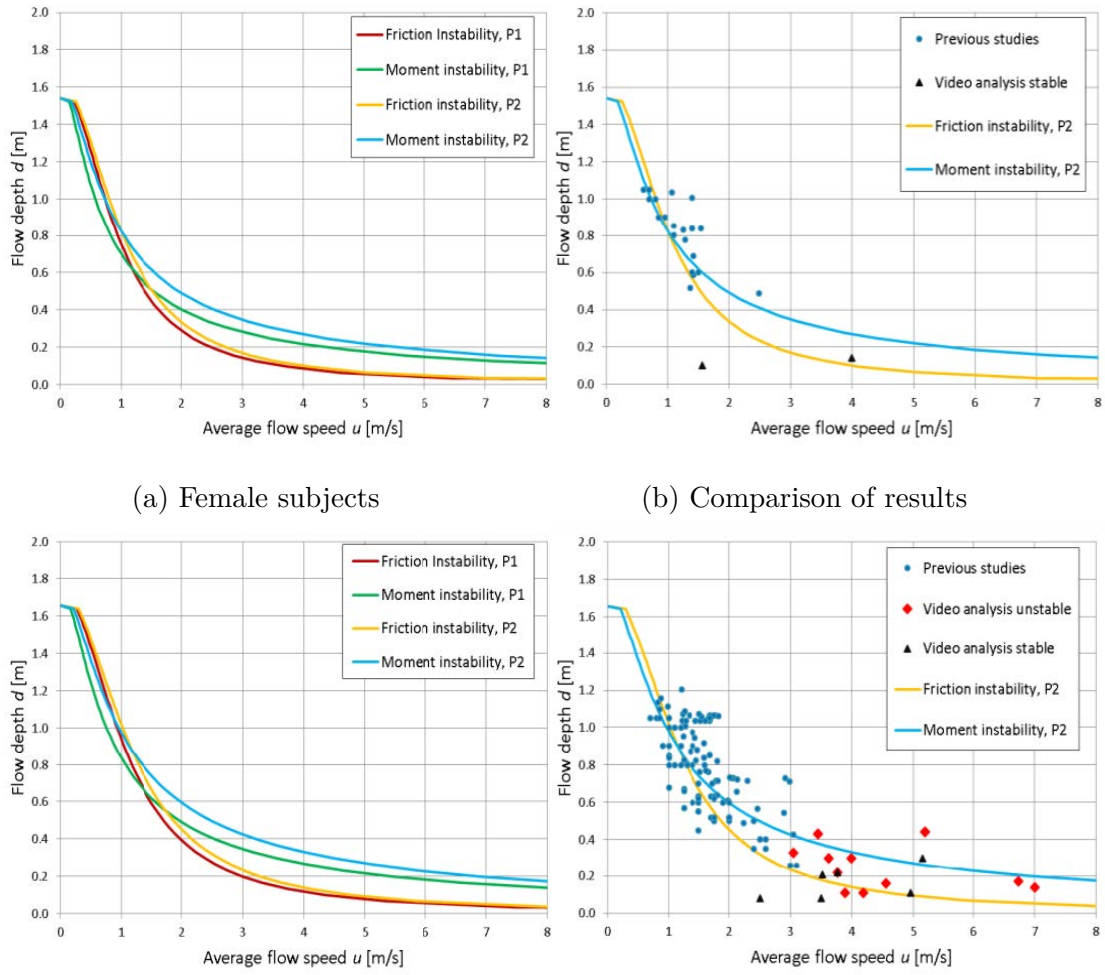

(a) Female subjects

(b) Comparison of results

(c) Male subjects

(d) Comparison of results

Figure 2.22: Comparison of instability prediction between "Position 1" and "Position 2" by Sandoval (2015) [10].

The last study analyzed within this thesis research is that of **Arrighi et al** (2015, 2017, 2019) [21] [23] [22] who, for the first time, compared the experimental data with the numerical model for the human and vehicles. They, from the data, identified relative submergence and the Froud number, as the most relevant parameters to estimate the vulnerability of pedestrians and parked vehicles for calculated the critical thresholds.

- **Vehicles vulnerability**

  The car is considered a rigid body and the forces acting on this are weight (W), buoyancy (B), drag, lift effect (L_i) and friction (friction coefficient μ is considered constant and equal to 0.2-0.5 because depends of vehicle type). Equilibrium to translation on a flat bed happens when friction forces is balanced by drag forces D acting on the car:

$$D = (W - B - L_i) \cdot \mu \tag{2.59}$$

$$D = 0.5\rho \cdot C_d \cdot (H_v - h_c) \cdot l \cdot U^2$$

$$W = \rho_c \cdot g \cdot (H_v - h_c) \cdot l \cdot L$$

$$B = \rho \cdot g \cdot (H_v - h_c) \cdot l \cdot L$$

$$L_i = 0.5g \cdot \rho \cdot C_l \cdot (H_v - h_c) \cdot l \cdot U^2$$

  where:

  - ρ_c is the car average density;
  - ρ is the water density;
  - H_v is the height of vehicle;
  - h_c is the distance of the chassis from the ground;
  - l and L are the the frontal width and the lenght of the vehicle;
  - H is the water depth;
  - U is the flow velocity;
  - C_d is the drag coefficient;
  - C_l is the lift coefficient

  Through these formulations it was possible to write:

$$\left(\frac{C_d}{\mu} + C_l\right) \cdot \frac{U^2}{g(H - h_c)} = 2L \cdot \frac{\rho_c(H_v - h_c) - \rho(H - h_c)}{\rho(H - h_c)(H_v - h_c)} \tag{2.60}$$

  the dimensional term is:

$$C \cdot Fr_v^2 = \theta_v \tag{2.61}$$

in which

$$Fr_v^2 = \frac{U^2}{g \cdot (H - h_c)} \tag{2.62}$$

and θ_v is defined as the mobility parameter of the vehicle.

The regression curve value-added by Arrighi et al can be written as:

$$\frac{H_{crV}}{H_V} = 0 - 0.05Fr + 0.34 \tag{2.63}$$

when $(H/H_{crV}) < H_V$ it has a safe condition otherwise unsafe condition

- **Human vulnerability**

  As for the vehicle also for the human can be possible individuated the equilibrium between the friction forces and drag forces:

$$D > (W - B - L_i) \cdot \mu \tag{2.64}$$

$$D = 0.5\rho \cdot C_d \cdot H_P \cdot l \cdot U^2$$

$$W = \rho_P \cdot g \cdot (d \cdot H_P \cdot l)$$

$$B = \rho \cdot g \cdot (d \cdot H \cdot l)$$

$$L_i = 0.5\rho \cdot C_l \cdot H_P \cdot l \cdot U^2$$

Through these formulations it was possible to write:

$$0.5U^2 \cdot C_D \cdot H_P + (0.55U^2 \cdot C_l \cdot H_P) \cdot \mu = [(g \cdot H_P \cdot d) - (g \cdot H \cdot d)] \cdot \mu \tag{2.65}$$

simplifying again you get:

$$\frac{U^2}{gH} \cdot \left(+ C_l \frac{C_D}{\mu} \right) = \frac{2d \cdot (H_P - H)}{H_P \cdot H} \tag{2.66}$$

in which

$$Fr_p^2 = \frac{U^2}{g \cdot H} \tag{2.67}$$

and the second term of the Eq 2.66, θ_P, is defined as the mobility parameter fro sliding instability of the people standing in floodwaters.

The regression curve from experimental human stability data can be written as:

$$\frac{H_{crP}}{H_P} = \frac{0.29}{0.24 + Fr} \tag{2.68}$$

when $(H/H_{crP}) < H_P$ it has a safe condition otherwise unsafe condition.

The Arrighi et al. (2019) results are summarized in this graphics:

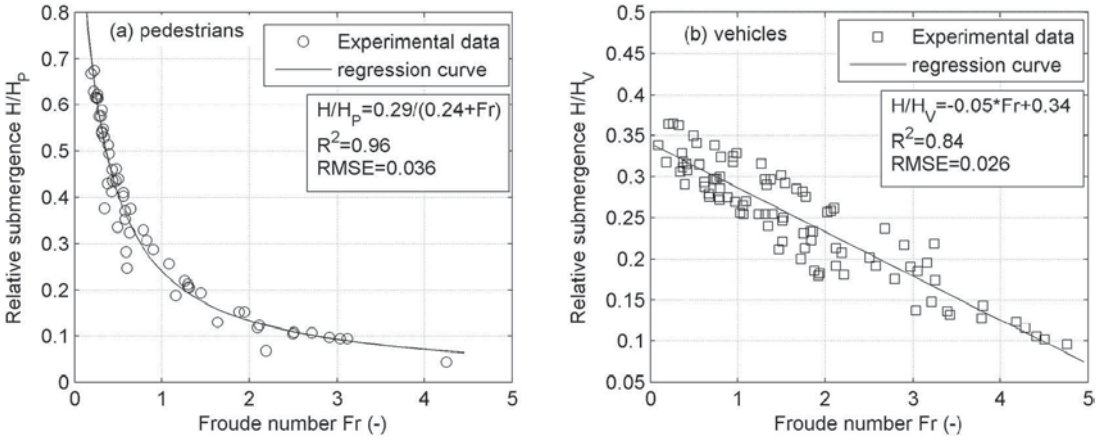

Figure 2.23: Regression curves used to assess the vulnerability of pedestrians (a) and parked vehicles (b) based on the experimental data [22]

CHAPTER 3

Case study

The geometrical layout used for the experimental campaign resembles the beach and coastal protection in the area of Premià de Mar, municipality in the Comarca of the Maresme in Catalonia, Spain.

Figure 3.1: Top view by Google Maps.

In particular, the area nearby the railway station has been studied. This stretch of the coast, in fact, present both railways and a bike path a few

very exposed to possible sea storms, being located at a few meters from the shore. See figure 3.2. Besides issues related to people safety, the vicinity of the railway to the sea has already caused in the past several problems and service interruption of the public transport for a line that is strategic for the zone, connecting it directly to the metropolitan area of Barcelona (e.g. https://www.elperiodico.com/es/sociedad/20190425/linea-r-1-rodalies-maresme-acumula-semana-retrasos-oleaje-7424487). Close to the railway station, the dike slope has been estimated equal to 1:1. In the physical model tests, the effect of the rubble mound has been neglected, considering a smooth slope, in stead. Due to lack of bathymetric data in the area, two different foreshore slope were considered, namely 1:15 (steep) and 1:30 (gentle). Different widths for the promenade between the dike edge and the station were considered to be representative of the different stretches along the coastline.

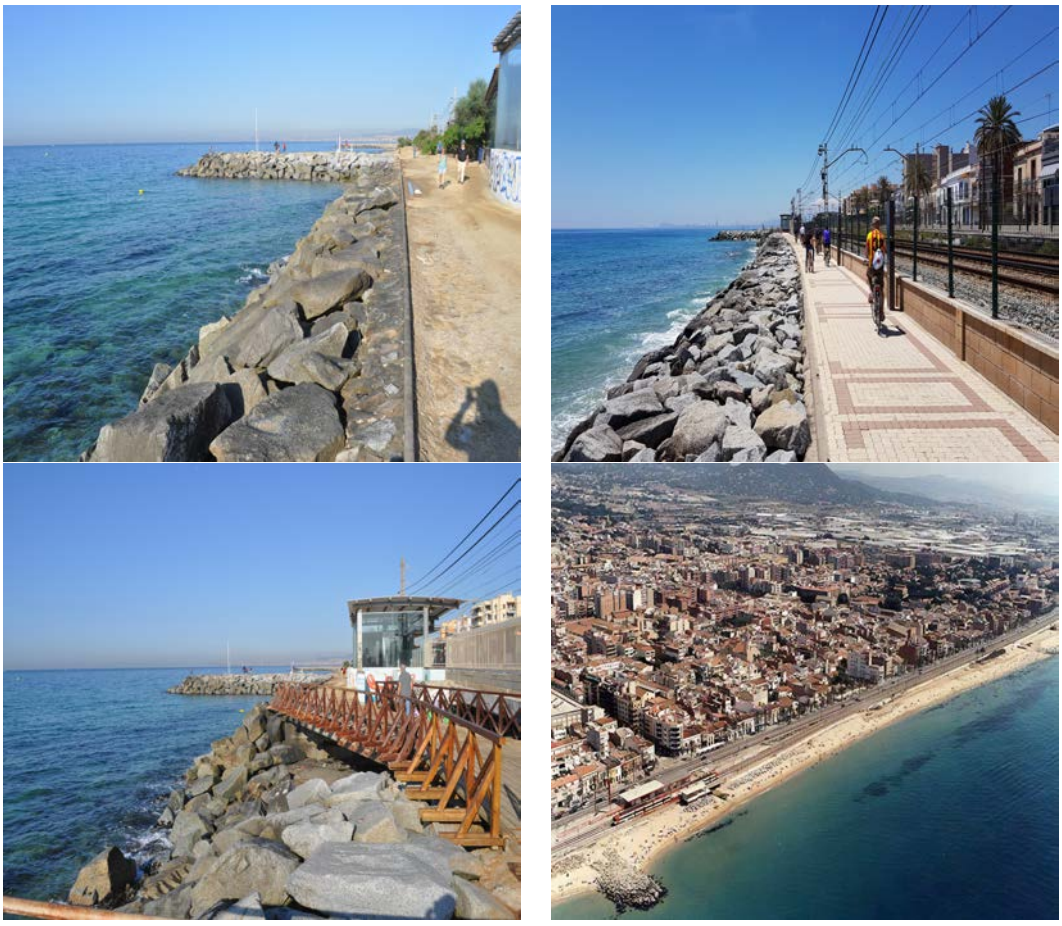

Figure 3.2: Case study framework.

CHAPTER 4

Experimental setup

In this chapter will be show how experiments were carried out. It will be described the whole procedure to execute a sensitivity analysis on the collected data.

4.1 CIEMito

Physical model experiments are carried out in the small scale "CIEMito" (Fig 4.1) wave flume at Laboratori d'Enginyeria Marìtima (LIM) from Universitat Politècnica de Catalunya-BarcelonaTech (UPC) in Barcelona.

Figure 4.1: "Views of the small scale wave flume at LIM/UPC"

CIEMito has a total length of 18m, with a useful section of 0.38m wide and 0.56m high and a maximum water depth of 0.36m. The supporting structure consists of square section metal profiles while the side and back walls are made of 5+5mm thick tempered glass. The wave generation is carried out using a piston wave-maker, whose motion is provided by a linear actuator with 1m maximum stroke and speed of response 1.6m/s. Water depths of 0.29 - 0.30 - 0.305 - 0.31m are tested, corresponding to 14.5m, 15m, 15.25m, 15.5m in prototype, assuming a model scale of 1:50. Two dikes were installed: the first with 1:15 foreshore slope and the second with 1:30 foreshore slope that corresponding at the real slope of the case study (Fig 4.2). The freeboards R_c, promenade width and toe depth h_{toe} varies between the valued summarized in this table:

	h_{toe}[m]	R_c [m]	Promenade [m]
Prot.	0.009-0.019-0.024-0.029	0.81-0.071-0.066-0.066	0.12-0.24
Model	0.45-0.905-1.2-1.45	4.05-3.55-3.3-3.05	6-12

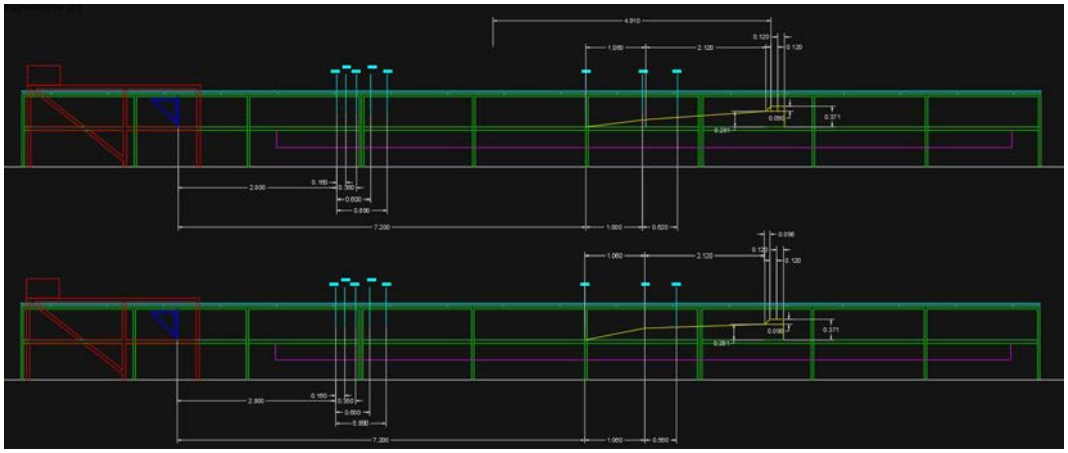

Figure 4.2: a) Case - slope 1:15; b) Case - slope 1:30

4.1.1 Measurement setup

Overtopping flow measurement system consists in:

- overtopping tank with two loads cells to measure the weight of the overtopping water later converted into volume;

- two high - speed cameras to measure overtopping flows and velocities;
- two ultrasonic sensors (AWG) on the dike top to measure flow depths and velocities [Appendix1];
- besides, eight resistive sensors have been placed along the flume to measure water surface elevation at different locations. The sensor consists in two stainless steel wires, the current that flows between the wires is converted in voltage that is directly proportional to the immersed depth.

(a) Loads cells

(b) Speed lateral camera

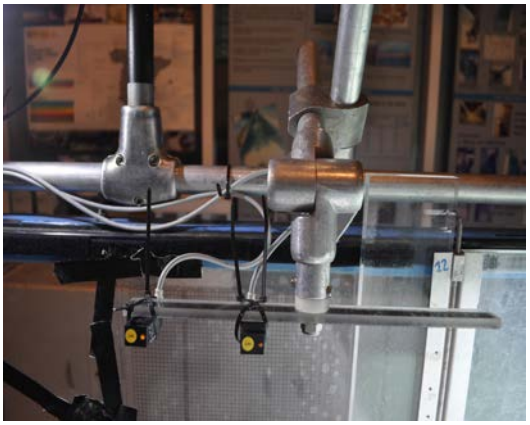

(c) Ultrasonic sensors

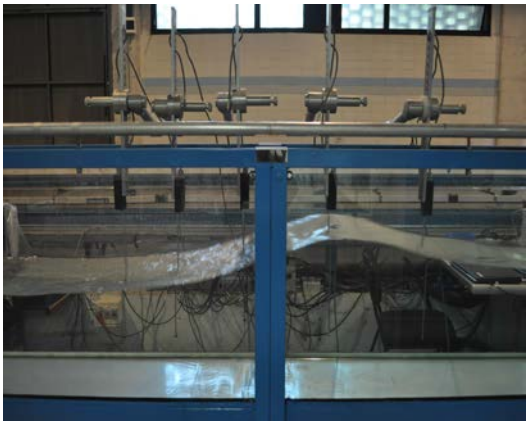

(d) Five resistive sensors

Figure 4.3: Measurement devices

4.1.2 Control system

The functioning of the CIEMito is based on the use of different software that are used both to generate the desired conditions and to convert the data obtained from the tools mentioned above. The system control consisted of:

- "CiemGen v.1.2" software developed by LIM/UPC allows the generation of regular and irregular waves and time series reproduction (Fig 4.4);
- "WaveLab 3.676" software developed by University of Aalborg allows calibration of eight resistive sensors and records data sensors during the test (Fig 4.5);

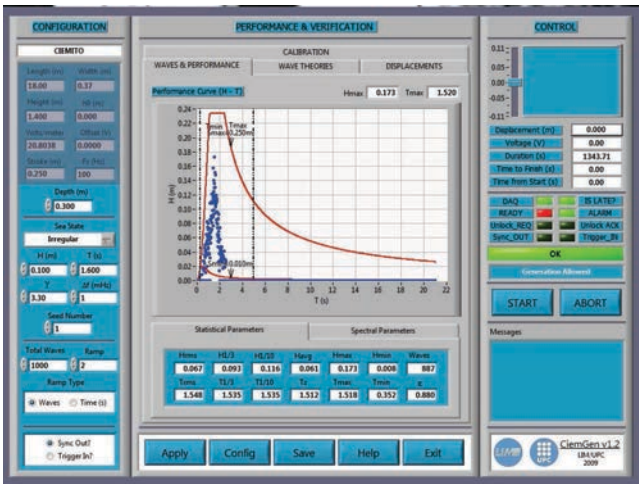

Figure 4.4: Window of "CiemGen v.1.2"

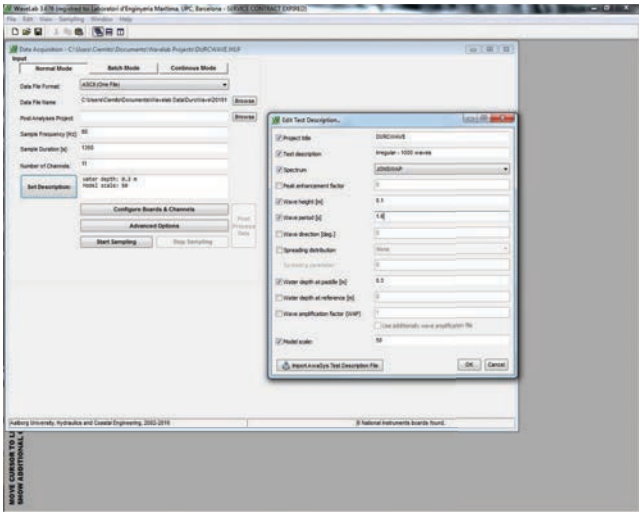

Figure 4.5: Window of "WaveLab 3.676"

- "CiemConv v1.2" software developed by LIM/UPC allows the conversion of WAVELAB data (Fig 4.6);

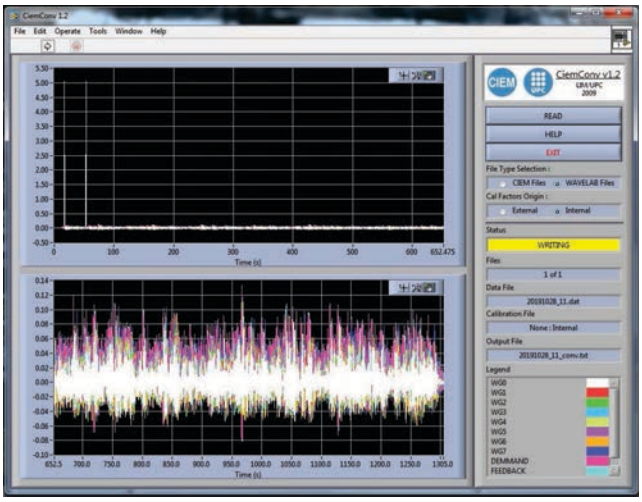

Figure 4.6: Window of "CiemConv v1.2"

- "CatManEasy V3.4.2" software developed by "HBM Italia s.r.l." allows calibration of two ultrasonic sensors and two load cells and records their data during the test (Fig 4.7);

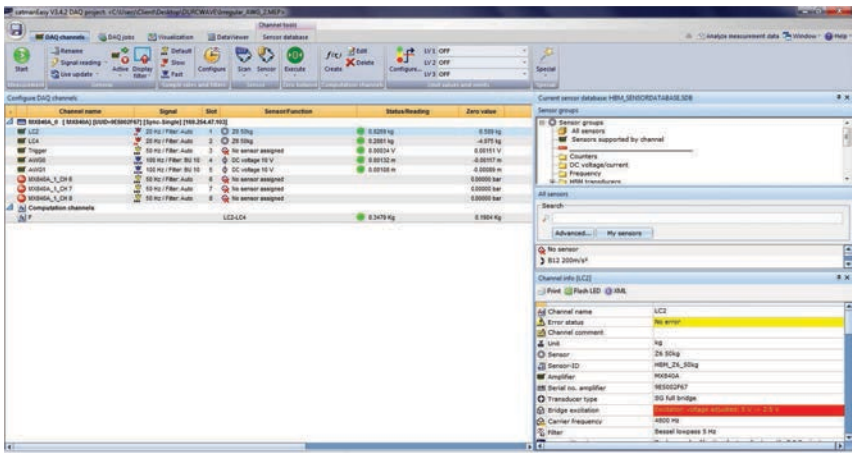

Figure 4.7: Window of "CatManEasy V3.4.2"

- "StreamPix 7x64 Edition SingleCamera or DubleCStreamPix 7.5.0.0" software developed by "NorPix, Inc." that allows to capture videos and images from the cameras (Fig 4.8).

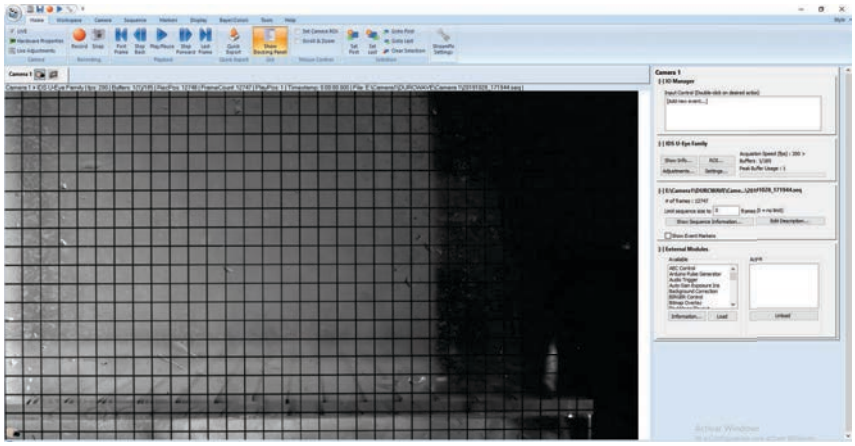

Figure 4.8: Window of "StreamPix 7.5.0.0"

In this table it's shown the distances between the instrument and the structures from the wave maker.

Sensors/layout	Dist. from the WM(1:15)	Dist. from the WM(1:30)
WG 0	2.80 m	2.80 m
WG 1	2.96 m	2.96 m
WG 2	3.15 m	3.15 m
WG 3	3.40 m	3.40 m
WG 4	3.69 m	3.69 m
WG 6	7.20 m	7.20 m
WG 7	8.20 m	8.26 m
WG 5	9.20 m	9.20 m
Dike toe	10.38 m	10.38 m
Dike crest	10.47 m	10.47 m
Start foreshore	7.20 m	7.20 m
Start transition slope	8.26 m	8.26 m
CAMERAS/AWG	≅10.60 m	≅10.60 m

4.2 Test procedure

The test in general is carried out in three distinct phases:

1. first phase, called calibration, in which all the instruments are tested to verify their proper functioning;
2. a second phase, is the test itself, in which the selected conditions are generated and the test is carried out;
3. a last phase in which the test is completed and the data from the various programs used are collected.

4.2.1 Calibration phase

- **AWG Calibration:**

  The AWG calibration is conducted with the software "CatManEasy V3.4.2" and a parallelepiped-shaped specimen (0.075m x 0.075m x 0.027m). The specimen is placed below the sensor and it is verified, through the use of two points, that the machine is working in the correct way (Fig 4.9).

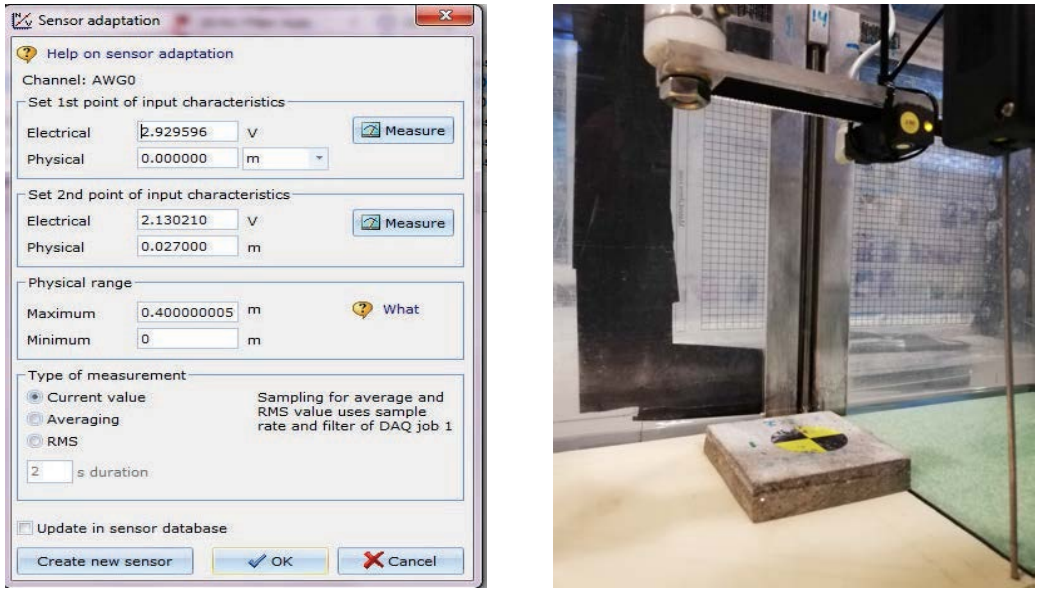

(a) Window of CatMan's Calibration (b) Measurement with spacemen

Figure 4.9: AWG calibration

- **Resistive sensors calibration:**

  The resistive sensors calibration is conducted with the software "WaveLab 3.676". The sensors are moved manually to two different points chosen before calibration (-0.04m and 0.00m), if they work correctly the software extracts a straight line that joins the selected points (fig 4.10).

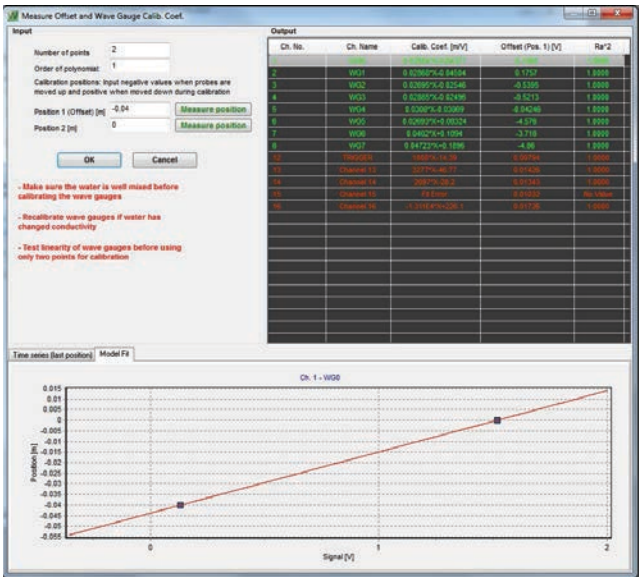

Figure 4.10: Window of "WaveLab 3.676"

- **Load cells calibration:**

  The Load cells calibration is conducted with the software "CatManEasy V3.4.2" and Excel and with the use of beakers. In order to evaluate its good functioning, variable quantities of water are introduced into the cells and through the "CatManEasy V3.4.2" software it is verified that the machines calculate the right force (Fig 4.11); subsequently all the various successions of water injections are plotted in Excel in a graph verifying that the empirical values and those of the machine coincide and that, therefore, it returns in output a regression line with a coefficient of determination of approximately equal to one (Fig 4.12).

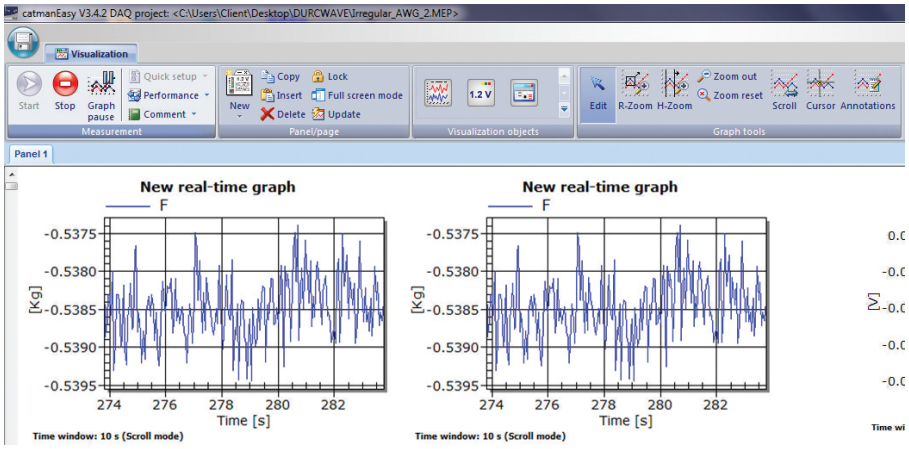

Figure 4.11: Calibration with "CatManEasy V3.4.2"

ENSAYO 1			
Y (agua)			X (fuerza)
0.054	0.054	0.055	0.055
0.078	0.132	0.123	0.068
0.014	0.146	0.13	0.007
0.022	0.168	0.145	0.015
0.014	0.182	0.1545	0.0095
0.034	0.216	0.183	0.0285
0.06	0.276	0.237	0.054
0.069	0.345	0.298	0.061
0.096	0.441	0.385	0.087
0.11	0.551	0.478	0.093
0.122	0.673	0.589	0.111
0.138	0.811	0.715	0.126
0.218	1.029	0.918	0.203
0.25	1.279	1.165	0.247
0.33	1.609	1.466	0.301
0.69	2.299	2.13	0.664

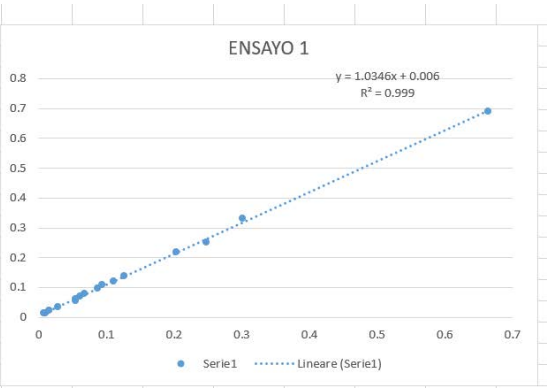

Figure 4.12: Output in "Excel"

4.2.2 During the test

Once the various instruments have been calibrated, the test can begin. First of all, the working conditions are set using the "CiemGen v.1.2" software (Fig 4.13), in that it's possible to set water depth, wave height H_{m0}, the peak period T_p, the value of spectra enhancement factor γ which is fixed and equal to 3.30 for a standard JONSWAP spectrum. Employing same wave conditions (H_{m0}, T_p), different time series can be generated varying a seed number, hence the phase assigned to each spectra wave component. More than four hundred tests were conducted during the thesis period, in which different conditions were considered depending on the slope of the beach, the promenade used and the desired return time.

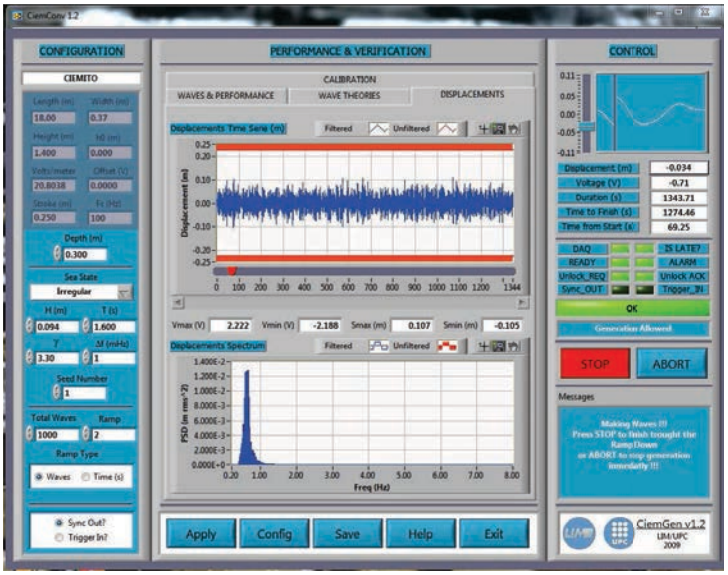

Figure 4.13: Windows of "CiemGen v.1.2"

In the following tables it is possible to see all the combinations studied, the scale used was 1:50:

Model scale:

Slope	T_R [y]	H_{m0} [m]	T_p [s]	SEED	Depth [m]	Prom. [m]
1:15	1	0.085	1.69	1;5	0.29-0.30-0.31	0.12-0.24
1:15	2	0.0882	1.74	1;5	0.29-0.30-0.31	0.12-0.24
1:15	5	0.10	1.79	1;5	0.29-0.30-0.31	0.12-0.24
1:15	>10	0.11	1.4	1;5	0.29-0.30-0.31	0.12-0.24
1:15	>10	0.10	1.4-1.5-1.6	1;5	0.29-0.30-0.31	0.12-0.24
1:15	>10	0.09	1.4-1.5-1.6-1.7	1;5	0.29-0.30-0.31	0.12-0.24

Slope	T_R [y]	H_{m0} [m]	T_p [s]	SEED	Depth [m]	Prom. [m]
1:30	1	0.085	1.69	1;5	0.305-0.31	0.12-0.24
1:30	2	0.0882	1.74	1;5	0.305-0.31	0.12-0.24
1:30	5	0.10	1.79	1;5	0.30-0.305-0.31	0.12-0.24
1:30	>10	0.11	1.4	1;5	0.305-0.31	0.12-0.24
1:30	>10	0.10	1.5-1.6	1;5	0.30-0.305-0.31	0.12-0.24
1:30	>10	0.09	1.4-1.5-1.6-1.7	1;5	0.305-0.31	0.12-0.24

Prototype scale:

Slope	T_R [y]	H_{m0} [m]	T_p [s]	SEED	Depth [m]	Prom. [m]
1:15	1	3.60	11.96	1;5	14.5-15-15.5	6-12
1:15	2	4.01	12.28	1;5	14.5-15-15.5	6-12
1:15	5	4.59	12.67	1;5	14.5-15-15.5	6-12
1:15	>10	5.55	9.9	1;5	14.5-15-15.5	6-12
1:15	>10	4.59	10.6-11.3	1;5	14.5-15-15.5	6-12
1:15	>10	4.50	9.9-10.6-11.3-12	1;5	14.5-15-15.5	6-12

Slope	T_R [y]	H_{m0} [m]	T_p [s]	SEED	Depth [m]	Prom. [m]
1:30	1	3.60	11.96	1;5	15.25-15.5	6-12
1:30	2	4.01	12.28	1;5	15.25-15.5	6-12
1:30	5	4.59	12.67	1;5	15-15.25-15.5	6-12
1:30	>10	5.55	9.9	1;5	15.25-15.5	6-12
1:30	>10	4.59	9.9-10.6-11.3	1;5	15-15.25-15.5	6-12
1:30	>10	4.50	9.9-10.6-11.3-12	1;5	15.25-15.5	6-12

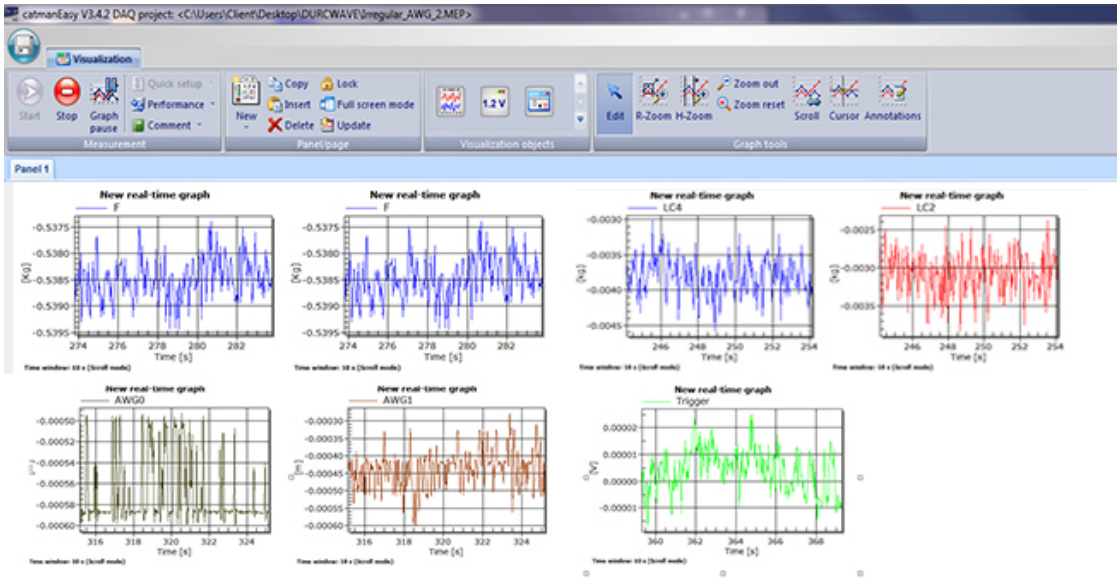

Figure 4.14: Data Acquisition with "CatManEasy V3.4.2"

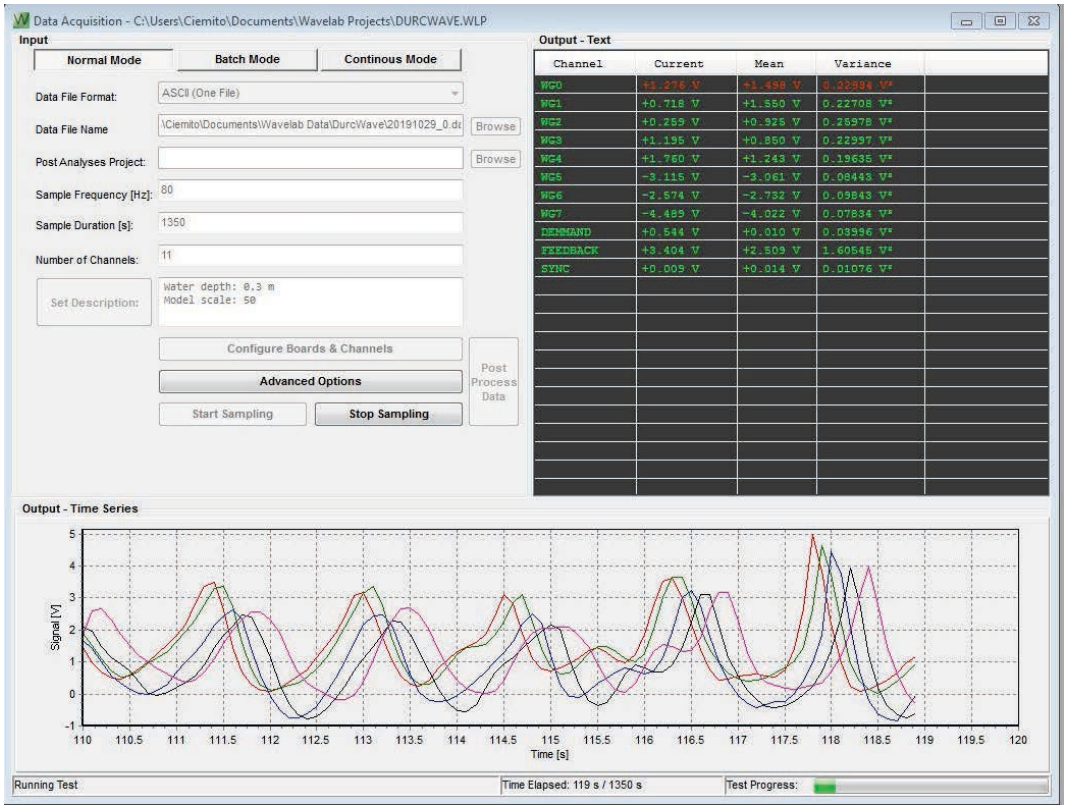

Figure 4.15: Data Acquisition with "WaveLab 3.676"

Once the working condition has been set, the test is ready to be started, usually it lasts between 20 and 25 minutes for 1000 waves. The acquisition of data from the sensors and the loads cells takes place through the two programs, namely "WaveLab 3.676" and "CatManEasy V3.4.2" (Fig 4.14 - 4.15). The tests with the same conditions were repeated twice: once without cameras, to obtain the values of the time and volume of the maximum event (after a post-processing with Matlab R2018a), and the second time using also the cameras for the next comparison.

4.2.3 Data collection

Once the test has been completed, the data are collected. In the following summary table it is possible to see all data collection:

OUTPUT	INSTRUMENTS	FILE FORMAT	EXTENSION
η	WG	text	.txt
u	AWG, cameras	text, image	.vol, .tif
λ	AWG, cameras	text, image	.vol, .tif
q, V	LC	text	.vol

Data from "CatManEasy V3.4.2" is saved within two text files that, subsequently the conversion file is plotted inside the calculation program "Matlab R2018a", in output we obtain the values of the discharge q in model and the total overflowing volume V_{tot}, the volumes in prototype, the total one $V_{max,prot}$, the $V_{1/3,prot}$ and the $V_{1/10,prot}$, which are the average of the third and tenth highest values in the series, the velocity (u_{AWG}) (Eq 4.1) and flow depth (λ_{AWG}) and the time of the peak overtopping event T_{max} (Fig 4.16).

$$u_{AWGt_{tip}};\ u_{AWGt_{maxVOL}} = AWG_{dist}/\Delta\ [m/s] \tag{4.1}$$

Where $\Delta = \Delta t_{tip}$ or Δt_{maxVOL} of AWG, respectively the temporal distance between the two maximum points and the distance at which it crosses a point set by the user in principle.

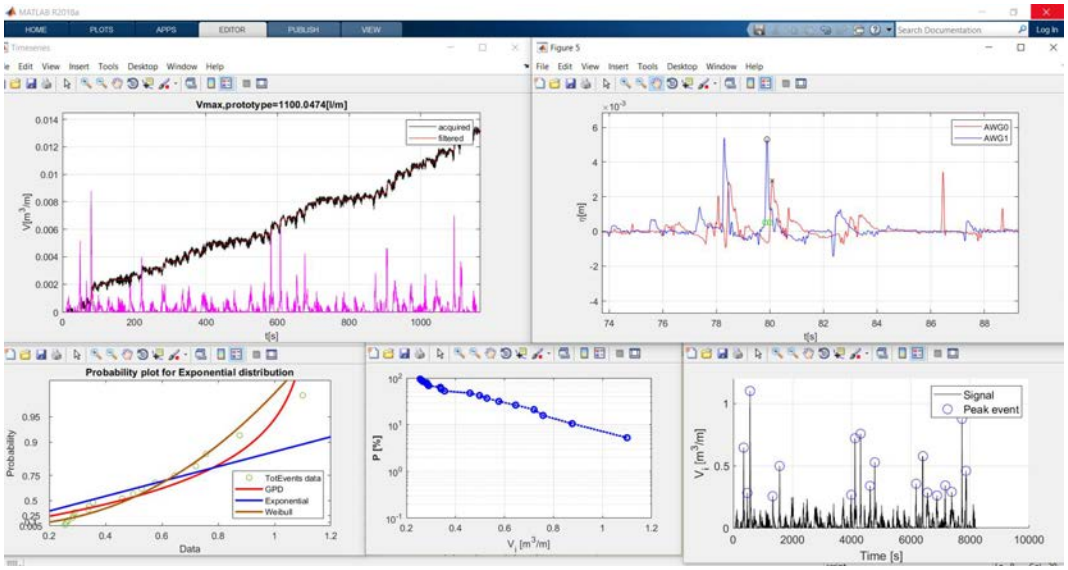

Figure 4.16: Example of output graphics and values by "Matlab R2018a"

As mentioned above, during the test, the maximum overtopping event is

resumed through the cameras, which work at 200 frames per second. From the acquired images we can obtain the velocity because we know the distance between the two sensors, the number of frames of the event, which will vary from case to case and the scale at which we are working. Knowing these data it's possible to use the conversion formula (Eq. 4.2):

$$u_{cam} = \frac{distance\ between\ AWG}{n_{frame}} \cdot 200 \cdot \sqrt{50} \tag{4.2}$$

The calculation of the velocity and the flow depth, through the cameras, is a manual procedure in which the images coming from the software are analysed.

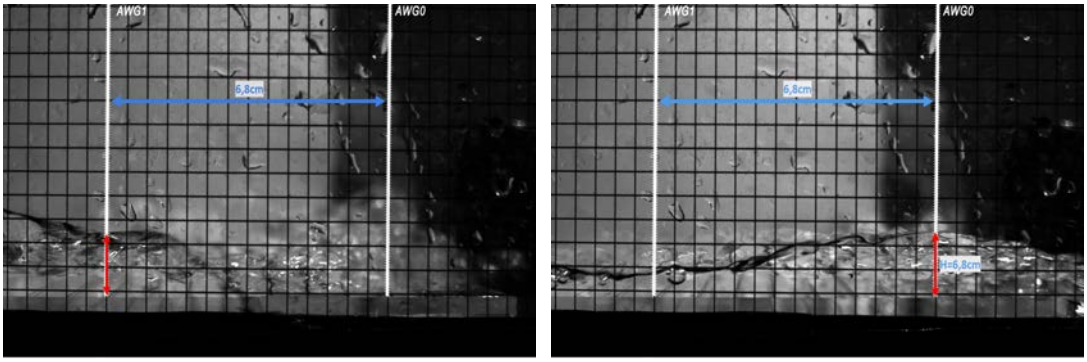

(a) First measuring point (b) Second measuring point

Figure 4.17: Example velocity measuring with lateral camera - n_{frame}=18

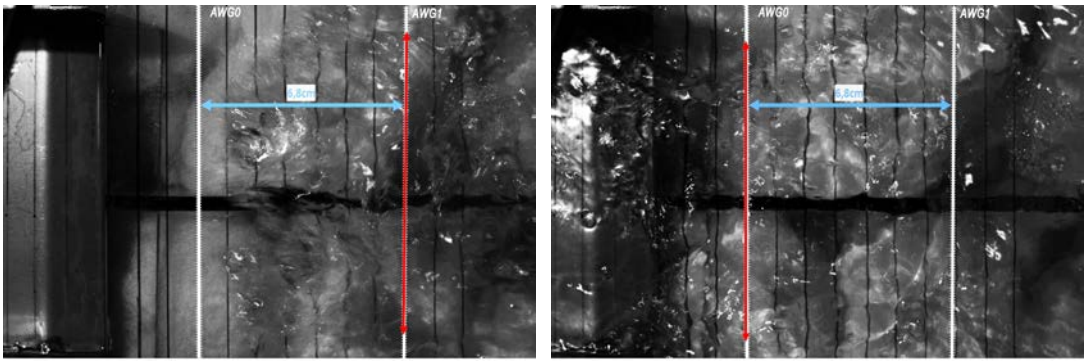

(a) First measuring point (b) Second measuring point

Figure 4.18: Example velocity measuring with upper camera - n_{frame}=16

As far as the velocity is concerned, it is first necessary to define the distance between the two AWGs then, subsequently, it is possible to identify the maximum height that one has for the two sensors to determine the exact number

of frames of the event (Fig 4.17 - 4.18). Guidelines were used to carry out the measurement: for the upper camera, lines of 1cm were marked on the promenade; while for the lateral camera a 0.5cm graph paper was applied. With the lateral camera it's possible calculated also the flow depth (λ_{cam}) using graph paper (Fig 4.17b). Once all the data has been collected, it is possible to implement an Excel database, which proved to be fundamental for the analysis of the results carried out later. The Excel file contains columns:

- the date of the text;
- the number of waves;
- the $H_{m0,o}$, T_p in model and prototype [m],[s];
- the water depth h in model and prototype [m];
- the promenade width in model and in prototype [m];
- values in model and prototype of h_{toe}=h-toe dike [m];
- values in model and prototype of R_c=dike height-h_{toe} [m];
- the values of q in model and prototype, $q_{prot} = q \cdot 50^{1.5}$ [l/s/m];
- the values of $V_{tot,mod}$ [m^3];
- the values of $V_{tot,prot}$, $V_{1/3,prot}$, $V_{1/10,prot}$ [l/m], which are the average of the third and tenth highest values in the series;
- the values of $T_{max,mod}$, fundamental for calculating the velocity and flow depth of the maximum overtopping event with the cameras [s];
- the distance between AWG [m];
- the λ_{cam} calculated with the lateral camera in prototype [m];
- the λ_{AWG} calculated with the AWG in prototype [m];
- the velocity calculated with the cameras (u_{cam}) using Equation 4.2 [m/s];

- Δt_{tip} and Δt_{maxVOL} of AWG, respectively the distance between the two maximum points and the distance at which it crosses a point set by the user in principle;
- the $u_{AWGt_{tip}} = AWG_{dist}/\Delta t_{tip} \cdot \sqrt{50}$ [m/s] in prototype;
- the $u_{AWGt_{maxVol}} = AWG_{dist}/\Delta t_{maxVOL} \cdot \sqrt{50}$ [m/s] in prototype;
- the average (u_{mean}) between velocities $u_{AWGt_{tip}}$, $u_{AWGt_{maxVol}}$ and u_{cam} [m/s];
- the average (λ_{mean}) between flow depths λ_{AWG} and λ_{cam} [m/s];
- any comments.

The complete data are contained in Appendix 2. The results obtained from all the tests are analyzed in the following chapter, in fact we will research the relationships between the various parameters that, subsequently, will be compared with the current literature and formulas of EurOtop (2018).

4.3 Incident wave conditions at the toe of the dike

The last tests were carried out removing the dike and placing in stead an horizontal bottom by absorption material (Fig 4.19). The scope was to calculate the incident wave conditions at the toe of the structure, minimizing the wave reflection. The values obtained from the resistive and acoustic sensors were compared.
The sensors WG6, WG8 and AWG were placed one at the beginning of the beach while the other at the toe of dike (=end of the foreshore) (Fig 4.20). It was possible to carry out this analysis for the 1:30 foreshore slope. The position of the WG7 sensor, on the other hand, has not been modified, since, starting from a visual analysis of the previous tests, it has been verified that in that area there is the breaking of the waves.

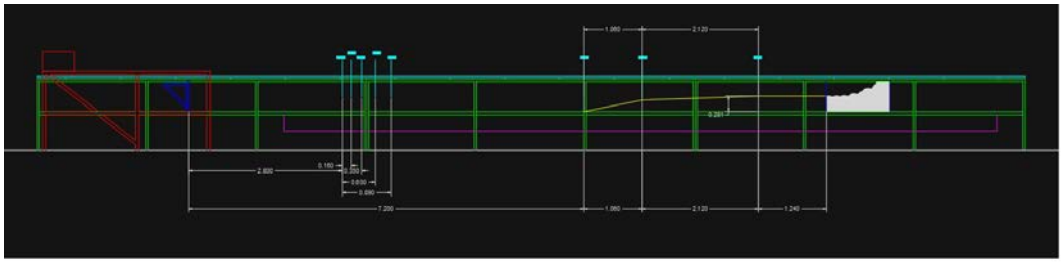

Figure 4.19: Case without dike

Figure 4.20: a)AWG1, WG6; b)AWG0, WG8; c)CIEMito without dike

The objectives of these new tests are two:

1. to obtain values at the toe of the structure that are also used in the current literature to be able to compare them;

2. spectrum filtering below a set value of $f < 1/T_{Re} = 0.05\ Hz$, where the resonance period has been calculated previously and equal to $T_{Re} = 15\ s$ (Fig 4.21). If we find oscillations of the period of the order of the characteristic period of resonance, $f, T_f \cong T_{Re}$, we can assume that such oscillation are due to the same resonance and therefore must be removed. Otherwise, let's consider a part of the energy that is created by model effects but that does not correspond to real cases, where the resonance is not present.

The results obtained from the tests have been of fundamental importance for the evaluation of scale effects, where viscosity and surface tension are evaluated.

Moreover, through this data it was possible to compare the results obtained experimentally with those obtained numerically through the "SWASH" program [25], fundamental for cases with 1:15 slope where this type of test was not carried out.

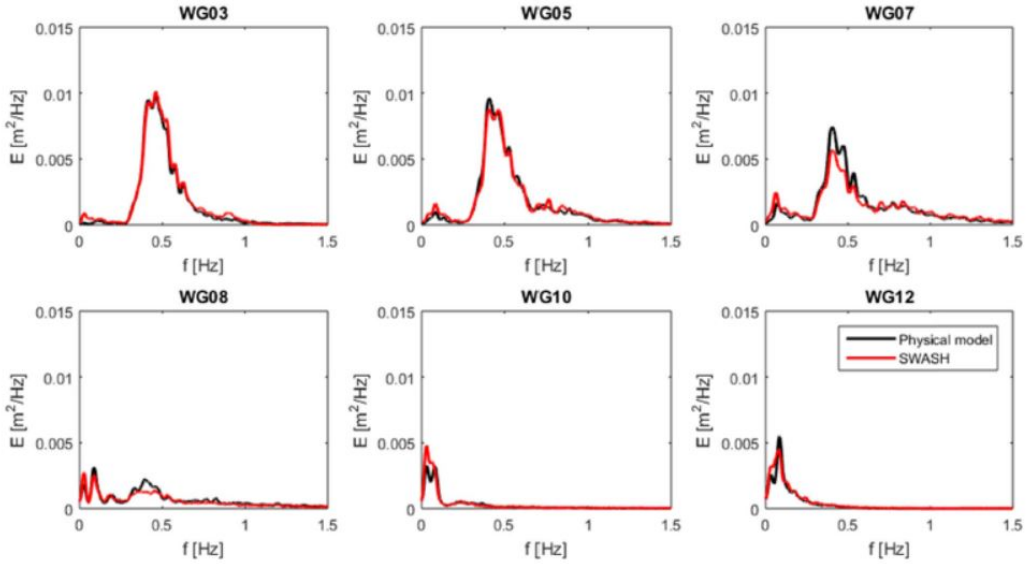

Figure 4.21: Example of a water surface energy spectra at different station, as it can see, they tend to move to the left and decrease its energy. Image by Suzuki et al. (2017) [20]

CHAPTER 5

Data analysis

The tests carried out were 419 and the data obtained are described in this chapter. First of all, all the data were analyzed to verify that none of them showed abnormal values. From this first sorting, 4 tests were eliminated in which the volume measurement was not present. The $u_{AWGt_{tip}}$ was not considered in the average velocity calculation (u_{mean}) because, it was verified that the method does not comply with the values obtained both from the cameras and Δt_{maxVOL}, so it was agreed to abandon this calculation methodology in order not to distort the analysis. Therefore, the values of the velocity (u_{mean}) and flow depth (λ_{mean}) of the overtopping event were not considered because, either they had a $u_{mean} > 15$ m/s, or a $\lambda_{mean} > 2$ m (u_{mean} and λ_{mean} values not conform with reality. In summary, the analyses were carried out on 415 tests: 193 cases with a 1:15 slope and the remaining 222 with a 1:30 slope of the beach. The study purposes are:

1. researching results;
2. comparison with the actual literature for the values of discharge, wave period evolution and overtopping volumes probability;
3. scale effects calculation.

5.1 Results

Here will be presented graphs containing the data divided for different wave overtopping parameters and different slopes.
In the Fig 5.1 is shown the discharge (q) versus the overtopping volume (V).

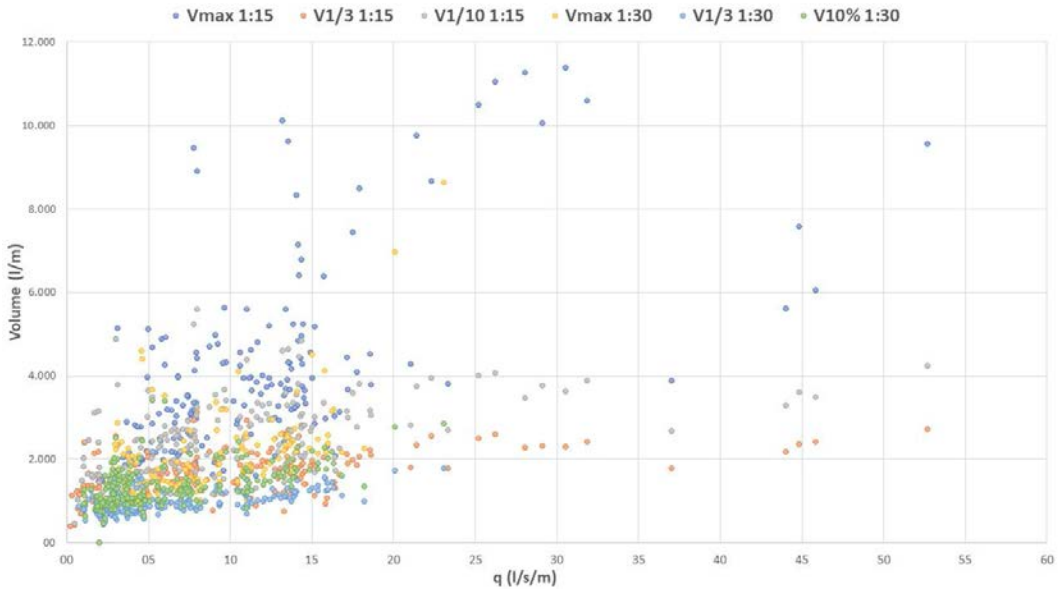

Figure 5.1: Discharge versus overtopping volume for different slopes

In this figure, the dates are divided according to the slope of the beach. The discharges have values between 0.2 - 52.7 l/s/m for slope 1:15 and 0.7 - 23.1 l/s/m for slope 1:30, while the volumes are within a range between 400 - 11000 m^3 for slope 1:15 and 460 - 8500 m^3 for slope 1:30. From the graph, it can be note that the $V_{1/3}$ and $V_{1/10}$ are grouped in a more uniform way, with few cases that move away from the main cloud, while the V_{max} it has more dispersion; for this reason, in the comparison with the literature, it will refer to the another volume (it will be defined later) and not to the maximum volume. The relationship between q and V seems pretty linear in fact, larger volumes correspond to higher discharges and vice versa. Higher values correspond to cases with larger T_p, H_{mo} and depths, lower values correspond to cases with lower inputs. It can also be noted that the slope of the beach plays a key role: for cases with 1:15 slope we have higher volumes and flow rates than the data

obtained with the real slope.

In the Fig 5.2 and 5.3 are shown the discharge (q) versus overtopping velocity (u) and flow depth (λ)

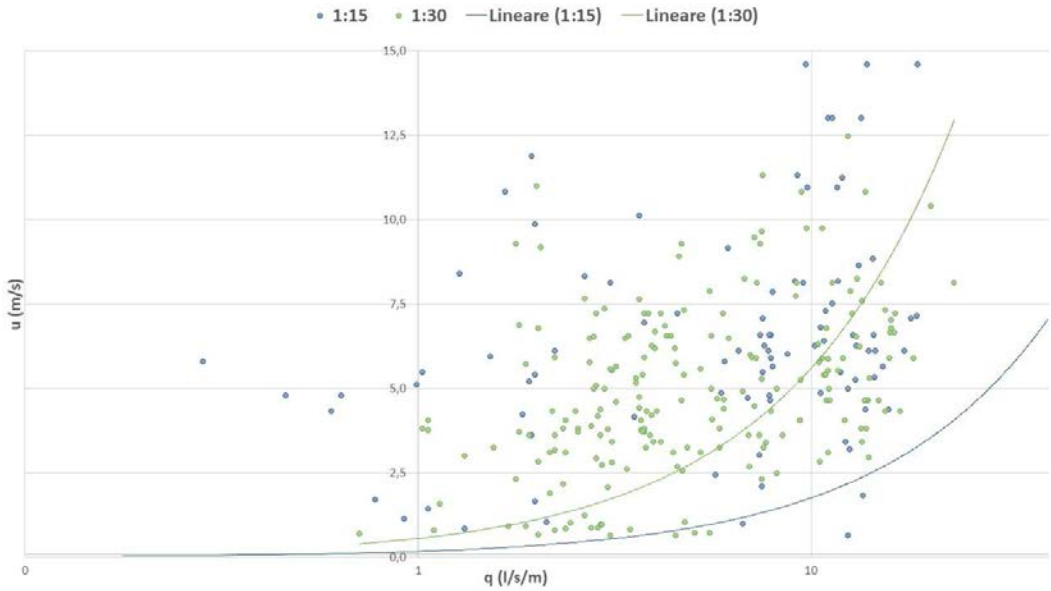

Figure 5.2: Discharge versus velocity for different slopes

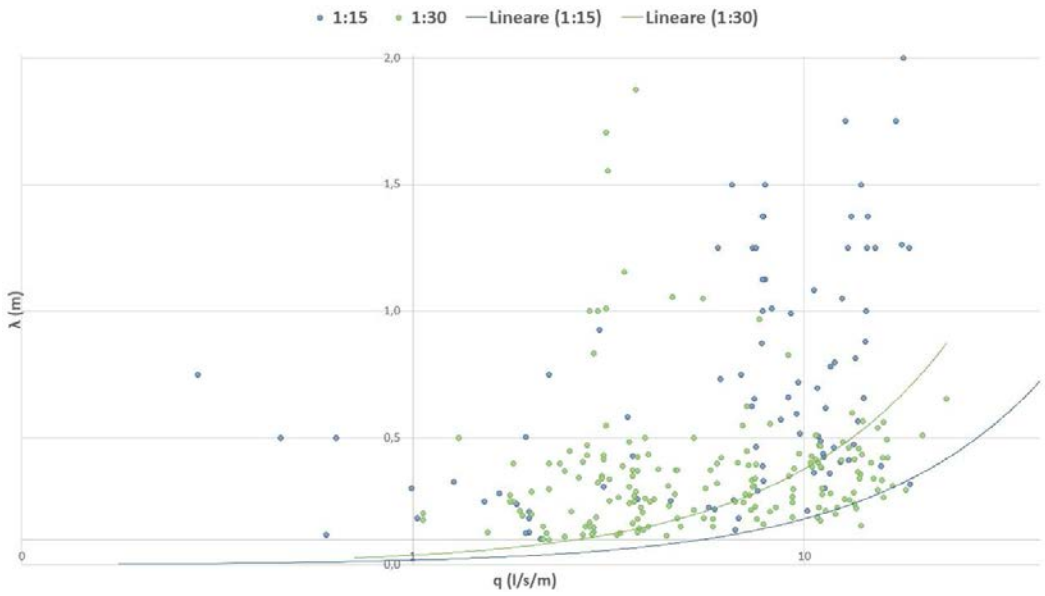

Figure 5.3: Discharge versus flow depth for different slopes

The velocity has values between 0.1 - 15 m/s for slope 1:15 and 0.74 - 15 l/s/m for slope 1:30, while the flow depth are within a range between 0.25 - 2.0 m

for slope 1:15 and 0.1 - 2.0 m for slope 1:30. The trend cases are exponential, in fact the discharges and the velocity, like depth, they can be different: for higher q , u and λ can had values higher or smaller according the overtopping event and vice versa. The slope role is fundamental in fact from the graphs it can be noted: the curve in the cases of slope 1:30 is always higher than the cases of slope 1:15, this means that the case 1:30 has the values more variables while for slope 1:15 the trend is more homogeneous.
In the Fig 5.4 is shown the overtopping velocity (u) versus flow depth (λ).

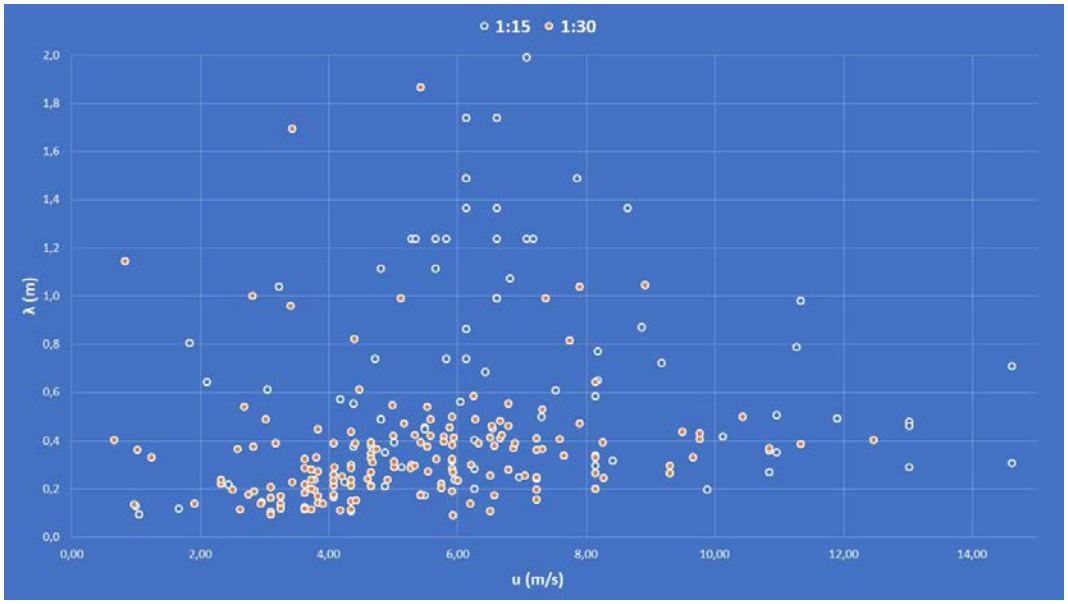

Figure 5.4: Velocity versus flow depth for different slopes

In this graph it can be seen, like the first relation between q and V, that the cases with the slope 1:30 stay in an homogeneous group while the others (slope 1:15) are arranged in different parts of the graph. It's important notes that u_{mean} and λ_{mean} don't have a linear relation, in fact it can had an overtopping velocity smaller and a splash (higher depth) or the contrary or again the two values may be proportional to each other.
Variability may depend on:

- promenade width;
- period of the overtopping wave;

- different slope;
- input condition

This results will be fundamental for the future analyses, especially the last figure because for the first time, the period of the overtopping event is important.

5.2 Comparison with the literature

In this section, the previous literature is compared with the experimental values, in particular the equations 2.17, 2.7, 2.30 used in the EurOtop (2018) [13]. All values have been separated for different slopes to check their behavior.

5.2.1 Overtopping discharge

The comparison with previous literature is complex because, none of the formulas is based on models with the same characteristics proposed in this thesis research. The application range of all the formulas is summarized in this table:

	Measured	Altomare et al.	Goda	Gallach
R_c/H_{m0}	1.85 - 6.9	1.4 - 3.8	0 - 3.9	0 - 3.25
h_{toe}/H_{m0}	0.68 - 1.38	-0.88 - 1.28	0 - 1.4	-
H_{m0}/h_{toe}	-	-	-	0.03 - 0.5
$\cot\alpha$	1	2 - 3.6	1 - 7	0 - 2.75
$\cot\theta$	15 - 30	35 - 50	10 - 30	-
$s_{m-1,0}$	-	0.0001 - 0.01	-	0.01 - 0.056
$\xi_{m-1,0}$	0.61 - 8.29	-	-	2 - 14.7

In the Fig 5.5 is proposed the comparison with the Altomare et al. (2016) formula (Eq 2.17), used also in the EurOtop manual (2018), in which all values have been considered in dimensional terms $Q = q/\sqrt{gH_{m0,toe}^3}$ and the heights

ratio.

As it can notice from the graph:

- many cases with slope 1:30 are within the formula range, the others exceed the upper limit;
- the cases with slope 1:15 are below the lower limit, except for few events.
- the yellow values range (slope 1:15) stay in the left part of graph while the orange values (slope 1:30) are in the right part, this means that the dimensionless height value is larger for the higher $\cot\theta$.

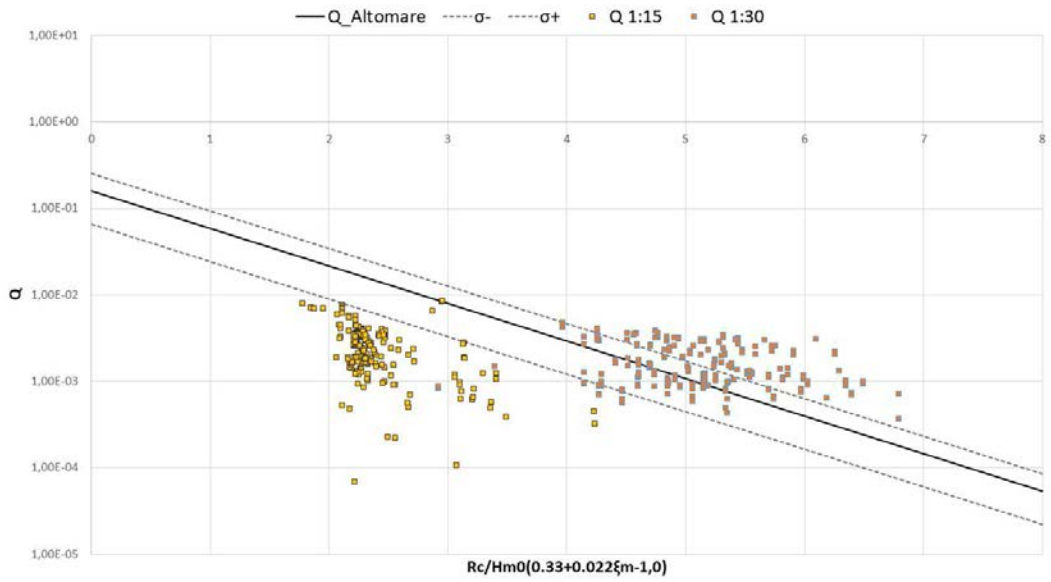

Figure 5.5: Comparison with Altomare et al. (2016) formula (Eq 2.17)

Altomare et al. (2016), in their studies did considered the shallow and very shallow condition, for this reason many cases are in accordance with his formula, moreover the lower limit $\cot\theta$ is similar with the one analyzed in the real case but, at the same time they didn't proposed a formulation for steep slopes, as 1:15 or dike slope, and for this reason the yellow points are not in conformity with the equation he suggested.

In the Fig 5.6 and 5.7 are shown the comparison with the Goda (2009) and Gallach (2018) formulas (Eq 2.12, 2.18). They, unlike Altomare et al. (2016), didn't considered the shallow and very shallow condition precisely for this, as

can be noted from the graphs, all values calculated with their formulations are upper the curves. In addition, the yellow values (slope 1:15) that have the values of $6 < R_c/H_{m0} < 7$ are the tests with less depth (0.29cm in model), this confirms the hypothesis initially made. Goda (2009) is the only one who has considerer the slope dike but, his dates are few for a true comparison.

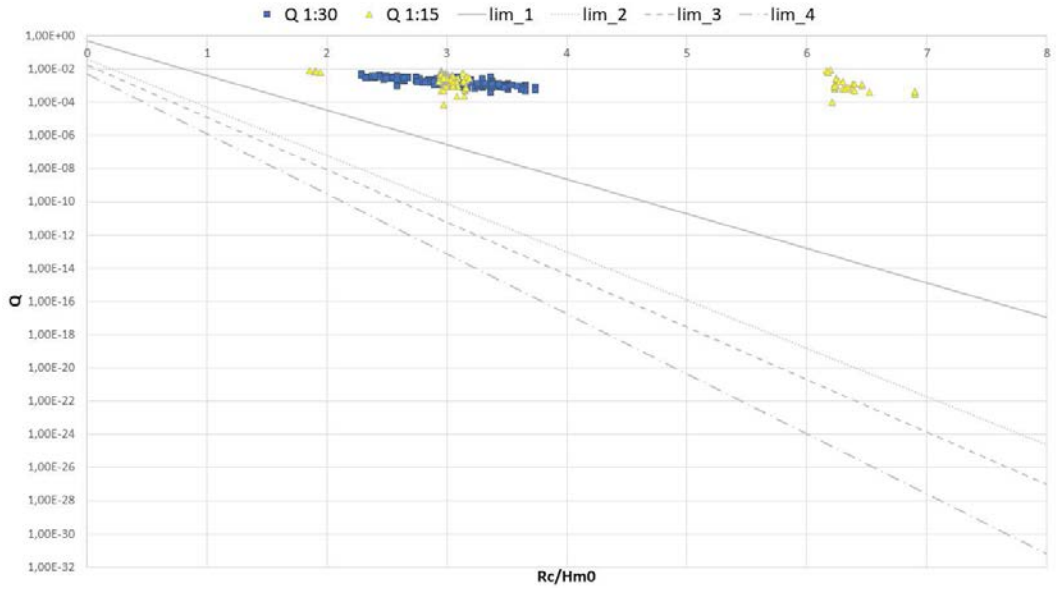

Figure 5.6: Comparison with Goda (2009) formula (Eq 2.12)

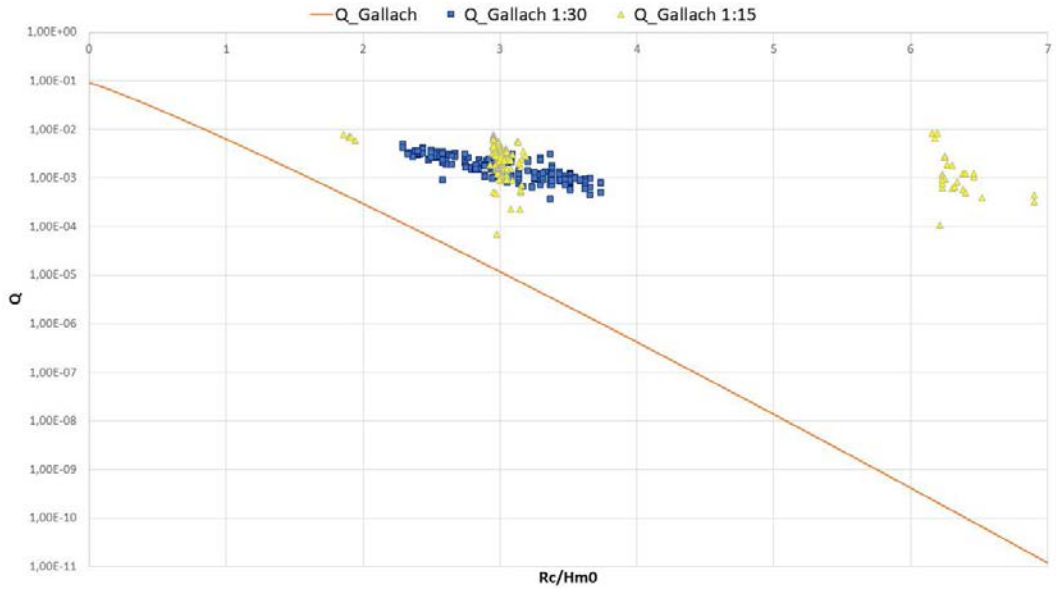

Figure 5.7: Comparison with Gallach (2015) formula (Eq 2.18)

Finally, the measured and calculated dimensional discharges have been com-

pared (Fig 5.8, 5.9, 5.10) for each formulation in the literature. It can be noted in all graphs that the calculated values are greater than those measured ($6.93 \cdot 10^{-5} < Q_{meas} < 8.54 \cdot 10^{-3}$), moreover the data with slope 1:30 are grouped, while the others (slope 1:15) are separated.

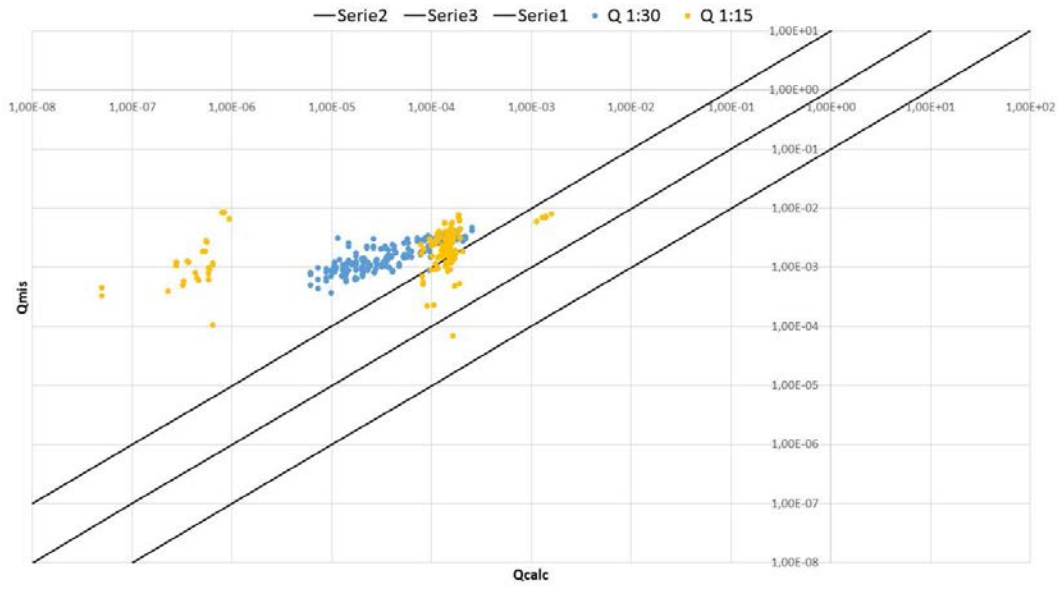

Figure 5.8: Q_{meas} versus Q_{cal} Altomare et al (2016) formula (Eq 2.17)

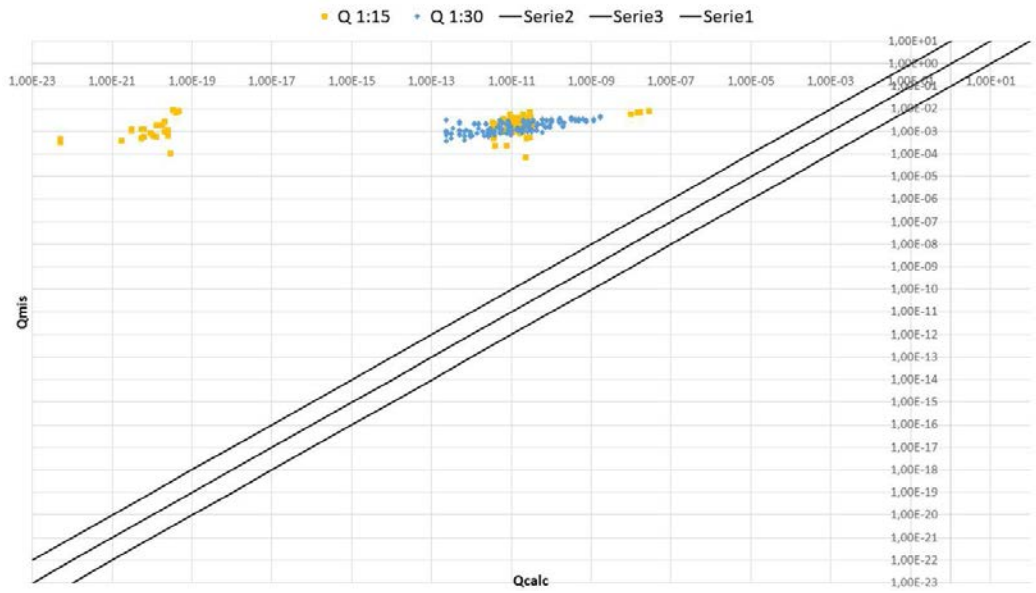

Figure 5.9: Q_{meas} versus Q_{cal} Goda (2009) formula (Eq 2.12)

In Altomare et al. (2016) (Fig 5.8), the data, as in the previous graph, are more near the formula limit, few values (slope 1:15) are within the range, but

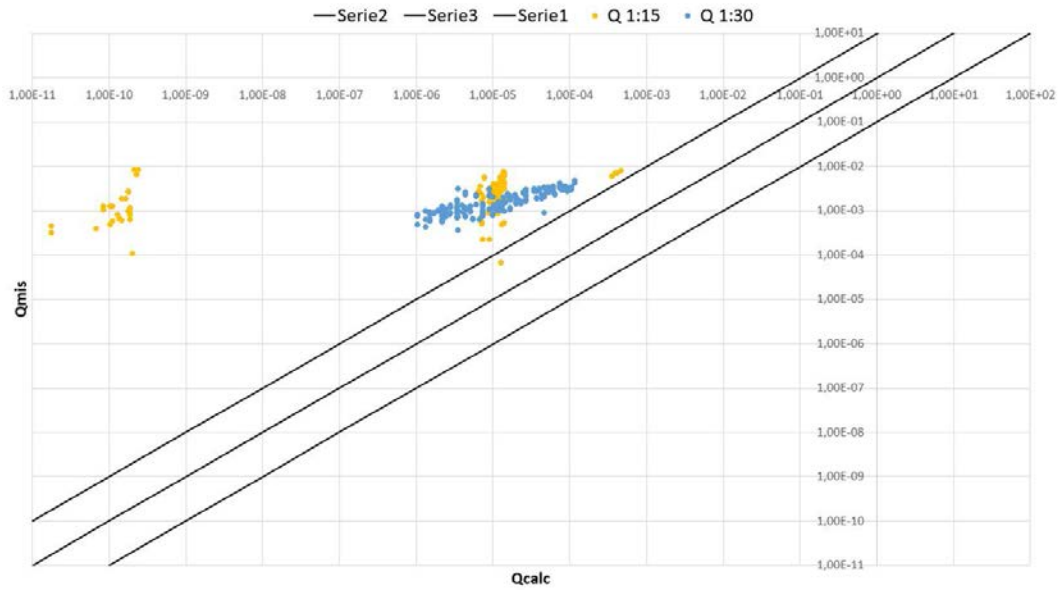

Figure 5.10: Q_{meas} versus Q_{cal} Gallach (2016) formula (Eq 2.18)

all others are higher. It gets this result because the equation considers shallow waters, unlike the others. In Goda (2009) and Gallach (2018) (Fig 5.9, 5.10) the values are further away from the limits, because the range of Q_{cal} is bigger than Altomare et al. results. The most distant data are always those with less depth.

In this table it is summarize the range of Q

	Altomare et al.	Goda	Gallach
$Q_{calc,min}$	$4.94 \cdot 10^{-8}$	$5.02 \cdot 10^{-23}$	$1.75 \cdot 10^{-11}$
$Q_{calc,max}$	$1.60 \cdot 10^{-3}$	$2.78 \cdot 10^{-8}$	$4.70 \cdot 10^{-4}$

5.2.2 Wave period evolution

As regards the assessment of wave period evolution, the Hofland et al. formula (2017) (Eq. 2.7) in EurOtop (2018) was compared. In this case, only tests with 1:30 slope were considered, as only in those tests were carried out experiments to calculate the toe conditions (to see chapter 4.3), for the comparison with the other slope (1:15) will be necessary the numerical model (SWASH, [25]) for calculate the missing data.

It can be noted from the Fig 5.11 the values are divided in three groups:

1. the first above the upper limit with depth equal 0.30cm in model;
2. the second, the largest, which is within the range of the formula with depths of 0.305 and 0.31cm;
3. the third, composed only by five values, below the lower limit with input conditions, in model: depth=0.31cm; H_{m0}=0.0882 - 0.085 [m]; T_s=1.74 - 1.69 [s].

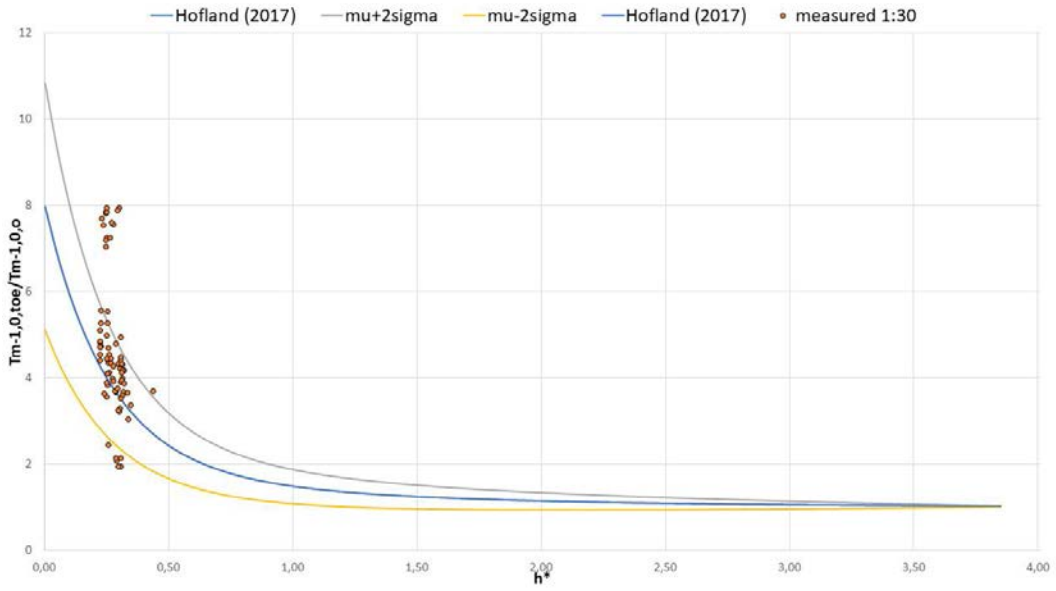

Figure 5.11: Comparison with Hofland et al. (2017) formula (Eq 2.7)

This results confirm the authors studies, in fact they worked under conditions similar to these (slope 1:35 and shallow condition) and came to the same conclusions:

- the formulation is valid for shallow and very shallow conditions;
- $T_{m-1,o}$ increases dramatically when the depth decreases and decreases when the depth increases (group 1 and group 3).

5.2.3 Individual overtopping volumes

For the overtopping volumes probability evaluation, for the fist time, it was considered another volume, $V_{10\%}$ with V_{max}. Unlike $V_{1/10}$, the $V_{10\%}$ is the volume value that is exceeded by only 10% of all values in the series, i.e. it's the minimum of the $V_{1/10}$ values of the series. The introduction of $V_{10\%}$ was fundamental for calculation of the Weibull volume distribution.
The steps performed were as follows:

1. Calculation of $V_{10\%,meas}$ trough the program "MATLAB" for each test;
2. Calculation of $P_{10\%,meas}$, the probability associated with the $V_{10\%,meas}$;
3. Calculation of α and β parameters of Weibull distribution;
4. Trough α and β it was possible to calculate $V_{10\%\ Weibull,calc}$ and compare it with the measured value.

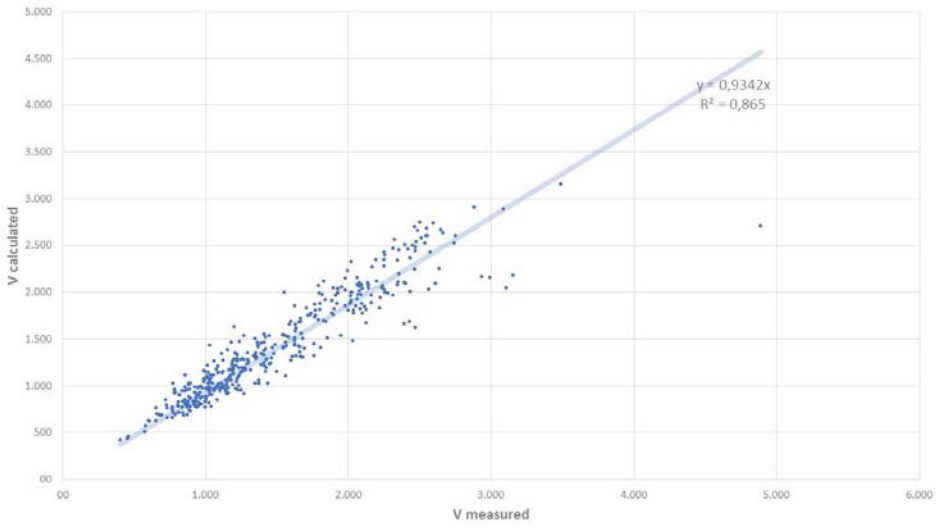

Figure 5.12: $V_{10\%,meas}$ versus $V_{10\%\ Weibull,cal}$

Fig 5.12 shows that the calculated and the measured values are similar, in fact the R^2 is approaching the unit. Once the hypothesis was verified it was possible the comparison with previous literature, in particular with the Zanuttingh et al. (2013) and Gallach (2018) formulas (Eq 2.29; 2.30).

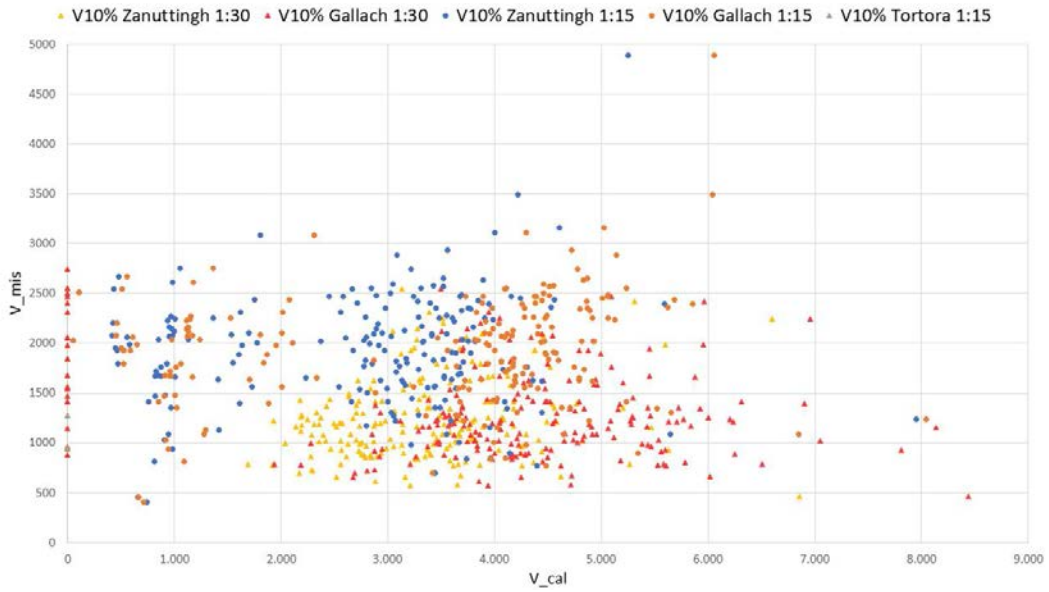

Figure 5.13: $V_{10\%,meas}$ versus $V_{10\%,cal}$

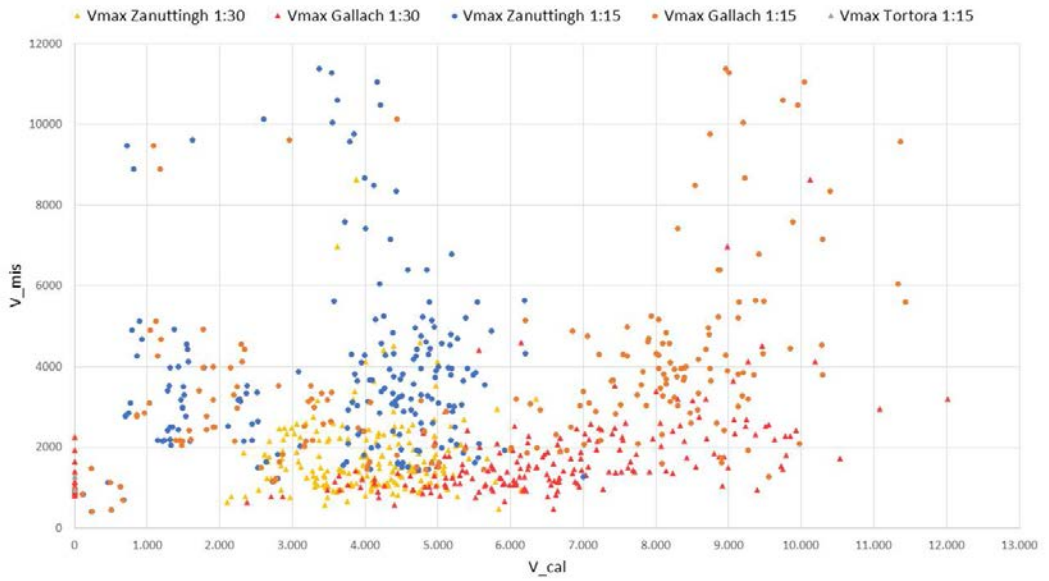

Figure 5.14: $V_{max,meas}$ versus $V_{max,cal}$

The Fig 5.13 and 5.14 show the relationship between the values measured and calculated, it can be noted:

- the $V_{10\%}$ values are grouped while the V_{max} are separate, so it will take more account of the first than the second;
- the values calculated with the Zanuttingh et al. (2013) formula are

approaching to those measured but, they are still larger;

- for Gallach (2018) formula, the calculate values are always higher than the measured values.

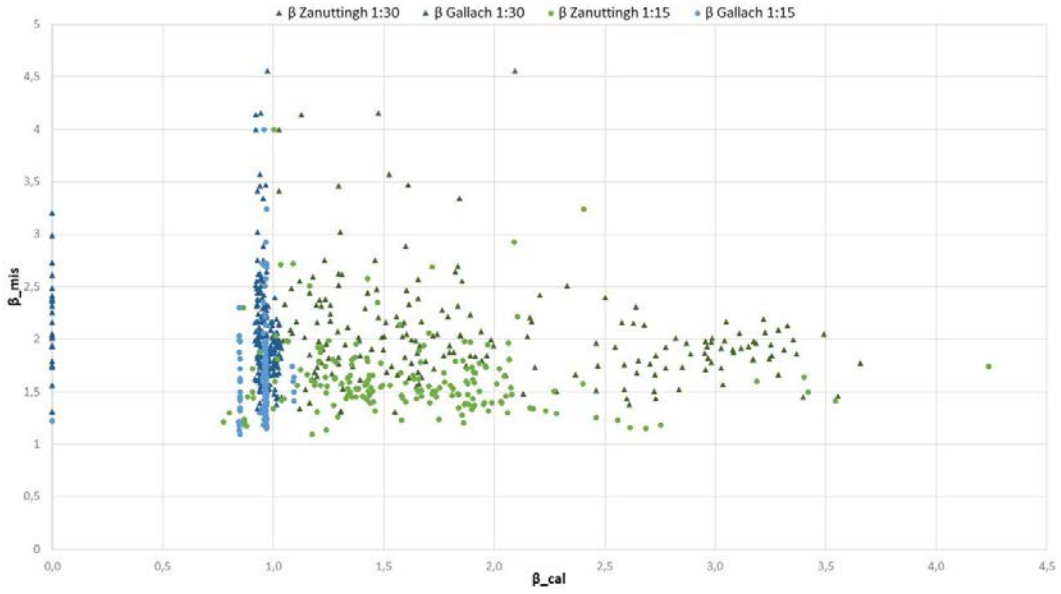

Figure 5.15: β_{meas} versus β_{cal}

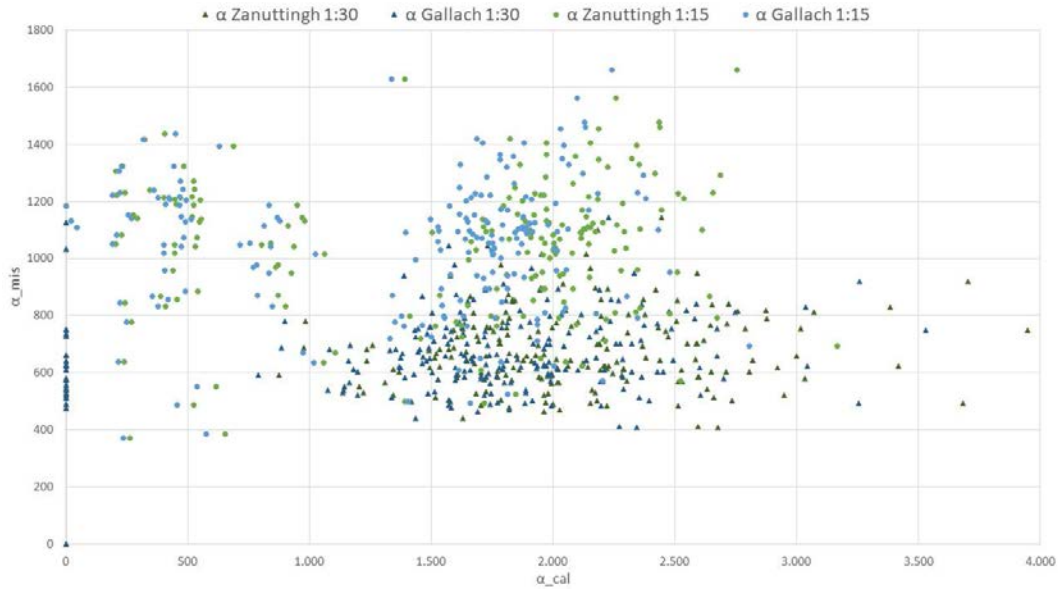

Figure 5.16: α_{meas} versus α_{cal}

The difference between two formulation is the definition of β coefficient and consequently also α coefficient (Fig 5.15, 5.16), in Gallach it is function of the ratio R_c/H_{m0} and remembering the experimental work condition, it's verified

that the Gallach values are upper because, in his studies, he didn't consider the shallow water. Looking at the figures it can be noted the above hypothesis are verified. Moreover, from the α formulation it shown the proportionality with discharge and, for this reason it can be verified the proportionality between q and V. Also P_{ov} value influences α calculation, in fact they are inversely proportional (Eq. 2.25). The formulas range are summarized in this table:

	Measured	Zanuttingh et al.$_{\text{cal}}$	Gallach$_{\text{cal}}$
α [l/m]	372 - 1661	20 - 3949	21 - 3530
β [s]	1.1 - 4.7	0.77 - 4.2	0.84 - 1.1

Both authors do not consider the promenade values, which can increase or decrease the overtopping volumes probability and this is the literature limit.

5.3 Scale effects

Scale and model effects result from incorrect reproduction of a prototype water-structure interaction in the scale model. Measurement effects are due different measurement equipment used for sampling the data in the prototype and model situations. These effects, which are referred to as "measurement effects" may significantly influence the comparison of results between prototype and model, or two identical models. It is therefore essential to quantify the effects and the uncertainty related to the different techniques available.
The method of calculating the scale effects is described within the EurOtop (2018) [13]:

1. first, it is necessary to calculate the run up value (Eq. 5.1, 5.2) and it is considered the minimum value between:

$$\frac{R_{2\%,max}}{H_{m0}} = 1.65 \cdot \gamma_b \cdot \gamma_f \cdot \gamma_\beta \cdot \xi_{m-1,0} \tag{5.1}$$

$$\frac{R_{2\%,min}}{H_{m0}} = 4 - \left(\frac{1.5}{\sqrt{\xi_{m-1,0}}} \right) \tag{5.2}$$

2. subsequently the limits imposed on viscosity (Reynolds Eq. 5.3) and surface tension (Weber Eq. 5.4) are assessed:

$$R_{eq,Reynolds} > R_{crit} = 10^3 \tag{5.3}$$

$$R_{eq,Weber} > R_{crit} = 10 \tag{5.4}$$

where:

$$R_{eq,Reynolds} = \frac{2(R_{2\%} \cdot R_c)^2}{\nu \cdot T} \tag{5.5}$$

$$R_{eq,Weber} = \frac{u_A \cdot h_A \cdot \rho_w}{\sigma_w} \tag{5.6}$$

3. then, the next scale factors correction are calculated:

$$f_{CLASH} = 1 \quad for\ q \geq 0.01 m^3/s/m \tag{5.7}$$

$$f_{CLASH} = 1 + 5\left[\left(-\frac{\log q + 2}{2}\right)^3\right] \quad for\ q < 0.01 m^3/s/m \tag{5.8}$$

$$f_{Schuttrumpf} = \sqrt{1 - \frac{64}{0.1 R_{eq}}} \tag{5.9}$$

4. finally, the new discharges are calculated:

$$q_{CLASH} = q_{prot} \cdot f_{CLASH} \tag{5.10}$$

$$q_{Schuttrumpf} = q_{prot} \cdot f_{Schuttrumpf} \tag{5.11}$$

For this particular case, the limit imposed on surface tension is always verified, except for 11 cases where the velocity calculated with the two methods (AWGs and cameras) are very different from each other. As further assessment of possible scale effect, the "Artificial Neural Networks" (ANNs) has been employed (see further details in EurOtop (2018) [13]). ANN was used to predict the mean overtopping discharge and compared it with measured values. Significant differences between predicted and measured, especially with lower measured discharges, would suggest possible scale effects values.
The input values for ANN are summarized as follow:

- test name.

- $cot\theta$ with slope 1:30 and $cot\alpha$;
- h_{toe}, h_t and R_c;
- $H_{m0,toe}$ and $T_{m-1,0,toe}$;
- Promenade width;
- γ_b, γ_f, γ_v;

By mean of the ANN it has been possible to compare the experimental data obtained with "CIEMito" and verify that they are inside the cloud derived by the method (Fig 5.17).

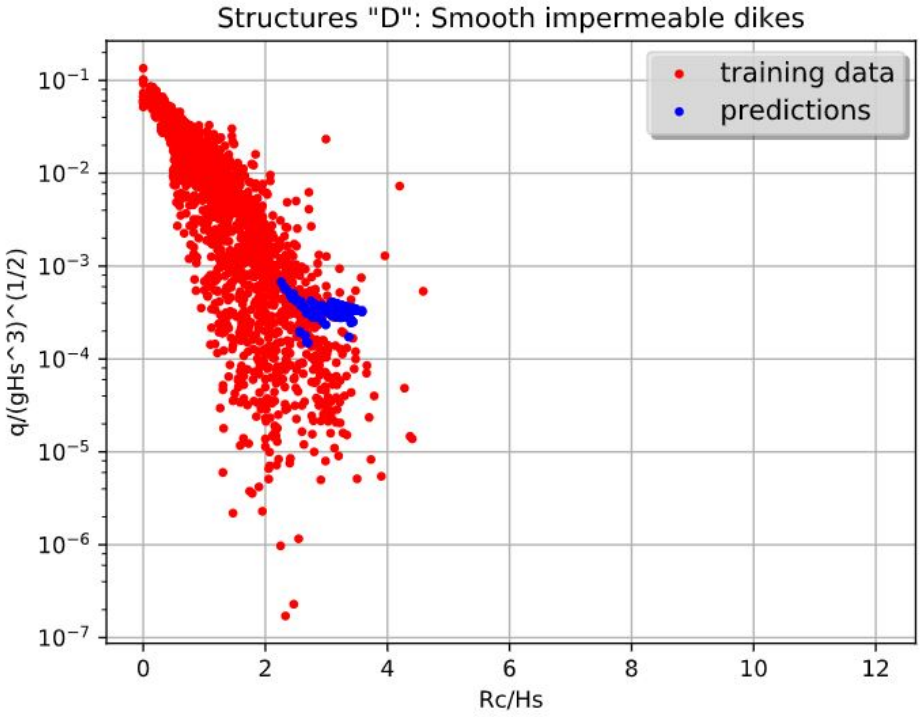

Figure 5.17: Results by Artificial Neural Networks, the values obtained by CIEMito are within the cloud, the scale effects are minimum

The $Q_{95\%,ANN}$, $Q_{mean,ANN}$, $Q_{5\%,ANN}$ were calculated (Eq. 5.12) and compared them with the measured discharges (Fig 5.18).

$$Q = \frac{q}{\sqrt{g \cdot H_{m0,toe}^3}} \tag{5.12}$$

Where $q = q_{95\%,ANN};\ q_{mean,ANN};\ q_{5\%,ANN}$ [$m^3/s/m$], the measured discharges, the discharge values that are exceeded by only 95%, 50% and 5% of all values in the series respectively. The values are within the limits and this verify also the hypothesis: the scale effects are minimum and may be overlooked.

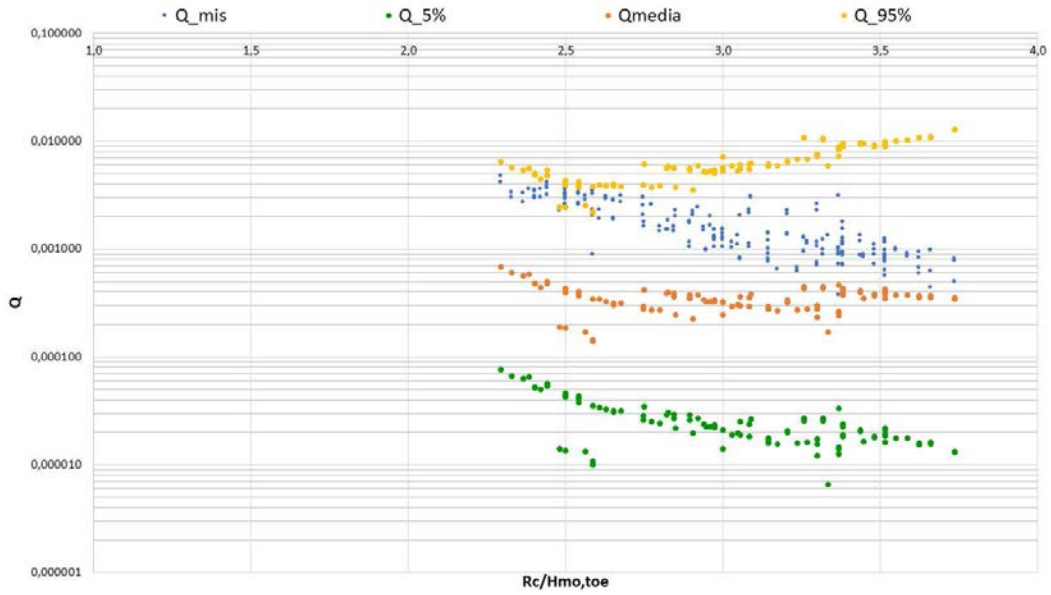

Figure 5.18: Q versus $R_c/H_{m0,toe}$

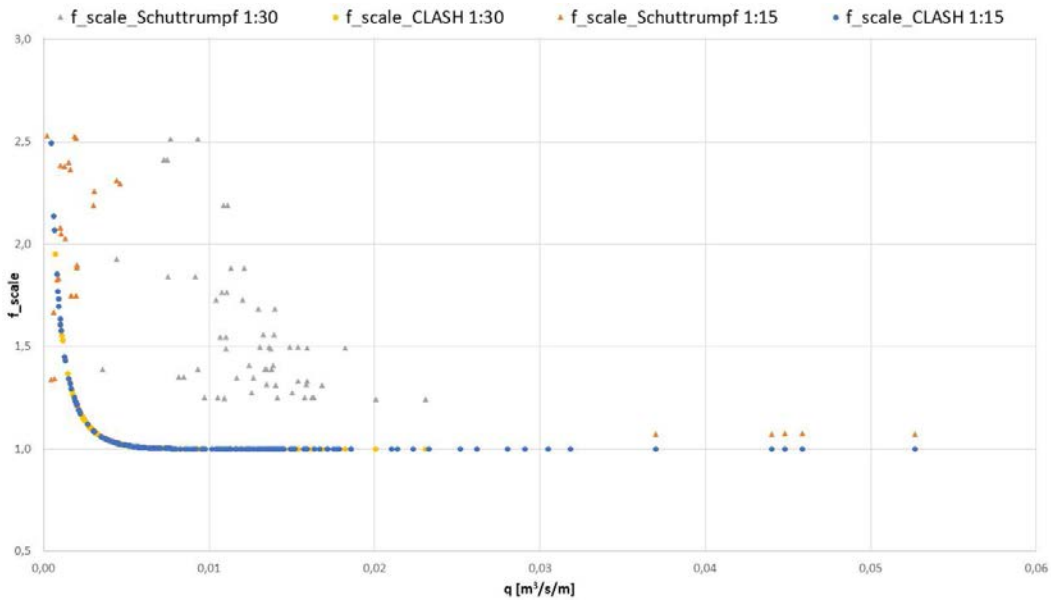

Figure 5.19: f_{scale} versus q [$m^3/s/m$]

Finally, the Fig 5.19 shows how the CLASH scale factor is almost always close

to unity and for this reason the discharge values do not change, while for Schuttrumpf (2001) [24], the result depends a lot on the conditions, especially on the value of the $\cot \alpha$. In fact considers lower slopes. Consequently, the coefficient within the formula should be changed, but the results are in line with the author's considerations (Fig 5.20).

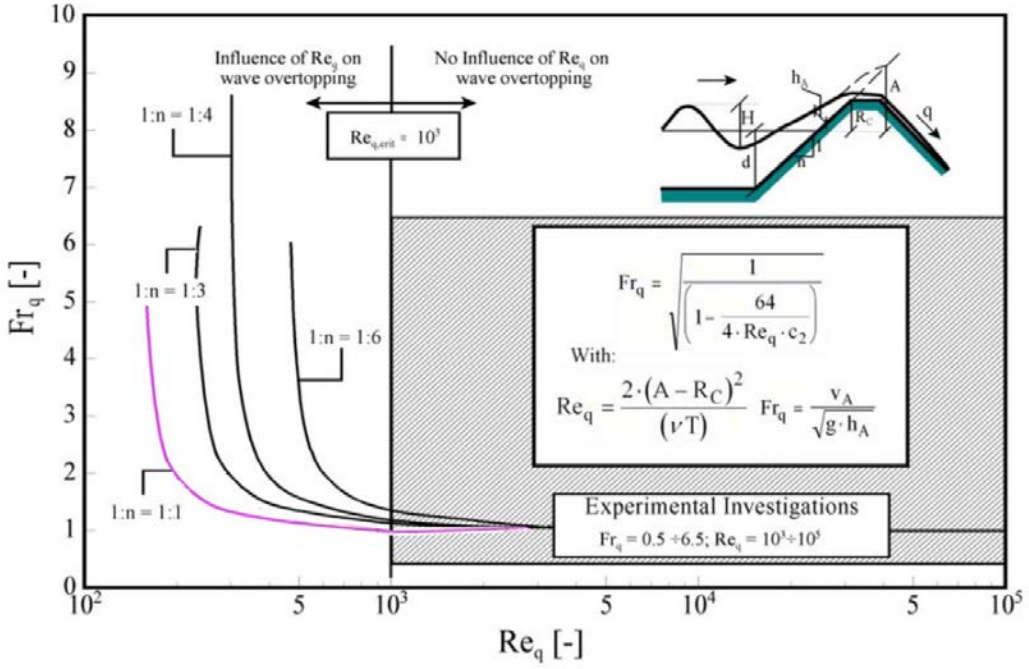

Figure 5.20: Influence of viscosity on wave run-up velocities [24]. The colored curve indicates the possible values of Froud and Reynold numbers for a dike slope 1:1.

CHAPTER 6

Discussion

In this chapter, the experimental results are compared with the EurOtop (2018) [13] limits (Fig 6.1) and with the Sandoval (2015) and Arrighi et al. (2019) stability curves (see chapter 2.2).

All values have been separated for different slopes and promenades to check their behavior.

Hazard type and reason	Mean discharge q (l/s per m)	Max volume V_{max} (l per m)
People at structures with possible violent overtopping, mostly vertical structures	No access for any predicted overtopping	No access for any predicted overtopping
People at seawall / dike crest. Clear view of the sea.		
H_{m0} = 3 m	0.3	600
H_{m0} = 2 m	1	600
H_{m0} = 1 m	10-20	600
H_{m0} < 0.5 m	No limit	No limit
Cars on seawall / dike crest, or railway close behind crest		
H_{m0} = 3 m	<5	2000
H_{m0} = 2 m	10-20	2000
H_{m0} = 1 m	<75	2000
Highways and roads, fast traffic	Close before debris in spray becomes dangerous	Close before debris in spray becomes dangerous

Figure 6.1: Overtopping limits for people and vehicles [13].

According EurOtop manual (2018) a structure could be considered safe for people and vehicles when the volume and the discharge values are within certain limits (Fig 6.1). Firstly, the experimental results, divided for different slopes and promenades, are compared with the EurOtop (2018) limits (Fig 6.2, 6.3, 6.4, 6.5).

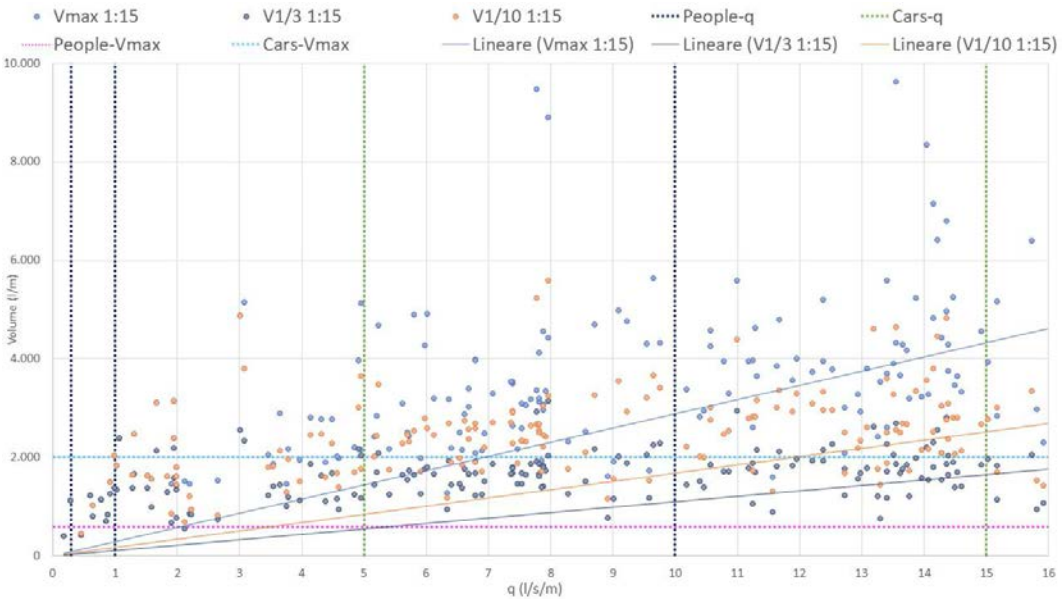

Figure 6.2: Volume versus discharge, comparison with the EurOtop (2018) limits (slope 1:15).

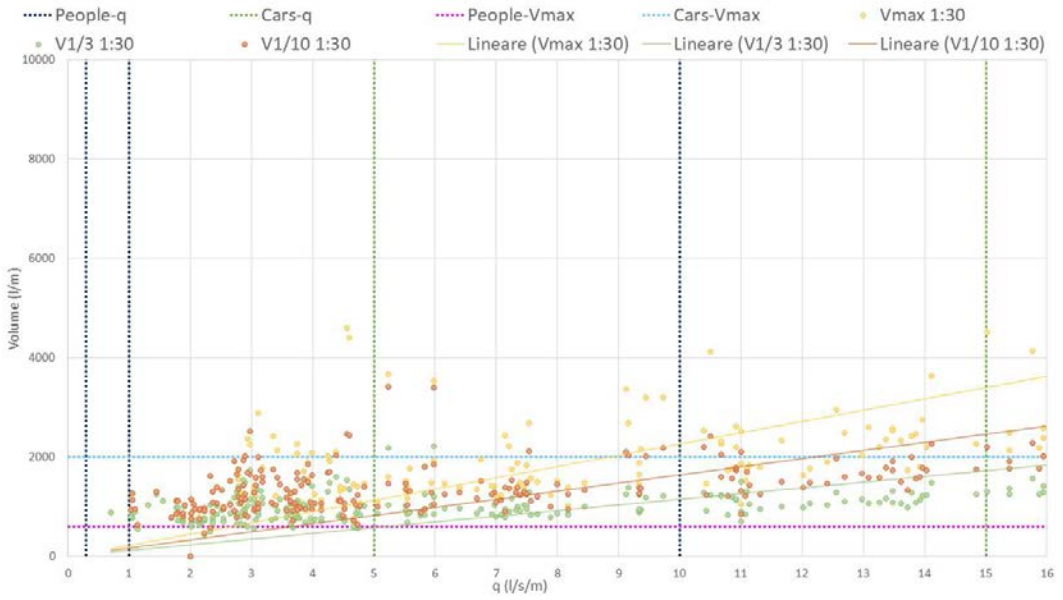

Figure 6.3: Volume versus discharge, comparison with the EurOtop (2018) limits (slope 1:30).

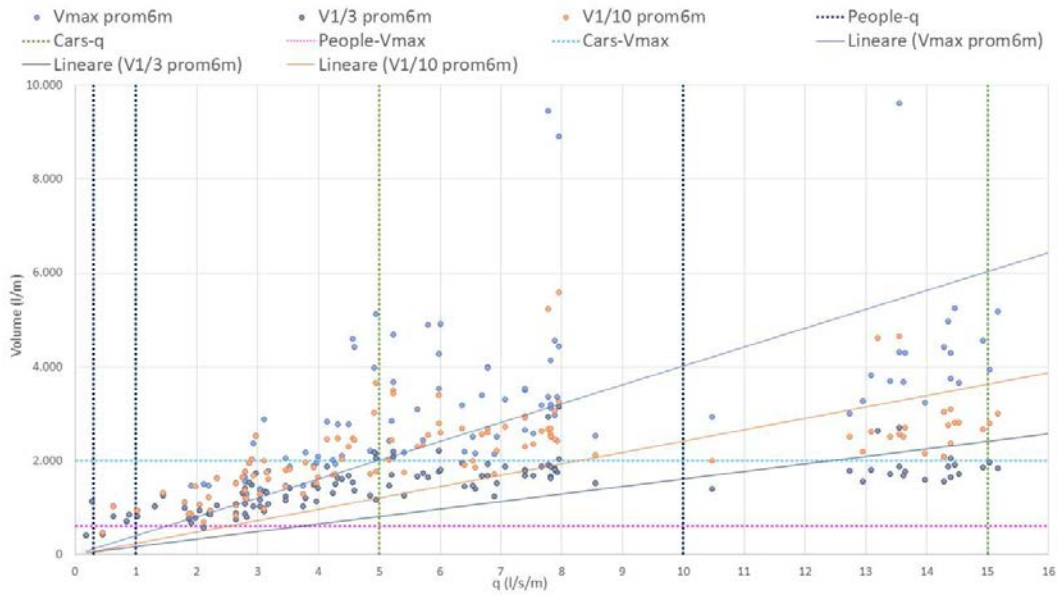

Figure 6.4: Volume versus discharge, comparison with the EurOtop (2018) limits (promenade 6m).

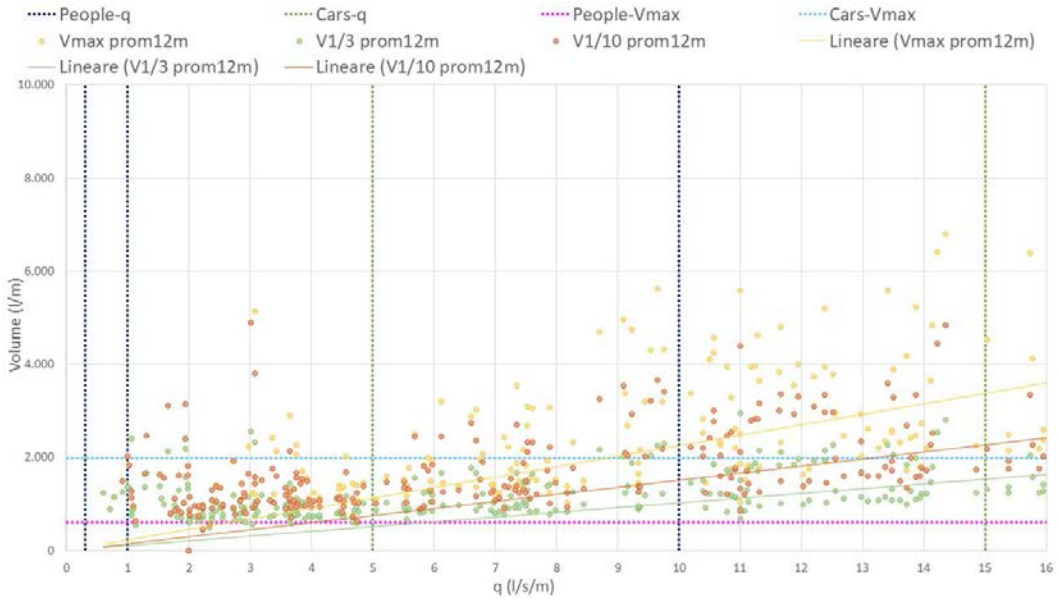

Figure 6.5: Volume versus discharge, comparison with the EurOtop (2018) limits (promenade 12m).

Figures 6.2, 6.3, 6.4, 6.5 show:

1. the volume values are not within the limits for the people (<600 m^3), except for few cases;

2. the volume values are within the limits for the vehicles for cases with

slope 1:30 (Fig 6.3), while it is not verified for the slope 1:15 (6.2) and different promenades (Fig 6.4, 6.5), in these the situations are similar (<2000 m^3)

3. the discharges values are within the limits for all conditions

Therefore the EurOtop (2018) limits are not verified for this particular case, the volume, based on these preliminary considerations, is the stronger limiting condition. Other parameters, u_{mean} and λ_{mean}, were considered for the safety assessment. The safety condition are evaluated through the stability curves of Sandoval and Arrighi et al. and the discharge values are divided in three range based on EurOtop manual (2018) ($q < 5;\ 5 < q < 15;\ q > 15$ [l/s/m]). Analyzing the graphs, it can be seen that:

- from the comparison with Sandoval and Arrighi's formulas (Fig 6.6; 6.7; 6.8; 6.10) it can be observed that not all values are in unsafe region, even if all cases present individual overtopping volumes higher than the threshold proposed in EurOtop (2018);

- the values within the safe zone for vehicles are verified also by the Arrighi's formula (2019) (Fig 6.9, 6.11);

- in the EurOtop (2018) the discharges values are almost always verified for the people. Here isn't true, in fact, considering the formulas, most of the cases are within the unsafe zone;

- the longest promenade (12m) has more values in the safe zone also for values of discharge higher, idem for the lower slope (1:30) in both formulations. In the Arrighi and Sandoval's formulas, the promenade has an important role, unlike in the EurOtop (2018), the beach slope ($\cot\theta$) has more relevance on the definition of safe and unsafe conditions;

- low input discharge values do not necessarily return an output value that is in the safe zone, the same happens in presence of high discharge values.

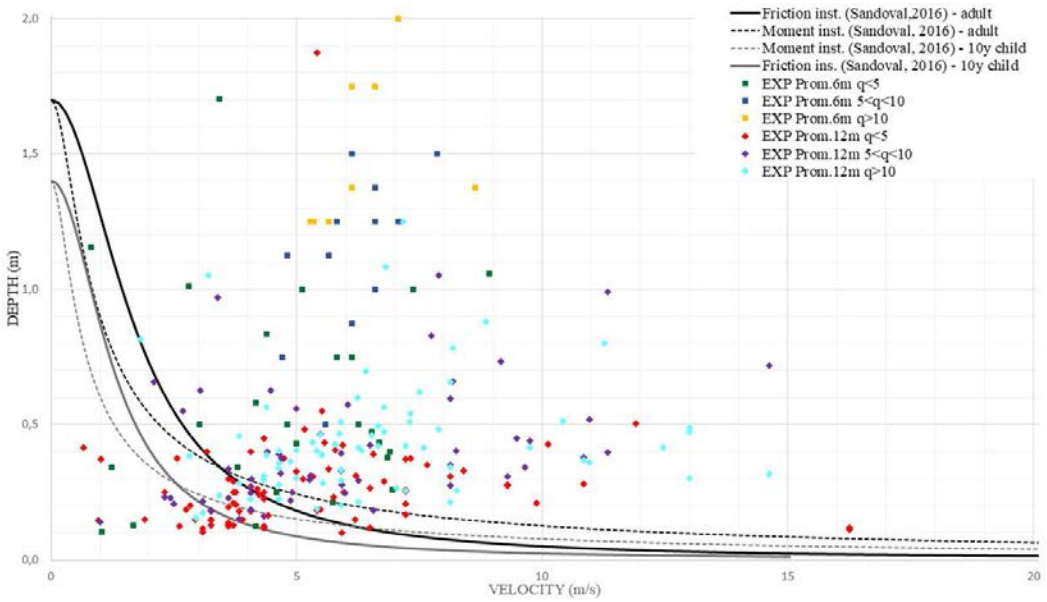

Figure 6.6: Flow depth versus velocity, comparison with Sandoval (2015) curves, the discharges are divided for different promenades.

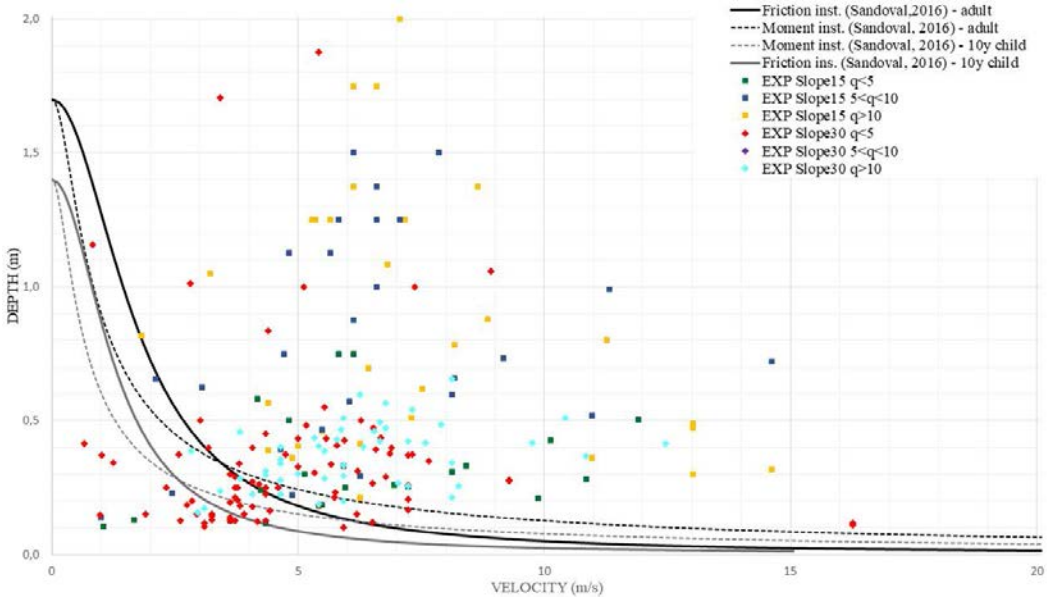

Figure 6.7: Flow depth versus velocity, comparison with Sandoval (2015) curves, the discharges are divided for different slopes.

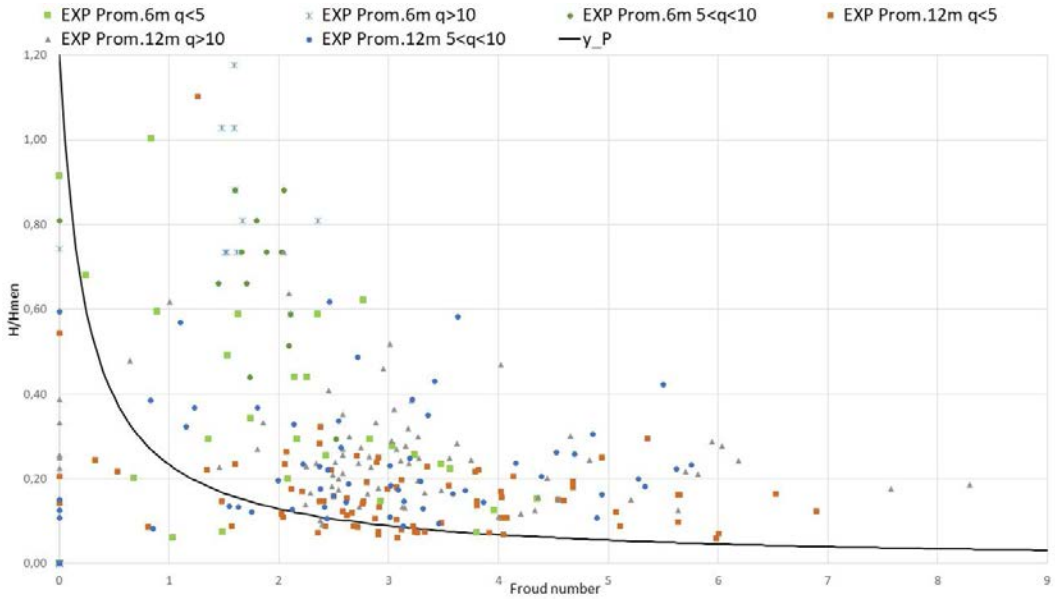

Figure 6.8: H/H_P (H=water depth; H_P=person height) versus Froud number, comparison with Arrighi et al. (2019) curve, the discharges are divided for different promenades.

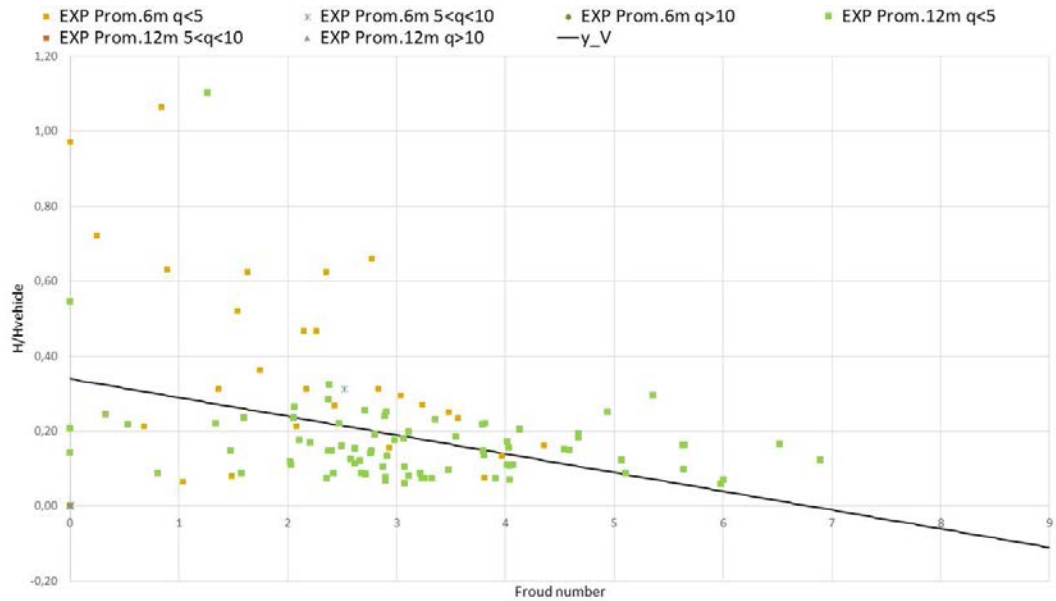

Figure 6.9: H/H_V (H=water depth; H_V=vehicle height) versus Froud number, comparison with Arrighi et al. (2019) curve, the discharges are divided for different promenades.

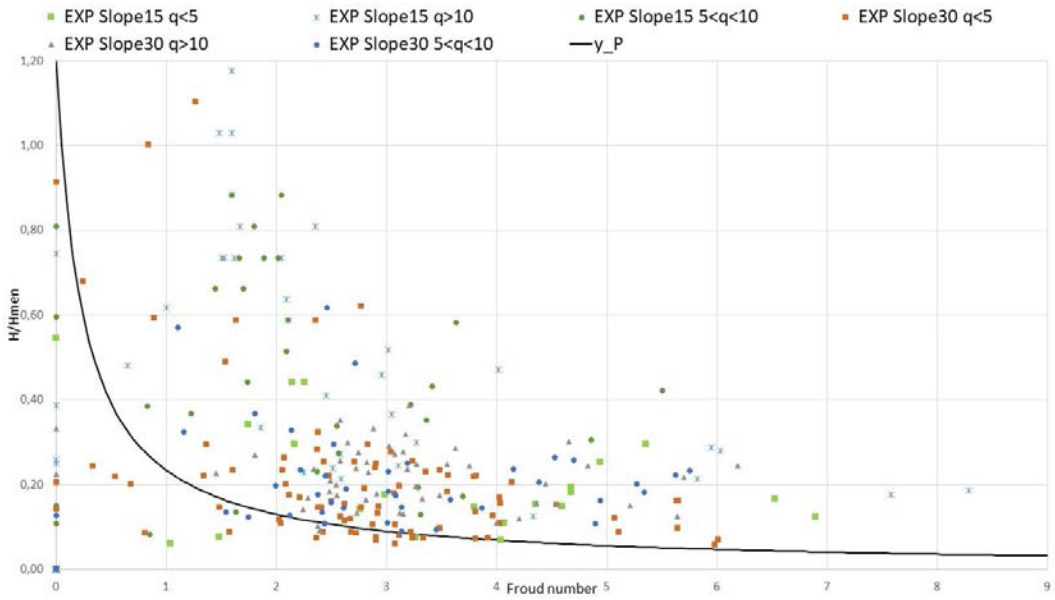

Figure 6.10: H/H_P (H=water depth; H_P=person height) versus Froud number, comparison with Arrighi et al. (2019) curve, the discharges are divided for different slopes.

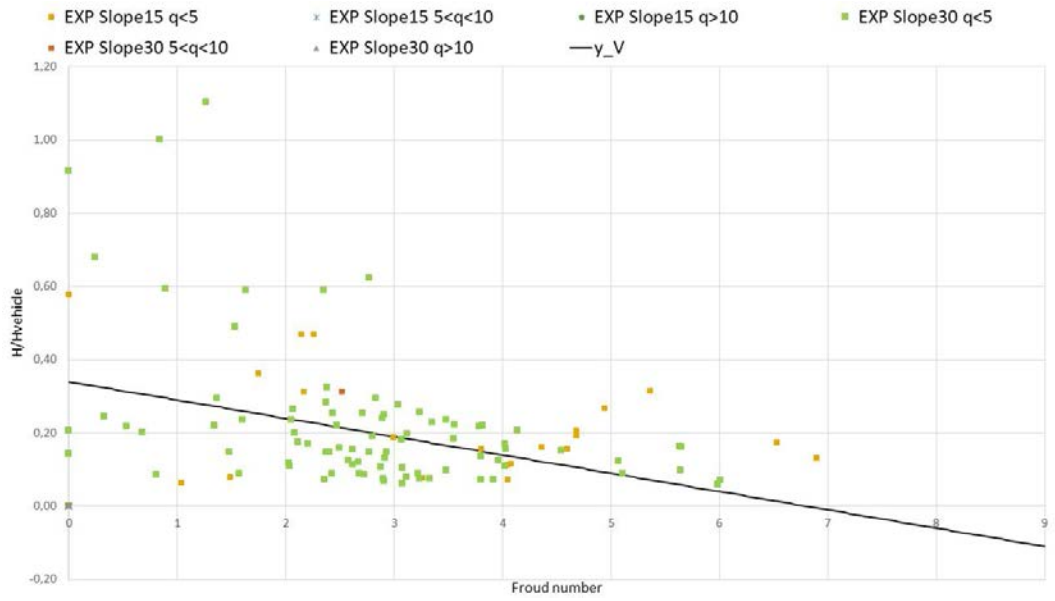

Figure 6.11: H/H_V (H=water depth; H_V=vehicle height) versus Froud number, comparison with Arrighi et al. (2019) curve, the discharges are divided for different slopes.

After performed studies, it seems that: promenade, beach slope, overtopping velocity and flow depth are very important for the assessment of coastal safety condition. In particular, the promenade variable in the analyzed study resulted dominant because the overtopping values are calculated at the end of the structure, where begins the railway and the people walk.
Considering two events with volume and discharge similar, but two different promenades width, it could have several results in terms of safety conditions because the promenade:

- affects unit volume. In fact, wave on the larger promenade runs and evolves differently and consequently it have more possibility to have lower overtopping volumes;
- affects overtopping velocity and depth. Increasing the promenade, the temporal distance between the sensors increases and therefore the velocity decreasing; while the overtopping flow depth, evaluated with AWG0 (the sensor more near the end of the promenade width), is less affected by splash and therefore smaller;
- from the previous point it is evident that higher discharges with larger promenade have more possibility to stay within the safe zone unlike shorter promenade.

Finally the result analysis shows that there is a fundamental lack in actual overtopping design criteria. Average discharges and individual overtopping volumes are key parameters for the design of coastal defense, especially for determining the structural freeboard and any element acting to mitigate overtopping events. Nevertheless, when looking carefully at post-overtopping processing, we should take into account how overtopping flows evolve, which is their maximum velocity and flow depth. These values must not lead to incipient instability for people or vehicles, if the rear side of coastal defenses is used by stakeholders. The outcomes of this work highlight, therefore, that more variables should be taken into account for the final design of coastal defenses.

CHAPTER 7

Conclusions

In this thesis work, the issue of coastal safety for the case located in Premìa de Mar has been addressed. Through the experimental work and then the analysis of the data, it has been possible to verify that the limits proposed by the current EurOtop manual (2018) are incomplete because they don't consider many variables that characterize the phenomenon. The current tables, therefore, can be used as a starting point for a preliminary evaluation, but must be accompanied by estimates of velocity, flow depth, geometric characteristics of the analyzed structure and the wave period of the sea event. Also the formulations of literature used to estimate overtopping discharge, wave period evolution and overtopping volume probability, are incomplete because do not consider all possible configurations as: shallow or very shallow wave conditions, 1:1 slope dike or presence of the dike. They, like the tables, can be used for a preliminary evaluation. Through the studies conducted, it seems obvious that:

1. the EurOtop (2018) limits for the safety of people and vehicle should be updated, searching other ranges for the overtopping parameters involved;

2. the scale effects evaluation must consider steep slopes dike;

3. as EurOtop limits, also the literature formulation should be updated,

considering all evaluated conditions and searching new correlation between the variables involved;

4. more experimental tests need to be carried out to find the overtopping parameters.

All points described before will be analyzed in a future work, but in fact:

- new tests will be performed on the CIEMito using the cars prototype for research new safety range;
- new correlations between the overtopping parameters will be obtained, which will update the current literature. The topic will be discussed in a nearby scientific paper;
- tests have already been carried out to compare the experimental model with the numerical model, using the meshless open-source "DualSPHysics" code (Crespo et al., 2015), to increase the number of conditions;

In accordance with the carried out study it is evident that for the design of coastal defense are essential the values of average discharges and individual overtopping volumes. However, to ensure their total safety, we should take into account how overtopping flows evolve, therefore we have to calculate maximum velocity and flow depth. These should not cause instability to people and vehicles, for this reason must be consider for the final design of coastal defenses.

Bibliography

[1] Van Gent, M. and Smith, G., *Physical model investigation on coastal structures with shallow foreshore: 2D model tests with singe and double - peaked wave energy spectra*, 1999.

[2] Van Der Meer, J.W., Allsop, N.W.H., Kortenhaus, A., Pullen, T., Schüttrumpf, *EurOtop, Manual on wave overtopping of sea defences and related structures, an overtopping manual largely based on european research, but for world - wide application*, 2007

[3] Technical Advisory Committee on Flood Defence, *TAW, Technical Report onWave Run-up andWave Overtopping at Dikes.*, 2002

[4] CIRIA C683, *The Rock Manual: The Use of Rock in Hydraulic Engineering*, II ed., London, 2007

[5] Hofland, B., Chen, X., Altomare, C., Oasterlo, P., *Prediction formula for the spectral wave period $T_{m-1,0}$, on mildly sloping hallow foreshores*, Coastal Engineering, 2017.

[6] Gallach Sanchez, D., *Experimental study of wave overtopping performance of steep low - crested structures*, PhD Thesis, Ghent University, 2018.

[7] Zanuttigh, B., Van Der Meer, J., Bruce, T., Hughens, S., *Statistical characterisation of extreme overtopping wave volumes*, 2013.

[8] Abt., S.R., Wittler, R.J., Taylor, A., Love, D.J., *Human stability in a high flood hazard zone. Wtaer resorces bullwtin*, Vol. 25, 1989.

[9] Endoh, K., Takahashi, S., *Numerically modeling personal danger on a promenade breakwater due to overtopping waves. Proceding of the 24 internation conference on coastal engineering*, Vol. 1, ASCE, 1994.

[10] Sandoval, C., *Direct personnel hazard in wave overtopping flows at seadikes*, PhD Thesis, Edinburgh University, 2015.

[11] Altomare, C., Suzuki, T., Chen, X., Verwaest, T., Kortenhaus, A., *Wave overtoppig of sea dikes with very shallow foreshore*, Coastal Engineering 116, Ghent University, 2016

[12] Van Der Meer, J.W., Allsop, N.W.H., Bruce, T., De Rouck, J., Kortenhaus, A., Pullen, T., Schüttrumpf, Troch, P., Zannuttigh, B., *EurOtop, Manual on wave overtopping of sea defences and related structures, an overtopping manual largely based on european research, but for world - wide application*, 2016.

[13] Van Der Meer, J.W., Allsop, N.W.H., Bruce, T., De Rouck, J., Kortenhaus, A., Pullen, T., Schüttrumpf, *EurOtop, Manual on wave overtopping of sea defences and related structures, an overtopping manual largely based on european research, but for world - wide application*, 2018.

[14] Goda, Y., *Derivatin of unified wave overtopping formuale for seawalls with smooth, impermeable surface based on selectes CLASH datasets,*, Coastal Engineering 56, 2009.

[15] Van Der Meer, J.W., Janssen, J.P.F.M., *Wave run-up and wave overtopping at dikes*, ASCE. In: Kobayashi, N., Demirbilek, Z. (Eds.), Wave Forces on Inclined and Vertical Wall Structures, 1995.

[16] Victor, L., Van Der Meer, J.W., Trock, P., *Probability distribution of individual wave overtopping volumes for smooth impermeable steep slopes with low crest freeboards*, Coastal Engineering 64, 2012.

[17] Tamada, T., Inoue, M., Tezuka, T., *Experimental studies on diagrams for the estimation of wave overtopping rate on gentle slope-type seawalls*

and these reduction effects on wave overtopping, Coastal Engineering 49, 2002.

[18] Hughes, S.A., Thortnton, C.I., Van Der Meer, J.W., Scholl, B.N., *Improvementsin describing wave overtopping processes*, Coastal Engineering 1(33):35, 2012.

[19] Hughes, S., Nadal, N., *Laboratory study of combined wave overtopping and storm surge overflow of a levee*, Coastal Engineering 56(3), 2009

[20] Tomohiro, S., Altomare, C., Veale, W., Verwaest, T., Trouw, K., Troch, P., Zijlema, M., *Efficient and robust wave overtopping estimation for impermeable coastal structures in shallow foreshores using SWASH*, Coastal Engineering 122(108-123), 2017

[21] Arrighi, C., Alcèrreca-Huerta, J.C., Oumeraci. H., Castelli, F., *Drag and lift contribution to the incipient motion of partly submerged flooded vehicles*, Journal pf Fluids and Structures 57, 2015

[22] Arrighi, C., Pregnolato, M., Dawson. R.J., Castelli, F., *Preparedness against mobility disruption by floods*, Science of Total Environment 654, 2019

[23] Arrighi, C., Pregnolato, Castelli, F., *Hydrodynamics of pedestrians' instability in floodwaters*, Hydrol. Earth Syst. Sci., 21, 515, 531, 2017

[24] Schüttrumpf, H., *Wellenüberlaufströmung bei Seedeichen - Experimentelle und Theoretische Untersuchungen*, PHD-Thesis, 2001

[25] Delft University of Technology, Environmental Fluid Mechanics Section, *SWASH - Implementation manual*, available from http://swash.sourceforge.net ,Version 6.01, August 2019

Appendices

.1 AWG data sheet

Ultrasonic distance measuring sensors

UNDK 20 (Sd = 400 mm)

sample drawing

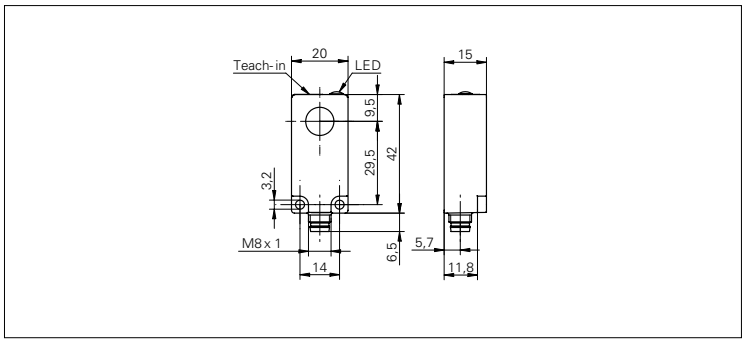

sample picture

general data	
scanning range sd	60 ... 400 mm
scanning range close limit Sdc	60 ... 400 mm
scanning range far limit Sde	60 ... 400 mm
repeat accuracy	< 0,5 mm
resolution	< 0,3 mm
response time ton	< 60 ms
release time toff	< 60 ms
temperature drift	< 2 % of distance to target So
sonic frequency	290 kHz
adjustment	Teach-in
alignment aid	target indication flashing
light indicator	yellow LED / red LED

electrical data	
voltage supply range +Vs	15 ... 30 VDC
output current	< 20 mA
residual ripple	< 10 % Vs
short circuit protection	yes
reverse polarity protection	yes
voltage output	
current consumption max. (no load)	35 mA
output signal	0 ... 10 V / 10 ... 0 V
current output	
current consumption max. (no load)	55 mA
output signal	4 ... 20 mA / 20 ... 4 mA
load resistance +Vs max.	< 1100 Ohm
load resistance +Vs min.	< 400 Ohm

mechanical data	
type	rectangular
housing material	polyester
width / diameter	20 mm
height / length	42 mm
depth	15 mm
connection types	connector M8

Ultrasonic distance measuring sensors

UNDK 20 (Sd = 400 mm)

ambient conditions	
operating temperature	-10 ... +60 °C
protection class	IP 67

order reference	output circuit
UNDK 20I6912/S35A	current output
UNDK 20U6912/S35A	voltage output

.2 Results in prototype

Test #	Overtopping				Velocity					Flow thickness				Promenade width	Comments
	q	Vmax	Vmax	V1/3	V1/10	u_cam1	u_cam2	u_AWG_tip	u_AWG_max	u_mean	ucam2-u_AWG_max/ucam2	λ_AWG1	λ_AWG0	λ_cam2(AWG0)	λ_mean	diffλ_cam2	w
	l/s/m	l/m (<2000)	l/m (<600)	l/m	l/m			m/s		(>15)				m			
20190710_0	15.9	2309.8	2309.8	1081.3	1425.8	NaN	NaN	NaN	NaN	#DIV/0!	#VALORE!	NaN	NaN	NaN	#DIV/0!	#VALORE!	NaN
20190710_1	11.6	1603.3	1603.3	891.1	1322.2	NaN	NaN	NaN	NaN	#DIV/0!	#VALORE!	NaN	NaN	NaN	#DIV/0!	#VALORE!	NaN
20190710_2	13.4	2608.7	2608.7	1180.8	1880.0	NaN	NaN	NaN	NaN	#DIV/0!	#VALORE!	NaN	NaN	NaN	#DIV/0!	#VALORE!	NaN
20190710_3	8.9	1625.0	1625.0	776.8	1169.8	NaN	NaN	NaN	NaN	#DIV/0!	#VALORE!	NaN	NaN	NaN	#DIV/0!	#VALORE!	NaN
20190710_4	11.2	2608.7	2608.7	1070.3	1740.5	NaN	NaN	NaN	NaN	#DIV/0!	#VALORE!	NaN	NaN	NaN	#DIV/0!	#VALORE!	NaN
20190711_0	15.2	2853.3	2853.3	1144.8	1699.9	NaN	NaN	NaN	NaN	#DIV/0!	#VALORE!	NaN	NaN	NaN	#DIV/0!	#VALORE!	NaN
20190711_1	13.3	2418.5	2418.5	1216.4	1762.4	NaN	NaN	NaN	NaN	#DIV/0!	#VALORE!	NaN	NaN	NaN	#DIV/0!	#VALORE!	NaN
20190711_2	12.7	2092.4	2092.4	1225.2	1691.5	5.70	NaN	NaN	NaN	#DIV/0!	#VALORE!	NaN	NaN	NaN	#DIV/0!	#VALORE!	NaN
20190711_3	13.8	3206.5	3206.5	1209.9	1735.2	NaN	NaN	NaN	NaN	#DIV/0!	#VALORE!	NaN	NaN	NaN	#DIV/0!	#VALORE!	NaN
20190712_0	14.6	3342.4	3342.4	1409.1	2138.0	6.34	NaN	NaN	NaN	#DIV/0!	#VALORE!	NaN	NaN	NaN	#DIV/0!	#VALORE!	NaN
20190712_1	9.6	1739.1	1739.1	1180.4	1527.2	NaN	NaN	NaN	NaN	#DIV/0!	#VALORE!	NaN	NaN	NaN	#DIV/0!	#VALORE!	NaN
20190712_2	9.0	1929.3	1929.3	1158.8	1576.1	NaN	NaN	NaN	NaN	#DIV/0!	#VALORE!	NaN	NaN	NaN	#DIV/0!	#VALORE!	NaN
20190712_3	14.1	3288.0	3288.0	1551.3	2179.7	NaN	NaN	NaN	NaN	#DIV/0!	#VALORE!	NaN	NaN	NaN	#DIV/0!	#VALORE!	NaN
20190712_4	6.3	1277.2	1277.2	953.5	1182.1	NaN	NaN	NaN	NaN	#DIV/0!	#VALORE!	NaN	NaN	NaN	#DIV/0!	#VALORE!	NaN
20190712_5	13.3	3532.6	3532.6	768.2	1455.1	NaN	NaN	NaN	NaN	#DIV/0!	#VALORE!	NaN	NaN	NaN	#DIV/0!	#VALORE!	NaN
20190715_0	16.4	2089.7	2089.7	1312.9	1739.6	NaN	NaN	NaN	NaN	#DIV/0!	#VALORE!	NaN	NaN	NaN	#DIV/0!	#VALORE!	NaN
20190715_1	16.7	3130.4	3130.4	1625.1	2266.8	NaN	NaN	NaN	NaN	#DIV/0!	#VALORE!	NaN	NaN	NaN	#DIV/0!	#VALORE!	NaN
20190715_2	16.4	3046.2	3046.2	1453.6	2049.4	5.36	NaN	NaN	NaN	#DIV/0!	#VALORE!	NaN	NaN	NaN	#DIV/0!	#VALORE!	NaN
20190715_3	14.5	3470.1	3470.1	1405.1	2075.5	4.27	NaN	NaN	NaN	#DIV/0!	#VALORE!	NaN	NaN	NaN	#DIV/0!	#VALORE!	NaN
20190715_4	15.8	2989.1	2989.1	939.4	1542.8	4.18	NaN	NaN	NaN	#DIV/0!	#VALORE!	NaN	NaN	NaN	#DIV/0!	#VALORE!	NaN
20190716_0	23.3	3812.5	3812.5	1781.4	2707.2	NaN	NaN	NaN	NaN	#DIV/0!	#VALORE!	NaN	NaN	NaN	#DIV/0!	#VALORE!	NaN
20190716_1	21.0	4293.5	4293.5	1806.6	2830.5	5.14	NaN	NaN	NaN	#DIV/0!	#VALORE!	NaN	NaN	NaN	#DIV/0!	#VALORE!	NaN
20190716_2	31.8	10597.8	10597.8	2421.8	3889.1	NaN	NaN	NaN	NaN	#DIV/0!	#VALORE!	NaN	NaN	NaN	#DIV/0!	#VALORE!	NaN
20190716_3	30.5	11385.9	11385.9	2302.9	3643.8	10.05	NaN	NaN	NaN	#DIV/0!	#VALORE!	NaN	NaN	NaN	#DIV/0!	#VALORE!	NaN
20190716_4	14.0	8342.4	8342.4	2215.1	3563.0	NaN	NaN	NaN	NaN	#DIV/0!	#VALORE!	NaN	NaN	NaN	#DIV/0!	#VALORE!	NaN
20190716_5	14.1	7146.7	7146.7	2308.4	3813.5	8.91	NaN	NaN	NaN	#DIV/0!	#VALORE!	NaN	NaN	NaN	#DIV/0!	#VALORE!	NaN
20190717_0	4.6	1997.3	1997.3	947.5	1391.9	NaN	NaN	NaN	NaN	#DIV/0!	#VALORE!	NaN	NaN	NaN	#DIV/0!	#VALORE!	6.00
20190717_1	4.4	1899.5	1899.5	1120.2	1602.9	3.61	NaN	NaN	NaN	#DIV/0!	#VALORE!	NaN	NaN	NaN	#DIV/0!	#VALORE!	6.00
20190717_2	29.1	10054.3	10054.3	2332.0	3764.0	NaN	NaN	NaN	NaN	#DIV/0!	#VALORE!	NaN	NaN	NaN	#DIV/0!	#VALORE!	6.00
20190717_3	28.0	11277.2	11277.2	2278.2	3478.7	11.76	NaN	NaN	NaN	#DIV/0!	#VALORE!	NaN	NaN	NaN	#DIV/0!	#VALORE!	6.00
20190717_4	26.2	11055.8	11055.8	2594.9	4072.1	8.77	NaN	NaN	NaN	#DIV/0!	#VALORE!	NaN	NaN	NaN	#DIV/0!	#VALORE!	6.00
20190718_0	22.3	8679.7	8679.7	2553.5	3956.3	6.13	NaN	#VALORE!	#VALORE!	#VALORE!	#VALORE!	NaN	NaN	NaN	#DIV/0!	#VALORE!	6.00
20190718_1	21.4	9756.1	9756.1	2342.8	3755.7	5.34	NaN	NaN	NaN	#DIV/0!	#VALORE!	NaN	NaN	NaN	#DIV/0!	#VALORE!	6.00
20190718_2	13.6	4300.1	4300.1	1766.1	2698.4	6.60	NaN	#VALORE!	#VALORE!	#VALORE!	#VALORE!	NaN	NaN	NaN	#DIV/0!	#VALORE!	6.00
20190718_3	10.5	2941.7	2941.7	1401.3	1998.1	7.07	NaN	#VALORE!	#VALORE!	#VALORE!	#VALORE!	NaN	NaN	NaN	#DIV/0!	#VALORE!	6.00
20190719_0	5.4	2165.8	2165.8	1246.4	1753.3	NaN	NaN	NaN	NaN	#DIV/0!	#VALORE!	NaN	NaN	NaN	#DIV/0!	#VALORE!	6.00
20190719_1	4.9	2154.9	2154.9	1173.4	1771.7	7.07	NaN	NaN	NaN	#DIV/0!	#VALORE!	NaN	NaN	NaN	#DIV/0!	#VALORE!	6.00
20190719_2	4.5	2771.7	2771.7	1683.3	2293.5	NaN	NaN	NaN	NaN	#DIV/0!	#VALORE!	NaN	NaN	NaN	#DIV/0!	#VALORE!	6.00
20190719_3	4.9	3978.3	3978.3	2178.0	3019.0	5.03	NaN	NaN	NaN	#DIV/0!	#VALORE!	NaN	NaN	NaN	#DIV/0!	#VALORE!	6.00
20190719_4	4.8	2201.1	2201.1	1256.1	1709.2	NaN	NaN	NaN	NaN	#DIV/0!	#VALORE!	NaN	NaN	NaN	#DIV/0!	#VALORE!	6.00
20190722_0	5.2	2418.5	2418.5	1458.9	2021.1	7.39	NaN	NaN	NaN	#DIV/0!	#VALORE!	NaN	NaN	NaN	#DIV/0!	#VALORE!	6.00
20190722_1	5.7	2445.7	2445.7	1739.1	2330.2	NaN	NaN	NaN	NaN	#DIV/0!	#VALORE!	NaN	NaN	NaN	#DIV/0!	#VALORE!	6.00
20190722_2	5.6	3097.8	3097.8	1658.3	2288.7	7.86	NaN	NaN	NaN	#DIV/0!	#VALORE!	NaN	NaN	NaN	#DIV/0!	#VALORE!	6.00
20190722_3	4.1	2820.7	2820.7	1874.7	2452.9	NaN	NaN	NaN	NaN	#DIV/0!	#VALORE!	NaN	NaN	NaN	#DIV/0!	#VALORE!	6.00
20190722_4	4.3	2771.7	2771.7	1628.3	2477.4	7.39	NaN	NaN	NaN	#DIV/0!	#VALORE!	NaN	NaN	NaN	#DIV/0!	#VALORE!	6.00
20190722_5	5.2	2853.3	2853.3	1702.6	2442.3	5.82	NaN	NaN	NaN	#DIV/0!	#VALORE!	NaN	NaN	NaN	#DIV/0!	#VALORE!	6.00
20190722_6	5.8	4891.3	4891.3	1651.2	2541.4	NaN	NaN	NaN	NaN	#DIV/0!	#VALORE!	NaN	NaN	NaN	#DIV/0!	#VALORE!	6.00
20190722_7	6.0	4269.0	4269.0	1768.9	2792.8	6.29	NaN	NaN	NaN	#DIV/0!	#VALORE!	NaN	NaN	NaN	#DIV/0!	#VALORE!	6.00
20190722_8	5.2	4684.8	4684.8	2089.2	3490.9	NaN	NaN	NaN	NaN	#DIV/0!	#VALORE!	NaN	NaN	NaN	#DIV/0!	#VALORE!	6.00
20190722_9	4.9	5130.4	5130.4	2045.0	3653.1	8.64	NaN	NaN	NaN	#DIV/0!	#VALORE!	NaN	NaN	NaN	#DIV/0!	#VALORE!	6.00
20190722_10	6.8	3991.8	3991.8	1925.1	2595.1	NaN	NaN	NaN	NaN	#DIV/0!	#VALORE!	NaN	NaN	NaN	#DIV/0!	#VALORE!	6.00
20190722_11	6.4	3184.8	3184.8	1942.4	2690.2	8.64	NaN	NaN	NaN	#DIV/0!	#VALORE!	NaN	NaN	NaN	#DIV/0!	#VALORE!	6.00

20190722_12	6.7	3399.5	3399.5	1673.9	2571.2	NaN	NaN	NaN	NaN	#DIV/0!	#VALORE!	NaN	NaN	NaN	#DIV/0!	#VALORE!	6.00			
20190722_13	6.8	3978.3	3978.3	1685.3	2687.0	5.34	NaN	NaN	NaN	#DIV/0!	#VALORE!	NaN	NaN	NaN	#DIV/0!	#VALORE!	6.00			
20190722_14	3.5	2057.1	2057.1	1239.2	1810.8	NaN	NaN	NaN	NaN	#DIV/0!	#VALORE!	NaN	NaN	NaN	#DIV/0!	#VALORE!	6.00			
20190722_15	3.8	2165.8	2165.8	1201.8	1964.2	7.86	NaN	NaN	NaN	#DIV/0!	#VALORE!	NaN	NaN	NaN	#DIV/0!	#VALORE!	6.00			
20190722_16	14.9	4565.2	4565.2	1857.3	2675.0	NaN	NaN	NaN	NaN	#DIV/0!	#VALORE!	NaN	NaN	NaN	#DIV/0!	#VALORE!	6.00			
20190722_17	13.5	4320.7	4320.7	1876.0	2560.4	8.64	NaN	NaN	NaN	#DIV/0!	#VALORE!	NaN	NaN	NaN	#DIV/0!	#VALORE!	6.00			
20190723_0	14.4	3750.0	3750.0	1645.5	2373.8	NaN	NaN	NaN	NaN	#DIV/0!	#VALORE!	NaN	NaN	NaN	#DIV/0!	#VALORE!	6.00			
20190723_1	14.3	3043.5	3043.5	1550.3	2086.7	NaN	NaN	NaN	NaN	#DIV/0!	#VALORE!	NaN	NaN	NaN	#DIV/0!	#VALORE!	6.00			
20190723_2	14.0	3233.7	3233.7	1593.0	2154.9	7.39	6.13	NaN	NaN	6.13	#VALORE!	NaN	NaN	1.50	1.500	#VALORE!	6.00			
20190723_4	14.4	4968.5	4968.5	1864.2	2757.9	NaN	NaN	NaN	NaN	#DIV/0!	#VALORE!	NaN	NaN	NaN	#DIV/0!	#VALORE!	6.00			
20190723_5	15.2	5174.2	5174.2	1843.5	3011.0	7.07	5.66	NaN	NaN	5.66	#VALORE!	NaN	NaN	1.25	1.250	#VALORE!	6.00			
20190723_6	13.1	3809.4	3809.4	1794.8	2608.5	NaN	NaN	NaN	NaN	#DIV/0!	#VALORE!	NaN	NaN	NaN	#DIV/0!	#VALORE!	6.00			
20190723_7	12.7	3006.9	3006.9	1776.6	2502.9	7.07	6.60	NaN	NaN	6.60	#VALORE!	NaN	NaN	1.75	1.750	#VALORE!	6.00	Splash		
20190724_0	13.4	3698.5	3698.5	1721.1	2513.1	NaN	NaN	NaN	NaN	#DIV/0!	#VALORE!	NaN	NaN	NaN	#DIV/0!	#VALORE!	6.00			
20190724_1	12.9	3275.7	3275.7	1561.5	2190.1	6.60	5.28	NaN	NaN	5.28	#VALORE!	NaN	NaN	1.25	1.250	#VALORE!	6.00			
20190724_2	6.6	2161.1	2161.1	1391.3	1854.2	NaN	NaN	NaN	NaN	#DIV/0!	#VALORE!	NaN	NaN	NaN	#DIV/0!	#VALORE!	6.00			
20190724_3	6.9	2144.6	2144.6	1244.7	1721.2	6.12	4.72	NaN	NaN	4.72	#VALORE!	NaN	NaN	0.75	0.750	#VALORE!	6.00			
20190724_4	7.7	3178.2	3178.2	1865.5	2641.3	NaN	NaN	NaN	NaN	#DIV/0!	#VALORE!	NaN	NaN	NaN	#DIV/0!	#VALORE!	6.00			
20190724_5	7.4	2651.5	2651.5	1682.0	2295.0	7.86	6.60	NaN	NaN	6.60	#VALORE!	NaN	NaN	1.25	1.250	#VALORE!	6.00			
20190724_6	6.4	2184.2	2184.2	1455.6	1909.6	NaN	NaN	NaN	NaN	#DIV/0!	#VALORE!	NaN	NaN	NaN	#DIV/0!	#VALORE!	6.00			
20190724_7	7.5	2587.7	2587.7	1686.5	2349.6	8.64	7.07	NaN	NaN	7.07	#VALORE!	NaN	NaN	1.25	1.250	#VALORE!	6.00			
20190725_0	7.9	3350.1	3350.1	1743.8	2423.8	NaN	NaN	NaN	NaN	#DIV/0!	#VALORE!	NaN	NaN	NaN	#DIV/0!	#VALORE!	6.00			
20190725_1	7.8	3361.8	3361.8	1916.6	2674.5	6.60	6.13	NaN	NaN	6.13	#VALORE!	NaN	NaN	0.88	0.875	#VALORE!	6.00			
20190725_2	6.9	2501.4	2501.4	1524.2	2209.7	NaN	NaN	NaN	NaN	#DIV/0!	#VALORE!	NaN	NaN	NaN	#DIV/0!	#VALORE!	6.00			
20190725_3	6.5	2513.1	2513.1	1463.2	1996.5	8.64	6.13	NaN	NaN	6.13	#VALORE!	NaN	NaN	1.50	1.500	#VALORE!	6.00			
20190725_4	7.4	3498.3	3498.3	1799.7	2946.1	NaN	NaN	NaN	NaN	#DIV/0!	#VALORE!	NaN	NaN	NaN	#DIV/0!	#VALORE!	6.00			
20190725_5	7.9	4561.2	4561.2	1837.5	3055.5	7.07	6.60	NaN	NaN	6.60	#VALORE!	NaN	NaN	1.38	1.375	#VALORE!	6.00			
20190725_6	7.1	3299.6	3299.6	1878.2	2719.7	NaN	NaN	NaN	NaN	#DIV/0!	#VALORE!	NaN	NaN	NaN	#DIV/0!	#VALORE!	6.00			
20190725_7	8.0	4429.5	4429.5	2039.5	3249.8	7.07	5.66	NaN	NaN	5.66	#VALORE!	NaN	NaN	1.13	1.125	#VALORE!	6.00			
20190725_8	7.9	2970.9	2970.9	1803.3	2451.7	NaN	NaN	NaN	NaN	#DIV/0!	#VALORE!	NaN	NaN	NaN	#DIV/0!	#VALORE!	6.00			
20190725_9	7.8	4132.0	4132.0	1873.4	2682.7	7.86	6.60	NaN	NaN	6.60	#VALORE!	NaN	NaN	1.00	1.000	#VALORE!	6.00			
20190725_10	8.6	2519.1	2519.1	1518.1	2113.2	NaN	NaN	NaN	NaN	#DIV/0!	#VALORE!	NaN	NaN	NaN	#DIV/0!	#VALORE!	6.00			
20190725_11	7.8	3133.4	3133.4	1666.5	2567.0	5.82	6.13	#VALORE!	#VALORE!	#VALORE!	#VALORE!	NaN	NaN	1.38	1.375	#VALORE!	6.00			
20190725_12	7.4	3531.6	3531.6	1782.0	2920.5	NaN	NaN	NaN	NaN	#DIV/0!	#VALORE!	NaN	NaN	NaN	#DIV/0!	#VALORE!	6.00			
20190725_13	7.8	3207.1	3207.1	1622.0	2511.4	5.03	4.80	NaN	NaN	4.80	#VALORE!	NaN	NaN	1.13	1.125	#VALORE!	6.00			
20190725_14	14.3	4424.9	4424.9	2085.2	3048.4	NaN	NaN	NaN	NaN	#DIV/0!	#VALORE!	NaN	NaN	NaN	#DIV/0!	#VALORE!	6.00			
20190725_15	14.4	4288.0	4288.0	2042.9	3096.7	6.13	6.60	NaN	NaN	6.60	#VALORE!	NaN	NaN	1.00	1.000	#VALORE!	6.00			
20190725_16	15.0	3947.7	3947.7	1967.1	2787.0	NaN	NaN	NaN	NaN	#DIV/0!	#VALORE!	NaN	NaN	NaN	#DIV/0!	#VALORE!	6.00			
20190725_17	14.5	5243.3	5243.3	1901.3	2811.5	7.86	5.34	NaN	NaN	5.34	#VALORE!	NaN	NaN	1.25	1.250	#VALORE!	6.00			
20190725_18	13.6	3678.4	3678.4	1678.6	2513.5	NaN	NaN	NaN	NaN	#DIV/0!	#VALORE!	NaN	NaN	NaN	#DIV/0!	#VALORE!	6.00			
20190725_19	14.5	3656.3	3656.3	1708.0	2814.2	7.39	6.13	NaN	NaN	6.13	#VALORE!	NaN	NaN	1.38	1.375	#VALORE!	6.00			
20190726_0	17.7	4093.3	4093.3	1866.6	2781.2	NaN	NaN	NaN	NaN	#DIV/0!	#VALORE!	1.658	1.264	NaN	1.264	#VALORE!	6.00			
20190726_1	17.2	3675.6	3675.6	1903.2	2990.3	5.66	6.13	#VALORE!	NaN	6.13	#VALORE!	NaN	NaN	1.75	1.750	#VALORE!	6.00	Splash		
20190726_2	17.5	7431.6	7431.6	1990.9	3600.4	NaN	NaN	NaN	NaN	#DIV/0!	#VALORE!	NaN	NaN	NaN	#DIV/0!	#VALORE!	6.00			
20190726_3	17.9	8498.6	8498.6	2070.4	3809.6	7.07	7.07	NaN	NaN	7.07	#VALORE!	NaN	NaN	2.00	2.000	#VALORE!	6.00	Splash		
20190726_4	7.8	9467.2	9467.2	2932.0	5239.4	NaN	NaN	NaN	NaN	#DIV/0!	#VALORE!	NaN	NaN	NaN	#DIV/0!	#VALORE!	6.00			
20190726_5	8.0	8902.6	8902.6	3147.2	5594.7	9.43	7.86	NaN	NaN	7.86	#VALORE!	NaN	NaN	1.50	1.500	#VALORE!	6.00			
20190726_6	13.5	9622.3	9622.3	2698.5	4646.4	NaN	NaN	NaN	NaN	#DIV/0!	#VALORE!	NaN	NaN	NaN	#DIV/0!	#VALORE!	6.00			
20190726_7	13.2	10124.6	10124.6	2630.7	4612.8	9.43	8.64	NaN	NaN	8.64	#VALORE!	NaN	NaN	1.38	1.375	#VALORE!	6.00			
20190726_8	25.2	10486.5	10486.5	2508.2	4005.1	NaN	NaN	NaN	NaN	#DIV/0!	#VALORE!	NaN	NaN	NaN	#DIV/0!	#VALORE!	6.00			
20190726_9	2.2	1474.3	1474.3	866.1	1215.1	NaN	NaN	NaN	NaN	#DIV/0!	#VALORE!	NaN	NaN	NaN	#DIV/0!	#VALORE!	6.00			
20190726_10	0.9	850.7	850.7	850.7	NaN	NaN	NaN	NaN	NaN	#DIV/0!	#VALORE!	NaN	NaN	NaN	#DIV/0!	#VALORE!	6.00			
20190726_11	2.2	940.2	940.2	849.5	939.6	6.13	6.13	NaN	NaN	6.13	#VALORE!	NaN	NaN	0.75	0.750	#VALORE!	6.00			
20190726_12	0.8	702.8	702.8	702.8	NaN	NaN	NaN	NaN	NaN	#DIV/0!	#VALORE!	NaN	NaN	NaN	#DIV/0!	#VALORE!	6.00			
20190726_13	0.5	455.9	455.9	422.4	455.9	5.82	4.80	NaN	NaN	4.80	#VALORE!	NaN	NaN	0.50	0.500	#VALORE!	6.00			

20190726_14	0.2	403.7	403.7	404.4	NaN	NaN	NaN	NaN	NaN	NaN	#DIV/0!	#VALORE!	NaN	NaN	NaN		#DIV/0!	#VALORE!	6.00			
20190726_16	0.6	1027.4	1027.4	811.1	1027.4	6.13	4.80	NaN	NaN		4.80	#VALORE!	NaN	NaN		0.50	0.500	#VALORE!	6.00			
20190726_17	0.3	1128.3	1128.3	1128.3	NaN	7.07	5.82	NaN	NaN		5.82	#VALORE!	NaN	NaN		0.75	0.750	#VALORE!	6.00			
20190726_18	6.0	4916.2	4916.2	1797.7	2598.6	7.07	5.82	NaN	NaN		5.82	#VALORE!	NaN	NaN		1.25	1.250	#VALORE!	6.00			
20190910_0	2.0	1452.6	1452.6	771.1	1452.6	NaN	NaN	1.74	1.67		1.67	#VALORE!	0.118	0.129	NaN		0.129	#VALORE!	6.00			
20190910_1	1.9	1462.7	1462.7	678.8	863.7	NaN	NaN	10.43	5.21		5.21	#VALORE!	NaN	NaN	NaN		#DIV/0!	#VALORE!	6.00			
20190910_2	2.1	1509.8	1509.8	561.2	692.8	NaN	NaN	1.02	1.04		1.04	#VALORE!	NaN	0.103	NaN		0.103	#VALORE!	6.00			
20190910_3	2.7	1526.8	1526.8	740.0	827.0	NaN	NaN	5.96	8.34		8.34	#VALORE!	0.147	NaN	NaN		#DIV/0!	#VALORE!	6.00			
20190910_4	3.5	1867.5	1867.5	1410.3	1815.3	NaN	NaN	4.17	4.17		4.17	#VALORE!	0.226	0.581	NaN		0.581	#VALORE!	6.00			
20190910_5	4.0	1951.6	1951.6	1124.6	1511.6	NaN	NaN	5.96	NaN		#DIV/0!	#VALORE!	NaN	NaN	NaN		#DIV/0!	#VALORE!	6.00	Δ_{tmax} non conforme		
20190910_6	3.7	1466.1	1466.1	1019.8	1296.4	NaN	NaN	6.95	6.95		6.95	#VALORE!	0.476	0.260	NaN		0.260	#VALORE!	6.00			
20190912_0	5.7	2505.9	2505.9	1558.1	2460.9	NaN	NaN	7.31	2.44		2.44	#VALORE!	0.371	0.228	NaN		0.228	#VALORE!	12.00			
20190912_1	6.6	2883.7	2883.7	1777.0	2742.3	NaN	NaN	6.26	#VALORE!		#VALORE!	#VALORE!	0.858	0.257	NaN		0.257	#VALORE!	12.00			
20190912_2	6.7	3029.2	3029.2	1677.4	2368.4	NaN	NaN	2.92	1.00		1.00	#VALORE!	0.182	0.139	NaN		0.139	#VALORE!	12.00			
20190912_3	7.4	3540.3	3540.3	1673.2	2706.5	6.26	5.48	0.76	0.61		3.04	89%	NaN	0.250		1.00	0.625	-75%	12.00			
20190912_4	7.5	2175.8	2175.8	1468.3	1894.4	3.51	2.92	2.74	1.29		2.11	56%	0.336	1.061		0.25	0.656	325%	12.00			
20190912_5	8.3	2323.1	2323.1	1259.7	1772.7	NaN	NaN	3.65	#VALORE!		#VALORE!	#VALORE!	1.309	1.013	NaN		1.013	#VALORE!	12.00			
20190913_0	13.7	4177.4	4177.4	1855.7	2680.8	NaN	NaN	6.26	4.38		4.38	#VALORE!	0.791	0.566	NaN		0.566	#VALORE!	12.00			
20190913_1	13.0	2934.7	2934.7	1691.1	2346.6	NaN	NaN	14.61	6.26		6.26	#VALORE!	0.260	0.414	NaN		0.414	#VALORE!	12.00			
20190913_2	13.5	3905.5	3905.5	2059.5	3290.3	NaN	NaN	5.48	1.83		1.83	#VALORE!	NaN	0.816	NaN		0.816	#VALORE!	12.00			
20190913_3	11.6	3852.9	3852.9	1826.7	3016.0	NaN	NaN	4.87	10.96		10.96	#VALORE!	0.354	0.361	NaN		0.361	#VALORE!	12.00			
20190913_4	13.9	5236.8	5236.8	1995.5	3353.5	NaN	NaN	1.83	14.61		14.61	#VALORE!	NaN	NaN	NaN		#DIV/0!	#VALORE!	12.00			
20190916_0	7.6	3058.9	3058.9	1653.9	2330.9	NaN	NaN	2.44	6.26		6.26	#VALORE!	0.502	0.293	NaN		0.293	#VALORE!	12.00			
20190916_1	7.5	3094.3	3094.3	1473.9	2339.6	6.26	5.48	5.48	5.48		5.48	0%	0.334	0.231		0.70	0.465	-67%	12.00			
20190916_2	9.8	4320.7	4320.7	2290.8	3415.7	NaN	NaN	#VALORE!	10.96		10.96	#VALORE!	0.732	0.518	NaN		0.518	#VALORE!	12.00			
20190916_3	9.7	5634.4	5634.4	2263.5	3670.4	2.51	NaN	6.26	14.61		14.61	#VALORE!	0.655	0.719	NaN		0.719	#VALORE!	12.00			
20190917_0	10.6	4573.7	4573.7	1859.6	2770.0	NaN	NaN	2.58	4.87		4.87	#VALORE!	0.371	0.362	NaN		0.362	#VALORE!	12.00			
20190917_1	11.2	3975.6	3975.6	1880.2	2825.7	NaN	NaN	2.92	#VALORE!		#VALORE!	#VALORE!	0.342	0.426	NaN		0.426	#VALORE!	12.00			
20190917_2	10.8	3952.6	3952.6	1717.6	2477.6	6.74	7.97	8.77	4.87		6.42	39%	0.605	0.394		1.00	0.697	-61%	12.00			
20190917_3	11.2	3955.3	3955.3	1795.0	2803.0	5.85	4.87	7.31	#VALORE!		#VALORE!	#VALORE!	0.518	0.325		0.55	0.438	-41%	12.00			
20190917_4	10.9	3292.6	3292.6	1713.9	2545.5	NaN	NaN	8.77	7.31		7.31	#VALORE!	0.449	0.509	NaN		0.509	#VALORE!	12.00			
20190917_5	11.3	3654.9	3654.9	2158.4	3163.7	7.31	8.77	10.96	6.26		7.52	29%	0.399	0.240		1.00	0.620	-76%	12.00			
20190918_0	14.2	6407.8	6407.8	2553.4	4458.1	NaN	NaN	14.61	#VALORE!		#VALORE!	#VALORE!	0.369	0.658	NaN		0.658	#VALORE!	12.00			
20190918_1	12.4	5207.3	5207.3	2158.5	3337.9	NaN	NaN	0.80	0.66		0.66	#VALORE!	0.600	NaN	NaN		#DIV/0!	#VALORE!	12.00			
20190918_2	14.4	6795.3	6795.3	2819.4	4838.6	7.31	6.74	3.65	10.96		8.85	-63%	0.595	0.260		1.50	0.880	-83%	12.00			
20190918_3	12.5	3792.7	3792.7	2274.5	2970.3	5.16	5.85	4.38	0.58		3.21	90%	0.176	NaN		1.05	1.050	#VALORE!	12.00			
20190918_4	6.8	2082.6	2082.6	1235.4	1908.1	NaN	NaN	14.61	#VALORE!		#VALORE!	#VALORE!	0.196	0.183	NaN		0.183	#VALORE!	12.00			
20190918_5	11.9	3568.7	3568.7	1843.5	2932.7	NaN	NaN	7.31	5.48		5.48	#VALORE!	0.348	0.460	NaN		0.460	#VALORE!	12.00			
20190918_6	15.7	6391.8	6391.8	2053.9	3347.4	NaN	NaN	5.48	4.38		4.38	#VALORE!	0.382	0.388	NaN		0.388	#VALORE!	12.00			
20190918_7	5.9	1989.3	1989.3	1261.2	1723.1	NaN	NaN	4.87	4.87		4.87	#VALORE!	0.245	0.221	NaN		0.221	#VALORE!	12.00			
20190918_8	10.2	3387.3	3387.3	1458.2	2228.5	NaN	NaN	4.87	6.26		6.26	#VALORE!	0.236	0.213	NaN		0.213	#VALORE!	12.00			
20190918_9	14.1	4838.6	4838.6	1795.6	2531.5	NaN	NaN	0.70	NaN		#DIV/0!	#VALORE!	NaN	NaN	NaN		#DIV/0!	#VALORE!	12.00	Δ_{tmax} non conforme		
20190918_10	10.4	2832.9	2832.9	1515.8	2029.1	NaN	NaN	10.96	NaN		#DIV/0!	#VALORE!	0.571	NaN	NaN		#DIV/0!	#VALORE!	12.00	Δ_{tmax} non conforme		
20190919_0	17.1	4443.5	4443.5	2130.5	3150.3	NaN	NaN	1.10	NaN		#DIV/0!	#VALORE!	NaN	NaN	NaN		#DIV/0!	#VALORE!	12.00	Δ_{tmax} non conforme		
20190919_1	18.6	4522.7	4522.7	2227.8	3175.2	NaN	10.96	3.37	3.37		7.17	69%	NaN	NaN		1.25	1.250	#VALORE!	12.00			
20190919_2	18.6	3791.3	3791.3	2111.8	3060.6	NaN	NaN	7.31	14.61		14.61	#VALORE!	0.242	0.317	NaN		0.317	#VALORE!	12.00			
20190919_3	1.0	1830.0	1830.0	1355.9	1830.0	NaN	NaN	4.38	5.48		5.48	#VALORE!	0.243	0.185	NaN		0.185	#VALORE!	12.00			
20190919_4	1.3	1651.9	1651.9	1376.1	1651.9	NaN	5.85	6.26	10.96		8.40	-88%	0.356	0.408		0.25	0.329	63%	12.00			
20190920_0	11.0	5596.2	5596.2	2947.8	4396.2	NaN	NaN	9.29	13.01		13.01	#VALORE!	0.817	0.488	NaN		0.488	#VALORE!	12.00			
20190920_1	1.9	2396.0	2396.0	1586.3	2396.0	NaN	NaN	3.83	3.61		3.61	#VALORE!	0.185	0.125	NaN		0.125	#VALORE!	12.00			
20190920_2	1.7	3110.3	3110.3	2144.0	3110.3	NaN	NaN	13.01	10.84		10.84	#VALORE!	0.501	0.281	NaN		0.281	#VALORE!	12.00			
20190920_3	1.8	1627.3	1627.3	1304.2	1627.3	NaN	7.12	5.42	1.36		4.24	81%	0.260	0.280		0.20	0.240	40%	12.00			
20190920_4	1.9	3156.8	3156.8	2195.9	3156.8	NaN	7.54	5.42	16.26		11.90	-116%	0.776	0.506		0.50	0.503	1%	12.00			
20190920_5	0.6	1240.5	1240.5	1240.5	NaN	NaN	NaN	4.34	4.34		4.34	#VALORE!	0.397	0.117	NaN		0.117	#VALORE!	12.00			
20190920_6	3.1	5148.0	5148.0	2339.2	3800.9	NaN	NaN	7.23	8.13		8.13	#VALORE!	0.460	0.308	NaN		0.308	#VALORE!	12.00			

20190920_7	**3.0**	**4888.6**	**4888.6**	**2557.3**	**4888.6**	NaN	12.82	1.97	#VALORE!	**#VALORE!**	**#VALORE!**	1.585	1.601	0.25	**0.925**	**540%**	12.00						
20190920_8	**2.0**	**1812.0**	**1812.0**	**1342.5**	**1812.0**	NaN	NaN	5.00	5.42	**5.42**	**#VALORE!**	0.352	0.183	NaN	**0.183**	**#VALORE!**	12.00						
20190920_9	**2.0**	**1624.3**	**1624.3**	**1427.9**	**1624.3**	NaN	6.75	6.51	13.01	**9.88**	**-93%**	0.282	0.218	0.20	**0.209**	**9%**	12.00						
20190923_0	**1.6**	**1561.8**	**1561.8**	**991.1**	**1561.8**	NaN	NaN	16.26	NaN	**#DIV/0!**	**#VALORE!**	NaN	NaN	NaN	**#DIV/0!**	**#VALORE!**	12.00	Δ_{tmax} non conforme					
20190923_1	**1.3**	**2473.2**	**2473.2**	**1670.6**	**2473.2**	NaN	NaN	0.84	0.84	**0.84**	**#VALORE!**	NaN	NaN	NaN	**#DIV/0!**	**#VALORE!**	12.00						
20190925_0	**0.9**	**1502.0**	**1502.0**	**1269.2**	**1502.0**	NaN	NaN	1.14	1.14	**1.14**	**#VALORE!**	NaN	NaN	NaN	**#DIV/0!**	**#VALORE!**	12.00						
20190925_1	**1.5**	**1639.4**	**1639.4**	**1379.2**	**1639.4**	NaN	10.68	1.25	1.23	**5.95**	**89%**	NaN	NaN	0.25	**0.250**	**#VALORE!**	12.00						
20190925_2	**1.0**	**2033.2**	**2033.2**	**1376.5**	**2033.2**	NaN	5.13	13.01	NaN	**5.13**	**#VALORE!**	NaN	NaN	0.30	**0.300**	**#VALORE!**	12.00	Δ_{tmax} non conforme					
20190925_3	**0.8**	**1151.7**	**1151.7**	**1151.7**	**NaN**	NaN	NaN	1.59	1.71	**1.71**	**#VALORE!**	NaN	NaN	NaN	**#DIV/0!**	**#VALORE!**	12.00						
20190925_4	**1.1**	**2395.3**	**2395.3**	**2395.3**	**NaN**	NaN	NaN	1.45	1.45	**1.45**	**#VALORE!**	NaN	NaN	NaN	**#DIV/0!**	**#VALORE!**	12.00						
20190925_5	**45.9**	**6057.2**	**6057.2**	**2417.7**	**3491.0**	NaN	NaN	8.13	9.29	**9.29**	**#VALORE!**	NaN	NaN	NaN	**#DIV/0!**	**#VALORE!**	12.00						
20190925_6	**44.8**	**7583.7**	**7583.7**	**2358.2**	**3614.6**	NaN	NaN	1.51	1.51	**1.51**	**#VALORE!**	NaN	NaN	NaN	**#DIV/0!**	**#VALORE!**	12.00						
20190925_7	**44.0**	**5609.8**	**5609.8**	**2194.5**	**3304.8**	NaN	NaN	5.00	10.84	**10.84**	**#VALORE!**	NaN	NaN	NaN	**#DIV/0!**	**#VALORE!**	12.00						
20190925_8	**37.0**	**3882.3**	**3882.3**	**1789.5**	**2680.0**	NaN	NaN	7.23	NaN	**#DIV/0!**	**#VALORE!**	NaN	NaN	NaN	**#DIV/0!**	**#VALORE!**	12.00	Δ_{tmax} non conforme					
20190925_10	**52.7**	**9572.5**	**9572.5**	**2717.1**	**4257.2**	NaN	NaN	3.83	2.03	**2.03**	**#VALORE!**	NaN	NaN	NaN	**#DIV/0!**	**#VALORE!**	12.00						
20190926_0	**12.2**	**3730.0**	**3730.0**	**1939.5**	**3092.5**	NaN	NaN	#VALORE!	3.42	**3.42**	**#VALORE!**	NaN	NaN	NaN	**#DIV/0!**	**#VALORE!**	12.00						
20190926_1	**12.0**	**4003.7**	**4003.7**	**1970.8**	**3305.0**	NaN	16.02	5.91	6.51	**11.26**	**59%**	NaN	NaN	0.80	**0.800**	**#VALORE!**	12.00						
20190926_2	**9.5**	**4305.0**	**4305.0**	**2055.2**	**3214.0**	NaN	NaN	#VALORE!	8.13	**8.13**	**#VALORE!**	0.644	0.597	NaN	**0.597**	**#VALORE!**	12.00						
20190926_3	**7.9**	**3074.7**	**3074.7**	**1423.6**	**2223.7**	NaN	NaN	5.42	5.91	**5.91**	**#VALORE!**	1.090	0.330	NaN	**0.330**	**#VALORE!**	12.00						
20190926_4	**7.8**	**1936.2**	**1936.2**	**1394.0**	**1720.3**	NaN	NaN	10.84	4.65	**4.65**	**#VALORE!**	0.258	0.391	NaN	**0.391**	**#VALORE!**	12.00						
20190926_5	**8.7**	**4697.4**	**4697.4**	**2176.7**	**3262.9**	NaN	8.01	13.01	4.07	**6.04**	**49%**	0.822	0.396	0.75	**0.573**	**-47%**	12.00						
20190926_6	**9.1**	**4974.6**	**4974.6**	**2025.6**	**3546.8**	NaN	9.86	16.26	6.51	**8.18**	**34%**	0.706	0.694	0.63	**0.660**	**11%**	12.00						
20190926_7	**4.6**	**2027.8**	**2027.8**	**1165.4**	**1685.0**	NaN	NaN	5.42	7.23	**7.23**	**#VALORE!**	0.771	0.252	NaN	**0.252**	**#VALORE!**	12.00						
20190926_8	**13.4**	**5588.4**	**5588.4**	**2270.6**	**3596.2**	NaN	NaN	#VALORE!	13.01	**13.01**	**#VALORE!**	0.679	0.474	NaN	**0.474**	**#VALORE!**	12.00						
20190926_9	**12.4**	**3953.3**	**3953.3**	**1937.4**	**2965.5**	NaN	NaN	9.29	5.00	**5.00**	**#VALORE!**	0.997	0.405	NaN	**0.405**	**#VALORE!**	12.00						
20190926_10	**11.3**	**4622.6**	**4622.6**	**1702.1**	**2833.5**	NaN	NaN	7.23	13.01	**13.01**	**#VALORE!**	1.001	0.301	NaN	**0.301**	**#VALORE!**	12.00						
20190927_0	**10.6**	**4257.5**	**4257.5**	**1861.2**	**3012.4**	NaN	7.12	16.26	6.51	**6.81**	**9%**	0.382	0.516	1.65	**1.083**	**-69%**	12.00						
20190927_1	**11.7**	**4798.8**	**4798.8**	**2118.4**	**3360.8**	NaN	9.86	10.84	6.51	**8.18**	**34%**	0.641	0.463	1.10	**0.782**	**-58%**	12.00						
20190927_2	**9.2**	**4756.5**	**4756.5**	**1884.3**	**2930.5**	14.46	18.59	6.51	4.07	**11.33**	**78%**	0.853	0.481	1.50	**0.990**	**-68%**	12.00						
20190927_3	**6.1**	**3196.2**	**3196.2**	**1670.0**	**2456.7**	8.67	11.83	4.07	6.51	**9.17**	**45%**	0.729	0.341	1.13	**0.733**	**-70%**	12.00						
20190927_4	**3.6**	**2894.9**	**2894.9**	**1448.3**	**2133.2**	11.83	13.01	5.42	7.23	**10.12**	**44%**	0.476	0.356	0.50	**0.428**	**-29%**	12.00						
20191003_0	**1.1**	**1273.6**	**1273.6**	**772.9**	**1273.6**	NaN	NaN	3.83	4.07	**4.07**	**#VALORE!**	0.177	0.178	NaN	**0.178**	**#VALORE!**	12.00						
20191003_1	**1.1**	**1144.6**	**1144.6**	**851.0**	**1144.6**	NaN	3.72	3.61	3.83	**3.77**	**-3%**	0.204	0.158	0.25	**0.204**	**-37%**	12.00						
20191003_2	**11.0**	**2514.9**	**2514.9**	**1504.5**	**2109.4**	NaN	NaN	3.10	3.10	**3.10**	**#VALORE!**	0.141	0.173	NaN	**0.173**	**#VALORE!**	12.00						
20191003_3	**9.2**	**2694.5**	**2694.5**	**1381.5**	**2041.8**	NaN	NaN	8.13	8.13	**8.13**	**#VALORE!**	0.640	0.350	NaN	**0.350**	**#VALORE!**	12.00						
20191003_4	**7.2**	**1752.2**	**1752.2**	**1168.0**	**1544.0**	NaN	NaN	9.29	8.13	**8.13**	**#VALORE!**	0.359	0.276	NaN	**0.276**	**#VALORE!**	12.00						
20191003_5	**5.2**	**1601.9**	**1601.9**	**1035.9**	**1475.7**	NaN	NaN	4.65	3.10	**3.10**	**#VALORE!**	0.124	0.217	NaN	**0.217**	**#VALORE!**	12.00						
20191003_6	**7.5**	**1392.2**	**1392.2**	**1037.4**	**1309.8**	NaN	5.91	#VALORE!	4.65	**5.28**	**21%**	0.256	0.199	0.43	**0.312**	**-53%**	12.00						
20191003_7	**7.5**	**2681.4**	**2681.4**	**1293.9**	**2118.4**	NaN	11.83	8.13	10.84	**11.34**	**8%**	0.437	0.366	0.43	**0.395**	**-14%**	12.00						
20191003_8	**10.7**	**2273.1**	**2273.1**	**1231.1**	**1602.0**	NaN	6.51	21.68	13.01	**9.76**	**-100%**	0.305	0.408	0.43	**0.416**	**-4%**	12.00						
20191003_9	**5.8**	**954.9**	**954.9**	**832.3**	**954.9**	NaN	NaN	3.25	3.83	**3.83**	**#VALORE!**	0.171	0.152	NaN	**0.152**	**#VALORE!**	12.00						
20191003_10	**15.0**	**4514.8**	**4514.8**	**1309.2**	**2197.9**	NaN	NaN	5.42	8.13	**8.13**	**#VALORE!**	1.096	0.342	NaN	**0.342**	**#VALORE!**	12.00						
20191003_11	**13.8**	**2424.1**	**2424.1**	**1281.4**	**2001.5**	NaN	NaN	3.25	3.83	**3.83**	**#VALORE!**	NaN	0.458	NaN	**0.458**	**#VALORE!**	12.00						
20191003_12	**10.8**	**1732.9**	**1732.9**	**835.1**	**1213.2**	NaN	NaN	1.59	5.42	**5.42**	**#VALORE!**	0.163	0.187	NaN	**0.187**	**#VALORE!**	12.00						
20191003_13	**13.4**	**2348.6**	**2348.6**	**1164.1**	**1793.8**	NaN	NaN	5.00	3.83	**3.83**	**#VALORE!**	0.830	0.285	NaN	**0.285**	**#VALORE!**	12.00						
20191003_14	**13.5**	**2574.5**	**2574.5**	**1087.7**	**1729.7**	NaN	8.67	5.91	6.51	**7.59**	**25%**	1.024	0.333	0.50	**0.417**	**-33%**	12.00						
20191003_15	**12.6**	**2960.3**	**2960.3**	**1287.7**	**1975.6**	NaN	9.29	10.84	6.51	**7.90**	**30%**	0.690	0.317	0.65	**0.484**	**-51%**	12.00						
20191003_16	**11.1**	**1538.3**	**1538.3**	**860.7**	**1217.2**	NaN	6.85	5.42	#VALORE!	**#VALORE!**	**#VALORE!**	0.141	0.242	0.53	**0.383**	**-54%**	12.00						
20191004_0	**18.2**	**2273.9**	**2273.9**	**992.5**	**1359.0**	NaN	NaN	21.68	5.91	**5.91**	**#VALORE!**	0.240	0.294	NaN	**0.294**	**#VALORE!**	12.00						
20191004_1	**13.5**	**2540.4**	**2540.4**	**1315.0**	**1925.2**	NaN	NaN	5.42	3.42	**3.42**	**#VALORE!**	0.187	0.238	NaN	**0.238**	**#VALORE!**	12.00						
20191004_2	**13.9**	**1800.0**	**1800.0**	**1141.7**	**1596.7**	NaN	NaN	13.01	4.65	**4.65**	**#VALORE!**	0.279	0.356	NaN	**0.356**	**#VALORE!**	12.00						
20191004_3	**15.9**	**2190.0**	**2190.0**	**1247.7**	**1765.7**	NaN	8.67	4.34	4.65	**6.66**	**46%**	1.042	0.219	0.63	**0.422**	**-65%**	12.00						
20191004_4	**13.3**	**2206.7**	**2206.7**	**1093.4**	**1594.7**	6.85	8.67	3.83	3.83	**6.25**	**56%**	0.315	0.320	0.88	**0.598**	**-63%**	12.00						
20191004_5	**23.1**	**8630.0**	**8630.0**	**1799.5**	**2863.4**	NaN	NaN	13.01	8.13	**8.13**	**#VALORE!**	1.260	0.656	NaN	**0.656**	**#VALORE!**	12.00						
20191008_0	**12.7**	**2480.5**	**2480.5**	**1112.5**	**1607.4**	NaN	NaN	2.96	7.23	**7.23**	**#VALORE!**	0.170	0.257	NaN	**0.257**	**#VALORE!**	12.00						

20191008_1	**12.0**	**1636.0**	**1636.0**	**991.6**	**1391.5**	NaN	NaN	4.65	5.91	**5.91**	**#VALORE!**	0.211	0.202	NaN	**0.202**	**#VALORE!**	12.00						
20191008_2	**15.9**	**2591.5**	**2591.5**	**1280.7**	**2025.0**	6.51	7.65	1.81	5.91	**6.78**	**23%**	0.271	0.255	0.88	**0.565**	**-71%**	12.00						
20191008_3	**20.1**	**6963.5**	**6963.5**	**1722.8**	**2787.7**	9.29	10.01	7.23	10.84	**10.43**	**-8%**	0.731	0.398	0.63	**0.512**	**-36%**	12.00						
20191008_4	**9.3**	**1651.5**	**1651.5**	**888.8**	**1386.9**	NaN	NaN	4.07	4.07	**4.07**	**#VALORE!**	0.217	0.269	NaN	**0.269**	**#VALORE!**	12.00						
20191008_5	**7.9**	**1236.4**	**1236.4**	**784.5**	**1010.8**	NaN	NaN	4.65	4.34	**4.34**	**#VALORE!**	0.117	0.161	NaN	**0.161**	**#VALORE!**	12.00						
20191008_6	**16.8**	**2158.7**	**2158.7**	**1132.1**	**1609.2**	NaN	NaN	1.91	4.34	**4.34**	**#VALORE!**	0.367	0.311	NaN	**0.311**	**#VALORE!**	12.00						
20191008_7	**13.9**	**2467.2**	**2467.2**	**1093.9**	**1577.1**	NaN	NaN	1.97	4.65	**4.65**	**#VALORE!**	0.209	0.339	NaN	**0.339**	**#VALORE!**	12.00						
20191008_8	**12.1**	**1766.6**	**1766.6**	**1076.9**	**1495.0**	NaN	NaN	7.23	4.07	**4.07**	**#VALORE!**	0.182	0.226	NaN	**0.226**	**#VALORE!**	12.00						
20191008_9	**14.0**	**2204.6**	**2204.6**	**1235.6**	**1730.4**	6.85	7.23	5.00	3.42	**5.33**	**53%**	0.205	0.170	0.70	**0.435**	**-76%**	12.00						
20191008_10	**12.4**	**1906.8**	**1906.8**	**1030.2**	**1466.7**	6.51	8.67	1.00	16.26	**12.47**	**-88%**	0.190	0.328	0.50	**0.414**	**-34%**	12.00						
20191008_11	**11.3**	**1802.9**	**1802.9**	**952.8**	**1258.9**	NaN	NaN	1.45	8.13	**8.13**	**#VALORE!**	0.134	0.212	NaN	**0.212**	**#VALORE!**	12.00						
20191008_12	**11.7**	**2335.3**	**2335.3**	**1011.3**	**1500.9**	7.23	7.65	4.34	3.42	**5.54**	**55%**	0.137	0.216	0.35	**0.283**	**-38%**	12.00						
20191009_0	**10.4**	**1466.9**	**1466.9**	**919.9**	**1238.0**	NaN	7.23	4.65	4.34	**5.78**	**40%**	0.260	0.232	0.63	**0.428**	**-63%**	12.00						
20191009_1	**7.7**	**1510.9**	**1510.9**	**852.0**	**1205.5**	NaN	5.42	4.65	1.38	**3.40**	**74%**	0.198	1.563	0.38	**0.969**	**317%**	12.00						
20191009_2	**7.0**	**1227.3**	**1227.3**	**808.8**	**1089.8**	NaN	7.65	4.65	4.34	**6.00**	**43%**	0.104	0.191	0.30	**0.245**	**-36%**	12.00						
20191009_3	**14.8**	**2264.2**	**2264.2**	**1254.0**	**1751.7**	NaN	NaN	5.42	4.65	**4.65**	**#VALORE!**	0.308	0.403	NaN	**0.403**	**#VALORE!**	12.00						
20191009_4	**16.3**	**3205.3**	**3205.3**	**1312.8**	**1906.4**	NaN	NaN	5.91	7.23	**7.23**	**#VALORE!**	0.548	0.422	NaN	**0.422**	**#VALORE!**	12.00						
20191009_5	**10.9**	**2212.6**	**2212.6**	**1144.0**	**1744.9**	NaN	NaN	4.07	4.65	**4.65**	**#VALORE!**	0.330	0.226	NaN	**0.226**	**#VALORE!**	12.00						
20191009_6	**8.4**	**1495.4**	**1495.4**	**1000.4**	**1341.7**	NaN	NaN	3.83	3.61	**3.61**	**#VALORE!**	0.185	0.228	NaN	**0.228**	**#VALORE!**	12.00						
20191009_7	**10.9**	**2613.1**	**2613.1**	**1150.7**	**1780.0**	NaN	7.65	5.91	5.91	**6.78**	**23%**	0.276	0.320	0.63	**0.472**	**-49%**	12.00						
20191009_8	**15.4**	**2484.1**	**2484.1**	**1246.5**	**1766.5**	NaN	6.51	1.51	8.13	**7.32**	**-25%**	0.264	0.207	0.88	**0.541**	**-76%**	12.00						
20191009_9	**8.2**	**1386.0**	**1386.0**	**859.7**	**1247.9**	NaN	5.91	3.25	4.07	**4.99**	**31%**	0.180	0.115	1.00	**0.558**	**-88%**	12.00						
20191009_10	**16.2**	**3152.1**	**3152.1**	**1461.8**	**2181.5**	NaN	8.67	5.91	4.65	**6.66**	**46%**	0.267	0.363	0.63	**0.494**	**-42%**	12.00						
20191010_0	**14.0**	**2747.4**	**2747.4**	**1219.7**	**1781.7**	NaN	NaN	4.34	2.96	**2.96**	**#VALORE!**	0.291	0.156	NaN	**0.156**	**#VALORE!**	12.00						
20191010_1	**11.1**	**1760.9**	**1760.9**	**1306.9**	**1702.3**	NaN	NaN	7.23	5.00	**5.00**	**#VALORE!**	0.226	0.302	NaN	**0.302**	**#VALORE!**	12.00						
20191010_2	**9.3**	**1883.9**	**1883.9**	**927.9**	**1254.2**	NaN	NaN	0.99	4.07	**4.07**	**#VALORE!**	0.182	0.186	NaN	**0.186**	**#VALORE!**	12.00						
20191010_3	**7.6**	**1567.1**	**1567.1**	**830.1**	**1126.1**	NaN	NaN	3.42	3.25	**3.25**	**#VALORE!**	0.260	0.181	NaN	**0.181**	**#VALORE!**	12.00						
20191010_4	**13.0**	**2033.6**	**2033.6**	**1157.4**	**1672.1**	NaN	7.65	6.51	5.42	**6.54**	**29%**	0.302	0.296	0.63	**0.461**	**-53%**	12.00						
20191010_5	**10.9**	**1768.9**	**1768.9**	**1197.6**	**1572.5**	NaN	6.51	5.00	4.34	**5.42**	**33%**	0.218	0.308	0.50	**0.404**	**-38%**	12.00						
20191010_6	**9.4**	**2173.4**	**2173.4**	**944.6**	**1373.8**	NaN	6.20	8.13	4.34	**5.27**	**30%**	0.280	0.219	0.38	**0.297**	**-42%**	12.00						
20191010_7	**7.1**	**1245.4**	**1245.4**	**837.1**	**1136.0**	NaN	6.85	#VALORE!	5.00	**5.93**	**27%**	0.258	0.182	0.38	**0.279**	**-51%**	12.00						
20191010_8	**15.4**	**2145.5**	**2145.5**	**1365.5**	**1915.5**	NaN	NaN	4.34	4.34	**4.34**	**#VALORE!**	0.412	0.296	NaN	**0.296**	**#VALORE!**	12.00						
20191010_9	**13.6**	**2340.0**	**2340.0**	**1078.5**	**1496.9**	NaN	NaN	0.72	4.65	**4.65**	**#VALORE!**	0.172	0.222	NaN	**0.222**	**#VALORE!**	12.00						
20191010_10	**13.1**	**2610.5**	**2610.5**	**1074.0**	**1592.7**	NaN	9.29	7.23	7.23	**8.26**	**22%**	0.233	0.163	0.35	**0.256**	**-54%**	12.00						
20191010_11	**15.9**	**2391.1**	**2391.1**	**1428.0**	**2026.9**	NaN	6.85	6.51	7.23	**7.04**	**-6%**	0.294	0.281	0.25	**0.265**	**12%**	12.00						
20191010_12	**11.1**	**1836.1**	**1836.1**	**1056.5**	**1435.7**	NaN	NaN	#VALORE!	4.65	**4.65**	**#VALORE!**	0.361	0.279	NaN	**0.279**	**#VALORE!**	12.00						
20191010_13	**11.0**	**1877.3**	**1877.3**	**907.6**	**1327.1**	NaN	8.13	#VALORE!	3.61	**5.87**	**56%**	0.207	0.184	0.75	**0.467**	**-75%**	12.00						
20191010_14	**15.8**	**4131.5**	**4131.5**	**1579.3**	**2283.9**	NaN	NaN	5.91	5.91	**5.91**	**#VALORE!**	0.918	0.334	NaN	**0.334**	**#VALORE!**	12.00						
20191010_15	**14.1**	**3641.8**	**3641.8**	**1483.3**	**2276.1**	NaN	9.29	7.23	#VALORE!	**#VALORE!**	**#VALORE!**	0.408	0.480	0.65	**0.565**	**-26%**	12.00						
20191011_0	**13.7**	**1734.3**	**1734.3**	**990.2**	**1345.6**	NaN	NaN	5.42	10.84	**10.84**	**#VALORE!**	0.215	0.368	NaN	**0.368**	**#VALORE!**	12.00						
20191011_1	**10.5**	**4116.6**	**4116.6**	**1234.1**	**2417.9**	NaN	NaN	2.60	2.83	**2.83**	**#VALORE!**	1.969	0.385	NaN	**0.385**	**#VALORE!**	12.00						
20191011_2	**9.3**	**1464.5**	**1464.5**	**962.0**	**1263.3**	NaN	NaN	5.00	4.07	**4.07**	**#VALORE!**	0.218	0.247	NaN	**0.247**	**#VALORE!**	12.00						
20191011_3	**9.7**	**3202.0**	**3202.0**	**1220.1**	**2180.2**	NaN	13.01	5.42	6.51	**9.76**	**50%**	NaN	0.505	0.38	**0.440**	**35%**	12.00						
20191011_4	**11.0**	**1050.0**	**1050.0**	**700.5**	**847.0**	NaN	7.23	4.65	3.83	**5.53**	**47%**	0.112	0.150	0.63	**0.387**	**-76%**	12.00						
20191011_5	**3.6**	**1356.1**	**1356.1**	**978.3**	**1356.1**	NaN	6.51	5.00	3.83	**5.17**	**41%**	0.182	0.216	0.75	**0.483**	**-71%**	12.00						
20191015_0	**4.4**	**1136.2**	**1136.2**	**799.0**	**1115.8**	NaN	NaN	21.68	#VALORE!	**#VALORE!**	**#VALORE!**	NaN	NaN	NaN	**#DIV/0!**	**#VALORE!**	12.00						
20191015_1	**4.5**	**1401.0**	**1401.0**	**841.7**	**1160.9**	NaN	NaN	2.50	3.10	**3.10**	**#VALORE!**	0.178	0.116	NaN	**0.116**	**#VALORE!**	12.00						
20191015_2	**4.1**	**1026.1**	**1026.1**	**703.1**	**944.0**	NaN	NaN	2.96	3.42	**3.42**	**#VALORE!**	0.129	NaN	NaN	**#DIV/0!**	**#VALORE!**	12.00						
20191015_3	**7.4**	**1889.8**	**1889.8**	**1000.0**	**1393.1**	NaN	NaN	4.65	3.61	**3.61**	**#VALORE!**	1.134	0.334	NaN	**0.334**	**#VALORE!**	12.00						
20191015_4	**2.2**	**785.7**	**785.7**	**666.3**	**748.0**	NaN	NaN	0.70	NaN	**#DIV/0!**	**#VALORE!**	NaN	NaN	NaN	**#DIV/0!**	**#VALORE!**	12.00	Δ_{tmax} non conforme					
20191015_5	**6.4**	**1391.2**	**1391.2**	**973.1**	**1292.1**	NaN	NaN	1.18	NaN	**#DIV/0!**	**#VALORE!**	NaN	NaN	NaN	**#DIV/0!**	**#VALORE!**	12.00	Δ_{tmax} non conforme					
20191015_6	**4.0**	**1055.4**	**1055.4**	**709.6**	**946.8**	NaN	6.20	16.26	NaN	**6.20**	**#VALORE!**	NaN	NaN	0.15	**0.150**	**#VALORE!**	12.00	Δ_{tmax} non conforme					
20191015_7	**3.7**	**1116.4**	**1116.4**	**845.7**	**1011.4**	NaN	4.34	3.42	3.10	**3.72**	**29%**	0.182	0.104	0.15	**0.127**	**-31%**	12.00						
20191015_8	**3.7**	**763.8**	**763.8**	**592.8**	**715.7**	NaN	6.51	1.03	1.03	**3.77**	**84%**	NaN	NaN	0.25	**0.250**	**#VALORE!**	12.00						
20191015_9	**6.8**	**1956.1**	**1956.1**	**961.7**	**1527.4**	NaN	10.01	6.51	6.51	**8.26**	**35%**	0.716	0.405	0.40	**0.403**	**1%**	12.00						

20191015_10	**5.8**	**895.8**	**895.8**	**816.7**	**891.0**	NaN	8.67	0.77	0.71	**4.69**	**92%**	NaN	NaN		0.38	**0.375**	**#VALORE!**	12.00			
20191015_11	**2.0**	**778.1**	**778.1**	**679.2**	**759.2**	NaN	4.82	0.86	0.86	**2.84**	**82%**	NaN	NaN		0.20	**0.200**	**#VALORE!**	12.00			
20191016_0	**5.1**	**1107.3**	**1107.3**	**875.5**	**1006.3**	NaN	NaN	0.74	0.74	**0.74**	**#VALORE!**	NaN	NaN	NaN		**#DIV/0!**	**#VALORE!**	12.00			
20191016_1	**7.5**	**1277.5**	**1277.5**	**1023.3**	**1247.2**	NaN	NaN	2.96	2.32	**2.32**	**#VALORE!**		0.163	0.231	NaN	**0.231**	**#VALORE!**	12.00			
20191016_2	**9.4**	**3198.2**	**3198.2**	**1191.4**	**2020.5**	NaN	NaN	9.29	10.84	**10.84**	**#VALORE!**		0.588	0.379	NaN	**0.379**	**#VALORE!**	12.00			
20191016_3	**4.5**	**980.4**	**980.4**	**788.1**	**946.2**	NaN	NaN	0.66	0.66	**0.66**	**#VALORE!**	NaN	NaN	NaN		**#DIV/0!**	**#VALORE!**	12.00			
20191016_4	**3.8**	**1100.0**	**1100.0**	**779.3**	**988.1**	NaN	NaN	3.25	3.25	**3.25**	**#VALORE!**		0.265	0.146	NaN	**0.146**	**#VALORE!**	12.00			
20191016_5	**4.7**	**1033.1**	**1033.1**	**868.7**	**1030.5**	NaN	4.34	0.78	0.81	**2.58**	**81%**	NaN	NaN		0.38	**0.375**	**#VALORE!**	12.00			
20191016_6	**7.0**	**1418.5**	**1418.5**	**1031.7**	**1291.0**	NaN	4.65	0.77	0.72	**2.68**	**84%**	NaN	NaN		0.55	**0.550**	**#VALORE!**	12.00			
20191016_7	**9.1**	**3378.2**	**3378.2**	**1247.5**	**2102.8**	NaN	10.84	1.91	4.65	**7.74**	**57%**		1.734	0.754		0.90	**0.827**	**-16%**	12.00		
20191016_8	**4.5**	**819.1**	**819.1**	**761.1**	**814.1**	NaN	6.51	10.84	5.91	**6.21**	**9%**		0.292	0.250		0.38	**0.312**	**-33%**	12.00		
20191016_9	**3.6**	**930.8**	**930.8**	**790.9**	**914.5**	NaN	7.23	3.42	3.42	**5.33**	**53%**		0.220	0.164		0.45	**0.307**	**-64%**	12.00		
20191016_10	**2.8**	**1093.1**	**1093.1**	**650.6**	**1093.1**	NaN	NaN	8.13	7.23	**7.23**	**#VALORE!**	NaN		0.168	NaN		**0.168**	**#VALORE!**	12.00		
20191016_11	**4.1**	**1145.8**	**1145.8**	**763.8**	**1078.2**	NaN	NaN	#VALORE!	7.23	**7.23**	**#VALORE!**		0.173	0.258	NaN		**0.258**	**#VALORE!**	12.00		
20191016_12	**8.0**	**1527.3**	**1527.3**	**874.2**	**1457.2**	NaN	NaN	21.68	#VALORE!	**#VALORE!**	**#VALORE!**	NaN	NaN	NaN		**#DIV/0!**	**#VALORE!**	12.00			
20191016_13	**3.0**	**1250.4**	**1250.4**	**566.5**	**930.9**	NaN	5.91	#VALORE!	#VALORE!	**#VALORE!**	**#VALORE!**	NaN	NaN		0.35	**0.350**	**#VALORE!**	12.00			
20191016_15	**7.5**	**1837.8**	**1837.8**	**954.2**	**1488.8**	NaN	10.01	8.13	9.29	**9.65**	**7%**		0.291	0.283		0.40	**0.341**	**-29%**	12.00		
20191017_0	**4.7**	**765.5**	**765.5**	**610.8**	**725.5**	NaN	NaN	2.60	9.29	**9.29**	**#VALORE!**		0.199	0.277	NaN		**0.277**	**#VALORE!**	12.00		
20191017_1	**8.2**	**1025.5**	**1025.5**	**831.3**	**949.5**	NaN	NaN	3.10	2.50	**2.50**	**#VALORE!**		0.124	0.209	NaN		**0.209**	**#VALORE!**	12.00		
20191017_2	**4.7**	**1447.0**	**1447.0**	**716.0**	**1127.1**	NaN	NaN	2.96	4.65	**4.65**	**#VALORE!**		0.214	NaN	NaN		**#DIV/0!**	**#VALORE!**	12.00		
20191017_3	**5.6**	**1405.1**	**1405.1**	**857.5**	**1327.8**	NaN	NaN	3.10	5.00	**5.00**	**#VALORE!**		0.130	NaN	NaN		**#DIV/0!**	**#VALORE!**	12.00		
20191017_4	**6.9**	**1420.3**	**1420.3**	**862.5**	**1249.5**	NaN	NaN	1.18	3.61	**3.61**	**#VALORE!**	NaN	NaN	NaN		**#DIV/0!**	**#VALORE!**	12.00			
20191017_5	**7.1**	**923.1**	**923.1**	**787.6**	**902.3**	NaN	7.23	1.48	1.71	**4.47**	**76%**		0.143	NaN		0.63	**0.625**	**#VALORE!**	12.00		
20191017_6	**4.7**	**655.6**	**655.6**	**579.3**	**631.4**	NaN	8.13	6.51	6.51	**7.32**	**20%**	NaN	NaN		0.38	**0.375**	**#VALORE!**	12.00			
20191017_7	**6.7**	**1362.1**	**1362.1**	**872.5**	**1178.5**	NaN	4.82	0.97	5.00	**4.91**	**-4%**		0.187	NaN		0.25	**0.250**	**#VALORE!**	12.00		
20191017_8	**5.6**	**1169.8**	**1169.8**	**683.5**	**1030.5**	NaN	5.91	4.07	7.23	**6.57**	**-22%**		0.186	0.117		0.25	**0.184**	**-53%**	12.00		
20191017_9	**4.5**	**1373.5**	**1373.5**	**707.4**	**1070.9**	NaN	6.85	2.24	4.65	**5.75**	**32%**		0.235	0.165		0.30	**0.233**	**-45%**	12.00		
20191017_10	**3.9**	**955.9**	**955.9**	**690.6**	**955.9**	NaN	NaN	3.61	3.61	**3.61**	**#VALORE!**		0.173	0.137	NaN		**0.137**	**#VALORE!**	12.00		
20191017_11	**2.5**	**947.0**	**947.0**	**700.5**	**947.0**	NaN	NaN	1.10	3.83	**3.83**	**#VALORE!**	NaN	NaN	NaN		**#DIV/0!**	**#VALORE!**	12.00			
20191017_12	**2.3**	**575.3**	**575.3**	**497.6**	**575.3**	NaN	NaN	21.68	2.17	**2.17**	**#VALORE!**	NaN	NaN	NaN		**#DIV/0!**	**#VALORE!**	12.00			
20191017_13	**3.6**	**1074.5**	**1074.5**	**670.0**	**1074.5**	NaN	5.42	3.10	3.42	**4.42**	**37%**		0.214	0.154		0.18	**0.165**	**-12%**	12.00		
20191017_14	**2.8**	**789.1**	**789.1**	**661.5**	**789.1**	NaN	4.20	2.83	3.61	**3.91**	**14%**		0.132	NaN		0.15	**0.150**	**#VALORE!**	12.00		
20191017_15	**2.2**	**463.6**	**463.6**	**438.4**	**463.6**	NaN	3.72	#VALORE!	8.13	**5.92**	**-119%**	NaN	NaN		0.10	**0.100**	**#VALORE!**	12.00			
20191021_0	**3.8**	**1434.0**	**1434.0**	**969.1**	**1434.0**	NaN	NaN	10.84	4.34	**4.34**	**#VALORE!**		0.268	0.226	NaN		**0.226**	**#VALORE!**	12.00		
20191021_1	**2.9**	**1251.9**	**1251.9**	**823.9**	**1251.9**	NaN	NaN	0.97	0.97	**0.97**	**#VALORE!**		0.117	0.147	NaN		**0.147**	**#VALORE!**	12.00		
20191021_2	**4.5**	**1321.0**	**1321.0**	**836.9**	**1100.6**	NaN	NaN	2.50	NaN	**#DIV/0!**	**#VALORE!**		0.151	NaN	NaN		**#DIV/0!**	**#VALORE!**	12.00	Δ_{tmax} non conforme	
20191021_3	**3.1**	**1205.4**	**1205.4**	**740.4**	**969.5**	NaN	NaN	0.87	NaN	**#DIV/0!**	**#VALORE!**		0.119	NaN	NaN		**#DIV/0!**	**#VALORE!**	12.00	Δ_{tmax} non conforme	
20191021_4	**5.8**	**1828.3**	**1828.3**	**1250.4**	**1807.5**	NaN	NaN	3.61	3.25	**3.25**	**#VALORE!**		0.228	0.182	NaN		**0.182**	**#VALORE!**	12.00		
20191021_5	**2.2**	**941.0**	**941.0**	**635.0**	**941.0**	NaN	NaN	1.25	3.10	**3.10**	**#VALORE!**		0.112	0.103	NaN		**0.103**	**#VALORE!**	12.00		
20191021_6	**1.1**	**634.4**	**634.4**	**550.1**	**634.4**	NaN	NaN	1.86	1.59	**1.59**	**#VALORE!**	NaN	NaN	NaN		**#DIV/0!**	**#VALORE!**	12.00			
20191021_7	**3.7**	**1310.8**	**1310.8**	**1056.2**	**1310.8**	NaN	NaN	4.07	5.42	**5.42**	**#VALORE!**		0.180	1.876	NaN		**1.876**	**#VALORE!**	12.00		
20191021_8	**5.5**	**1486.6**	**1486.6**	**927.1**	**1472.7**	NaN	NaN	0.79	0.73	**0.73**	**#VALORE!**		0.194	NaN	NaN		**#DIV/0!**	**#VALORE!**	12.00		
20191021_9	**7.2**	**2226.4**	**2226.4**	**903.4**	**1377.6**	NaN	NaN	21.68	5.91	**5.91**	**#VALORE!**		0.464	0.392	NaN		**0.392**	**#VALORE!**	12.00		
20191021_10	**3.3**	**1086.0**	**1086.0**	**736.2**	**1086.0**	NaN	NaN	#VALORE!	16.26	**16.26**	**#VALORE!**	NaN		0.117	NaN		**0.117**	**#VALORE!**	12.00		
20191021_11	**2.7**	**917.0**	**917.0**	**889.1**	**917.0**	NaN	NaN	5.42	6.51	**6.51**	**#VALORE!**		0.210	0.120	NaN		**0.120**	**#VALORE!**	12.00		
20191022_0	**3.6**	**1266.0**	**1266.0**	**921.1**	**1266.0**	NaN	5.66	1.10	3.83	**4.74**	**32%**	NaN	NaN		0.38	**0.375**	**#VALORE!**	12.00			
20191022_1	**2.8**	**1065.2**	**1065.2**	**799.9**	**1065.2**	NaN	5.20	1.23	0.68	**2.94**	**87%**		0.117	NaN		0.15	**0.150**	**#VALORE!**	12.00		
20191022_2	**2.2**	**952.7**	**952.7**	**681.8**	**952.7**	NaN	4.34	1.48	NaN	**4.34**	**#VALORE!**	NaN	NaN		0.13	**0.125**	**#VALORE!**	12.00	Δ_{tmax} non conforme		
20191022_3	**6.0**	**1945.3**	**1945.3**	**1198.4**	**1851.7**	NaN	4.34	4.07	5.00	**4.67**	**-15%**		0.233	0.242		0.40	**0.321**	**-40%**	12.00		
20191022_4	**4.8**	**1464.1**	**1464.1**	**1021.3**	**1396.6**	NaN	3.25	1.12	NaN	**3.25**	**#VALORE!**		0.136	NaN		0.15	**0.150**	**#VALORE!**	12.00	Δ_{tmax} non conforme	
20191022_5	**3.4**	**1213.7**	**1213.7**	**767.0**	**1038.7**	NaN	3.25	0.79	1.97	**2.61**	**39%**	NaN	NaN		0.13	**0.125**	**#VALORE!**	12.00			
20191022_6	**5.6**	**1779.3**	**1779.3**	**884.9**	**1313.7**	NaN	3.52	0.89	4.65	**4.08**	**-32%**		0.122	NaN		0.30	**0.300**	**#VALORE!**	12.00		
20191022_7	**7.1**	**2436.0**	**2436.0**	**958.6**	**1389.9**	NaN	10.84	8.13	8.13	**9.49**	**25%**		0.441	0.395		0.50	**0.448**	**-21%**	12.00		
20191022_8	**3.6**	**1118.6**	**1118.6**	**841.3**	**1118.6**	NaN	7.65	#VALORE!	NaN	**7.65**	**#VALORE!**		0.178	0.264		0.44	**0.349**	**-39%**	12.00	Δ_{tmax} non conforme	
20191022_9	**3.1**	**1073.4**	**1073.4**	**833.5**	**1073.4**	NaN	7.23	2.83	3.83	**5.53**	**47%**		0.102	NaN		0.55	**0.550**	**#VALORE!**	12.00		

20191022_10	**0.7**	**883.8**	**883.8**	**883.8**	**NaN**	NaN	NaN		0.78	0.71	**0.71**	**#VALORE!**		0.269	NaN		NaN		**#DIV/0!**	**#VALORE!**	12.00		
20191022_11	**3.4**	**2424.7**	**2424.7**	**1041.1**	**1758.3**	NaN	NaN		9.29	6.51	**6.51**	**#VALORE!**		0.402		0.265	NaN		**0.265**	**#VALORE!**	12.00		
20191022_12	**1.1**	**954.8**	**954.8**	**896.6**	**954.8**	NaN	NaN		1.08	0.81	**0.81**	**#VALORE!**		0.111	NaN		NaN		**#DIV/0!**	**#VALORE!**	12.00		
20191022_13	**2.4**	**1409.8**	**1409.8**	**1012.9**	**1394.3**	NaN	NaN		3.61	1.02	**1.02**	**#VALORE!**		0.264		0.371	NaN		**0.371**	**#VALORE!**	12.00		
20191022_14	**2.0**	**1148.8**	**1148.8**	**600.4**	**1148.8**	NaN	NaN		0.74	0.67	**0.67**	**#VALORE!**	NaN		NaN		NaN		**#DIV/0!**	**#VALORE!**	12.00		
20191022_15	**3.1**	**1434.1**	**1434.1**	**924.5**	**1434.1**	NaN	NaN		1.28	0.66	**0.66**	**#VALORE!**		0.642		0.415	NaN		**0.415**	**#VALORE!**	12.00		
20191022_16	**3.4**	**2131.4**	**2131.4**	**921.6**	**1595.4**	NaN	7.23	#VALORE!		5.91	**6.57**	**18%**		0.339		0.182		0.60	**0.391**	**-70%**	12.00		
20191022_17	**3.1**	**1585.6**	**1585.6**	**1044.2**	**1585.6**	NaN	6.51		5.00	4.65	**5.58**	**29%**		0.284		0.265		0.60	**0.433**	**-56%**	12.00		
20191022_18	**2.4**	**1301.7**	**1301.7**	**721.4**	**1301.7**	NaN	4.07		3.42	NaN		**4.07**	**#VALORE!**		0.165	NaN			0.40	**0.400**	**#VALORE!**	12.00	Δ_{tmax} non conforme	
20191023_0	**5.9**	**1491.4**	**1491.4**	**1041.6**	**1293.8**	NaN	NaN		5.42	7.23	**7.23**	**#VALORE!**	NaN		NaN		NaN		**#DIV/0!**	**#VALORE!**	12.00		
20191023_1	**4.8**	**1067.6**	**1067.6**	**841.2**	**1023.1**	NaN	NaN		0.99	1.05	**1.05**	**#VALORE!**	NaN		NaN		NaN		**#DIV/0!**	**#VALORE!**	12.00		
20191023_2	**4.7**	**1410.6**	**1410.6**	**934.7**	**1242.1**	NaN	NaN		10.84	5.42	**5.42**	**#VALORE!**		0.818		0.185	NaN		**0.185**	**#VALORE!**	12.00		
20191023_3	**7.3**	**1392.9**	**1392.9**	**932.2**	**1291.7**	NaN	NaN		5.91	NaN		**#DIV/0!**	**#VALORE!**	NaN		0.215	NaN		**0.215**	**#VALORE!**	12.00	Δ_{tmax} non conforme	
20191023_4	**7.4**	**1494.1**	**1494.1**	**920.5**	**1237.6**	NaN	NaN		9.29	9.29	**9.29**	**#VALORE!**		0.355		0.309	NaN		**0.309**	**#VALORE!**	12.00		
20191023_5	**10.7**	**2322.7**	**2322.7**	**1225.1**	**2047.0**	NaN	NaN		5.91	5.91	**5.91**	**#VALORE!**		0.733		0.510	NaN		**0.510**	**#VALORE!**	12.00		
20191023_6	**5.5**	**1524.2**	**1524.2**	**1019.9**	**1347.0**	NaN	6.51		6.51	9.29	**7.90**	**-43%**	NaN		NaN			1.05	**1.050**	**#VALORE!**	12.00		
20191023_7	**3.9**	**1560.0**	**1560.0**	**995.5**	**1500.3**	NaN	4.07		3.61	4.34	**4.20**	**-7%**		0.261		0.126		0.40	**0.263**	**-69%**	12.00		
20191023_8	**4.0**	**1248.4**	**1248.4**	**751.6**	**1070.5**	NaN	4.34		2.03	NaN		**4.34**	**#VALORE!**	NaN		NaN		0.25	**0.250**	**#VALORE!**	12.00	Δ_{tmax} non conforme	
20191023_9	**10.4**	**2533.3**	**2533.3**	**1282.0**	**2209.2**	NaN	7.65		5.42	5.00	**6.33**	**35%**		0.303		0.303		0.50	**0.402**	**-39%**	12.00		
20191023_10	**6.0**	**1202.5**	**1202.5**	**850.7**	**1047.5**	NaN	6.20		2.96	2.60	**4.40**	**58%**	NaN		NaN			0.40	**0.400**	**#VALORE!**	12.00		
20191023_11	**6.2**	**1463.5**	**1463.5**	**979.2**	**1255.7**	NaN	6.51		8.13	6.51	**6.51**	**0%**		0.208		0.223		0.63	**0.424**	**-64%**	12.00		
20191023_12	**2.4**	**1073.8**	**1073.8**	**846.5**	**1073.8**	NaN	NaN		16.26	16.26	**16.26**	**#VALORE!**		NaN		0.112	NaN		**0.112**	**#VALORE!**	12.00		
20191023_13	**2.5**	**1000.5**	**1000.5**	**774.6**	**992.8**	NaN	3.72	#VALORE!	NaN		**3.72**	**#VALORE!**		NaN		0.173		0.25	**0.211**	**-31%**	12.00	Δ_{tmax} non conforme	
20191024_0	**1.8**	**884.9**	**884.9**	**728.9**	**884.9**	NaN	3.72	#VALORE!	NaN		**3.72**	**#VALORE!**		NaN		NaN		0.25	**0.250**	**#VALORE!**	12.00	Δ_{tmax} non conforme	
20191024_1	**2.4**	**1085.1**	**1085.1**	**782.6**	**1085.1**	NaN	NaN		2.60	3.10	**3.10**	**#VALORE!**		0.105	NaN		NaN		**#DIV/0!**	**#VALORE!**	12.00		
20191024_2	**2.9**	**947.0**	**947.0**	**638.3**	**839.7**	NaN	NaN		3.10	3.61	**3.61**	**#VALORE!**		0.158		0.127	NaN		**0.127**	**#VALORE!**	12.00		
20191024_3	**3.7**	**1070.5**	**1070.5**	**766.0**	**942.5**	NaN	NaN		4.65	3.83	**3.83**	**#VALORE!**	NaN			0.180	NaN		**0.180**	**#VALORE!**	12.00		
20191024_4	**4.0**	**1125.8**	**1125.8**	**769.4**	**1084.1**	NaN	NaN		3.83	3.42	**3.42**	**#VALORE!**		0.303	NaN		NaN		**#DIV/0!**	**#VALORE!**	12.00		
20191024_5	**2.2**	**913.1**	**913.1**	**718.1**	**913.1**	NaN	3.52		2.60	2.83	**3.17**	**20%**		0.132	NaN			0.40	**0.400**	**#VALORE!**	12.00		
20191024_6	**2.9**	**804.2**	**804.2**	**611.5**	**804.2**	NaN	3.25		3.10	2.24	**2.75**	**31%**		0.170		0.122		0.25	**0.186**	**-51%**	12.00		
20191024_7	**3.7**	**1325.9**	**1325.9**	**773.9**	**1069.6**	NaN	3.83		5.91	3.61	**3.72**	**6%**		0.202		0.153		0.43	**0.289**	**-64%**	12.00		
20191024_8	**3.7**	**934.4**	**934.4**	**734.6**	**916.1**	NaN	4.07		3.25	4.07	**4.07**	**0%**		0.226		0.141		0.40	**0.271**	**-65%**	12.00		
20191024_9	**3.7**	**2272.6**	**2272.6**	**1117.5**	**1680.2**	NaN	NaN		5.42	7.23	**7.23**	**#VALORE!**		0.244		0.371	NaN		**0.371**	**#VALORE!**	12.00		
20191024_10	**3.6**	**1184.9**	**1184.9**	**961.1**	**1184.9**	NaN	NaN		#VALORE!	NaN		**#DIV/0!**	**#VALORE!**	0.244		0.243	NaN		**0.243**	**#VALORE!**	12.00	Δ_{tmax} non conforme	
20191024_11	**2.9**	**1438.0**	**1438.0**	**943.9**	**1438.0**	NaN	NaN		1.00	0.87	**0.87**	**#VALORE!**		0.188	NaN		NaN		**#DIV/0!**	**#VALORE!**	12.00		
20191024_12	**1.7**	**794.7**	**794.7**	**778.3**	**794.7**	NaN	NaN		0.77	0.93	**0.93**	**#VALORE!**	NaN		NaN		NaN		**#DIV/0!**	**#VALORE!**	12.00		
20191024_13	**3.7**	**2065.0**	**2065.0**	**1070.5**	**1562.2**	NaN	4.65		5.91	7.23	**5.94**	**-56%**		0.339		0.401		0.45	**0.425**	**-11%**	12.00		
20191024_14	**1.8**	**852.1**	**852.1**	**851.6**	**852.1**	NaN	2.60		2.10	2.03	**2.32**	**22%**	NaN		NaN			0.25	**0.250**	**#VALORE!**	12.00		
20191024_15	**3.2**	**1504.0**	**1504.0**	**1193.5**	**1504.0**	NaN	4.82		10.84	6.51	**5.66**	**-35%**		0.492		0.247		0.43	**0.336**	**-42%**	12.00		
20191024_16	**2.5**	**1345.8**	**1345.8**	**930.8**	**1345.8**	NaN	7.65		0.99	1.03	**4.34**	**87%**		0.162	NaN			0.45	**0.450**	**#VALORE!**	12.00		
20191028_0	**3.9**	**1716.8**	**1716.8**	**1055.1**	**1546.6**	NaN	NaN		6.51	7.23	**7.23**	**#VALORE!**		0.443		0.207	NaN		**0.207**	**#VALORE!**	12.00		
20191028_1	**2.9**	**1153.2**	**1153.2**	**887.8**	**1153.2**	NaN	NaN		0.96	NaN		**#DIV/0!**	**#VALORE!**	NaN		NaN			**#DIV/0!**	**#VALORE!**	12.00	Δ_{tmax} non conforme	
20191028_2	**2.2**	**972.0**	**972.0**	**778.6**	**972.0**	NaN	NaN		0.93	0.79	**0.79**	**#VALORE!**	NaN		NaN		NaN		**#DIV/0!**	**#VALORE!**	12.00		
20191028_3	**2.1**	**961.1**	**961.1**	**720.7**	**961.1**	NaN	NaN		#VALORE!	NaN		**#DIV/0!**	**#VALORE!**	NaN		NaN			**#DIV/0!**	**#VALORE!**	12.00	Δ_{tmax} non conforme	
20191028_4	**1.9**	**810.9**	**810.9**	**687.6**	**810.9**	NaN	NaN		0.90	0.92	**0.92**	**#VALORE!**	NaN		NaN		NaN		**#DIV/0!**	**#VALORE!**	12.00		
20191028_5	**3.0**	**2249.9**	**2249.9**	**1159.6**	**1656.2**	NaN	NaN		8.13	5.00	**5.00**	**#VALORE!**		0.918		0.326	NaN		**0.326**	**#VALORE!**	12.00		
20191028_6	**1.9**	**1039.0**	**1039.0**	**1007.8**	**1039.0**	NaN	NaN		8.13	3.61	**3.61**	**#VALORE!**		0.252		0.194	NaN		**0.194**	**#VALORE!**	12.00	Δ_{tmax} non conforme	
20191028_7	**2.4**	**898.7**	**898.7**	**673.4**	**898.7**	NaN	NaN		0.66	0.84	**0.84**	**#VALORE!**	NaN		NaN		NaN		**#DIV/0!**	**#VALORE!**	12.00		
20191028_8	**2.7**	**1922.7**	**1922.7**	**1188.8**	**1922.7**	NaN	5.66		6.51	5.91	**5.79**	**-5%**		0.346		0.315		0.50	**0.407**	**-37%**	12.00		
20191028_9	**2.2**	**919.5**	**919.5**	**762.4**	**919.5**	NaN	3.61	#VALORE!	NaN		**3.61**	**#VALORE!**		NaN		0.197		0.40	**0.299**	**-51%**	12.00	Δ_{tmax} non conforme	
20191028_10	**2.0**	**873.7**	**873.7**	**658.8**	**873.7**	NaN	7.65		10.84	5.91	**6.78**	**23%**		0.104		0.130		0.45	**0.290**	**-71%**	12.00		
20191028_11	**2.2**	**957.1**	**957.1**	**723.6**	**957.1**	NaN	3.03		0.79	0.79	**1.91**	**74%**	NaN		NaN			0.15	**0.150**	**#VALORE!**	12.00		
20191029_0	**1.8**	**1125.5**	**1125.5**	**980.0**	**1125.5**	NaN	NaN		#VALORE!	9.29	**9.29**	**#VALORE!**		0.178		0.276	NaN		**0.276**	**#VALORE!**	12.00		
20191029_1	**1.6**	**1125.3**	**1125.3**	**1125.3**	**NaN**	NaN	NaN		3.42	3.25	**3.25**	**#VALORE!**		0.104		0.128	NaN		**0.128**	**#VALORE!**	12.00		
20191030_0	**3.5**	**1458.2**	**1458.2**	**1152.9**	**1456.2**	NaN	NaN		1.12	0.82	**0.82**	**#VALORE!**		1.171		1.156	NaN		**1.156**	**#VALORE!**	6.00		

20191030_1	**4.6**	**4599.1**	**4599.1**	**1539.0**	**2477.6**	NaN	NaN		2.87		2.70	**2.70**	**#VALORE!**	NaN	NaN	NaN		**#DIV/0!**	**#VALORE!**	6.00	
20191030_2	**2.9**	**2368.6**	**2368.6**	**1022.9**	**1684.8**	NaN	NaN		0.96		0.98	**0.98**	**#VALORE!**	NaN	NaN	NaN		**#DIV/0!**	**#VALORE!**	6.00	
20191030_3	**2.8**	**1648.8**	**1648.8**	**1309.2**	**1648.8**	NaN	NaN		0.85		0.88	**0.88**	**#VALORE!**		1.959	NaN	NaN		**#DIV/0!**	**#VALORE!**	6.00	
20191030_4	**4.6**	**4411.9**	**4411.9**	**1354.2**	**2435.1**	NaN		8.92	7.66	NaN		**8.92**	**#VALORE!**		0.704	0.366		1.75	**1.058**	**-79%**	6.00	
20191030_5	**4.2**	**2016.8**	**2016.8**	**1308.5**	**1693.0**	NaN		6.86	0.51	NaN		**6.86**	**#VALORE!**		1.633	0.257		0.50	**0.378**	**-49%**	6.00	Δ_{tmax} non conforme
20191030_6	**3.1**	**2887.6**	**2887.6**	**1339.7**	**2001.3**	NaN		5.94	1.12		0.90	**3.42**	**85%**		0.969	1.908		1.50	**1.704**	**27%**	6.00	
20191030_7	**2.9**	**2025.9**	**2025.9**	**1488.6**	**2025.9**	NaN		7.43	1.02		1.35	**4.39**	**82%**		0.481	0.168		1.50	**0.834**	**-89%**	6.00	
20191031_0	**2.8**	**1547.0**	**1547.0**	**872.3**	**1207.4**	NaN	NaN		11.49	NaN		**#DIV/0!**	**#VALORE!**	NaN	NaN	NaN		**#DIV/0!**	**#VALORE!**	6.00	Δ_{tmax} non conforme
20191031_1	**2.7**	**1048.2**	**1048.2**	**874.6**	**1040.2**	NaN	NaN		1.07		1.24	**1.24**	**#VALORE!**		1.167	0.343	NaN		**0.343**	**#VALORE!**	6.00	
20191031_2	**1.9**	**872.7**	**872.7**	**752.2**	**872.7**	NaN	NaN		1.02		5.75	**5.75**	**#VALORE!**		1.550	0.214	NaN		**0.214**	**#VALORE!**	6.00	
20191031_3	**1.4**	**1300.4**	**1300.4**	**1261.9**	**1300.4**	NaN	NaN		1.84	NaN		**#DIV/0!**	**#VALORE!**		1.213	NaN	NaN		**#DIV/0!**	**#VALORE!**	6.00	Δ_{tmax} non conforme
20191031_4	**3.1**	**980.6**	**980.6**	**910.2**	**971.6**	NaN		4.60	0.82		1.02	**2.81**	**78%**		1.757	0.522		1.50	**1.011**	**-65%**	6.00	
20191031_5	**2.8**	**1292.7**	**1292.7**	**801.8**	**1178.1**	NaN		5.11	#VALORE!		5.11	**5.11**	**0%**		1.203	NaN		1.00	**1.000**	**#VALORE!**	6.00	
20191031_6	**1.3**	**1030.7**	**1030.7**	**1030.7**	**NaN**	NaN		5.41	0.92		0.63	**3.02**	**88%**		1.513	NaN		0.50	**0.500**	**#VALORE!**	6.00	
20191105_0	**3.2**	**1788.3**	**1788.3**	**1078.0**	**1605.5**	NaN	NaN		4.18		4.60	**4.60**	**#VALORE!**		0.390	0.251	NaN		**0.251**	**#VALORE!**	6.00	
20191105_1	**2.9**	**1938.4**	**1938.4**	**1540.9**	**1938.4**	NaN	NaN		3.83		4.18	**4.18**	**#VALORE!**		0.250	0.123	NaN		**0.123**	**#VALORE!**	6.00	
20191105_2	**2.1**	**1055.8**	**1055.8**	**940.9**	**1055.8**	NaN	NaN		3.06		9.19	**9.19**	**#VALORE!**		0.164	NaN	NaN		**#DIV/0!**	**#VALORE!**	6.00	
20191105_3	**1.0**	**940.3**	**940.3**	**805.7**	**940.3**	NaN	NaN		3.28		3.83	**3.83**	**#VALORE!**		0.116	NaN	NaN		**#DIV/0!**	**#VALORE!**	6.00	
20191105_4	**3.0**	**2527.9**	**2527.9**	**1739.3**	**2527.9**	NaN		7.07	6.57		7.66	**7.37**	**-8%**		0.252	NaN		1.00	**1.000**	**#VALORE!**	6.00	
20191105_5	**2.3**	**1619.9**	**1619.9**	**1039.2**	**1619.9**	NaN	NaN		4.60		3.83	**3.83**	**#VALORE!**		0.282	NaN	NaN		**#DIV/0!**	**#VALORE!**	6.00	
20191105_6	**1.8**	**1117.8**	**1117.8**	**990.2**	**1117.8**	NaN		4.60	1.18		9.19	**6.89**	**-100%**		0.168	NaN		0.40	**0.400**	**#VALORE!**	6.00	
20191106_0	**6.0**	**3532.2**	**3532.2**	**2214.3**	**3401.9**	NaN	NaN		#VALORE!		#VALORE!	**#VALORE!**	**#VALORE!**	NaN	NaN	NaN		**#DIV/0!**	**#VALORE!**	6.00	
20191106_1	**4.4**	**2108.8**	**2108.8**	**1607.9**	**2033.1**	NaN	NaN		6.57		6.57	**6.57**	**#VALORE!**		0.132	NaN	NaN		**#DIV/0!**	**#VALORE!**	6.00	
20191106_2	**3.1**	**1741.6**	**1741.6**	**1324.5**	**1741.6**	NaN	NaN		3.28		#VALORE!	**#VALORE!**	**#VALORE!**		0.190	1.554	NaN		**1.554**	**#VALORE!**	6.00	
20191106_3	**3.0**	**1398.1**	**1398.1**	**1019.8**	**1290.7**	NaN	NaN		2.09		2.09	**2.09**	**#VALORE!**		0.133	NaN	NaN		**#DIV/0!**	**#VALORE!**	6.00	
20191106_4	**3.0**	**1377.3**	**1377.3**	**1162.4**	**1287.4**	NaN		6.13	5.75		1.48	**3.81**	**76%**		0.186	0.432		0.25	**0.341**	**73%**	6.00	
20191106_5	**5.2**	**3668.2**	**3668.2**	**2195.1**	**3423.5**	NaN		6.57	5.75		4.60	**5.58**	**30%**		0.223	NaN		0.50	**0.500**	**#VALORE!**	6.00	
20191106_6	**3.9**	**1899.2**	**1899.2**	**1492.7**	**1850.0**	NaN		8.36	7.66		4.18	**6.27**	**50%**		0.273	NaN		0.50	**0.500**	**#VALORE!**	6.00	
20191106_7	**2.8**	**1643.2**	**1643.2**	**1078.6**	**1351.7**	NaN		5.41	7.66		7.66	**6.53**	**-42%**		0.359	0.194		0.75	**0.472**	**-74%**	6.00	
20191106_8	**4.3**	**1925.8**	**1925.8**	**1496.0**	**1711.9**	NaN	NaN		5.11		6.57	**6.57**	**#VALORE!**		0.295	NaN	NaN		**#DIV/0!**	**#VALORE!**	6.00	
20191106_9	**2.7**	**1518.5**	**1518.5**	**1075.5**	**1518.5**	NaN	NaN		6.57		7.66	**7.66**	**#VALORE!**	NaN	NaN	NaN			**#DIV/0!**	**#VALORE!**	6.00	
20191106_10	**4.0**	**2091.4**	**2091.4**	**1418.9**	**1636.5**	NaN		4.18	5.11		9.19	**6.69**	**-120%**		0.214	0.120		0.75	**0.435**	**-84%**	6.00	
20191106_11	**2.8**	**1762.7**	**1762.7**	**1408.9**	**1762.7**	NaN		5.41	7.66		4.60	**5.00**	**15%**		0.325	0.113		0.75	**0.432**	**-85%**	6.00	